APPENDIX A

Part 1. Asphalt Surface Aging Prediction (ASAP) Program—Final Report

Part 2. ASAP SDD Software Design

Part 3. ASAP SDD Software Headers

Part 4. ASAP Final Report Software Diagrams

APPENDIX A

Part 1. Asphalt Surface Aging Prediction (ASAP) Program—Final Report

Asphalt Surface Aging Prediction (ASAP) Program

Final Report

Prepared under:
USDOT
Research and Innovative Technology Administration
Cooperative Agreement
DTOS59-07-

Western Research Institute

INNOVA ENGINEERING

Preface

The document has been prepared for inclusion into the Final Report for the Asphalt Surface Aging Prediction (ASAP) System under USDOT Cooperative Agreement #DTOS59-07-H-0006 involving USDOT Research and Innovative Technology Administration (RITA) and The Western Research Institute (WRI) at the University of Wyoming. Under this agreement WRI established a subcontract with Innova Engineering, LLC, to develop a field-capable Fourier Transform Infrared (FTIR) spectrometer system that would potentially replicate asphalt-signature phenomenology observed in WRI's laboratory.

WRI has discovered a promising means to predict the aging of asphalt binder materials by analyzing asphalt infrared spectral signatures for the presence of carbonyl molecular vibration modes at corresponding spectral regions of interest. Specific absorption bands relate to the presence of carbonyl in asphalt samples. Applying various means to normalize the carbonyl signature to other molecular signatures that indicate asphalt presence, the resulting Carbonyl Index (CI) may be derived. The normalized CI laboratory observations have repeatedly demonstrated a linear relationship to the log of the shear modulus (G*). This relationship provides a quantitative measure that enables the prediction of asphalt degradation using the G* relationship. Various types of FTIR spectrometer measurements have been used in their laboratory including traditional transmission accessories and photoacoustic (PAS) accessories to name a few. Each of these approaches to demonstrating the CI-to-Log(G*) linear correspondence have involved preparation of the asphalt sample or contact with the asphalt sample.

Under the ASAP program, Innova Engineering provided its best effort to develop a technical capability that could detect and quantify the carbonyl (C=O) content in asphalt surfaces using non-contact methods. This required development of a field-capable FTIR spectrometer that could operate in rugged environments. The capability would range from close-in non-contact measurements out to longer ranges commensurate with remote sensing standoff ranges. The targeted regions of the IR spectrum are ~1700-1725 cm^{-1} region and 1150-1250 cm^{-1} region (see Figure 1.2-1 in Section 1.0). Furthermore, in this scenario there would be no preparation of asphalt binder samples. The FTIR spectrometer could only collect spectral signatures from some standoff distance. This would require some type of diffuse reflectance measurement from the surface—using an IR source to illuminate the asphalt surface, or passively observe the surface using solar illumination.

A key enabling technology was the development of a monolithic optical block that could provide the interferometer function performed internal to all FTIR spectrometer instruments. PLX, Inc., had developed this monolithic interferometer block technology under internal funding based on its development of other monolithic precisely-aligned optical components for other applications. The monolithic interferometer block eliminated the sensitivities to environment factors such as shock, vibration, and temperature. Many laboratory spectrometer instruments require precise alignment of various mirrors, beamsplitter, compensator, and other optical components

that comprise the interferometer function. For the monolithic interferometer, the components are aligned with extreme optical precision relative to the other components in the interferometer using a proprietary alignment and adhesion process. Furthermore, the various "glass" materials are very insensitive to temperature variations due to the low thermal coefficient of expansion of these materials. These factors not only support ruggedized operation, but also minimize the need to perform routine maintenance and calibration of the internal optics required by many laboratory spectrometer instruments.

The ASAP FTIR spectrometer was designed, developed and tested exclusively for this program. All aspects of the FTIR design were directed to ensuring the instrument would be capable of operating in stressing test environments in fielded scenarios. The FTIR base ¾" aluminum plate provides the foundation for the FTIR internal optical functions and components. The sides of the FTIR are ½" aluminum plates. Among the bottom plate and the sides plates, all optical components and other mechanical and electrical devices and components are internally mounted. In addition, some external components such as the IR source, the special detector batteries, and the DRIFTS optical arms assembly were mounted to the exterior walls of the FTIR housing which also provided stable structural mounting. The top plate is 3/16" thick aluminum lid that completes the ruggedized FTIR housing.

Furthermore, the FTIR housing was mounted using four specialized shock mounts to isolate the FTIR from external shock and vibration influences. These shock mounts in term mounted the FTIR to the dove-tail plate that was developed for quick installation before tests and quick removal after the tests. The V-notch in the plate mounting assembly also provided precise alignment of the FTIR each time it was installed in the van. The plate also had an opening to allow the DRIFTS optical arms and end-effector to lower through the van floor and collect measurements from the asphalt surface below.

Being that this was a new development effort, all aspects of the designs for the ASAP program involved extensive research, detailed design and systems engineering tradeoffs, prototyping of the leading candidate designs, and implementation of the final designs into working systems, and test of key functions that were to be performed. Examples of these processes ranged from the survey of numerous van vehicles and models relative to the requirement to have a hole for viewing of the asphalt surface below with minimal structural changes to the van chassis structure—to complex algorithms to control the moving mirror motion or use the HeNe laser to provide measurement of the mirror position with extreme precision (~0.15 micron) for sampling the IR channel data. A considerable amount of research went into numerous technical issues associated with the intricacies of a Michelson-interferometer FTIR spectrometer including the requirements for extreme precision required for the dynamic interferometer function. In particular the requirement for a diffuse reflectance (DR) measurement from the asphalt surface posed significant challenges, and substantial research was devoted to developing a comprehensive understanding of various means used to achieve this form of measurement using various DR FTIR accessory components. During the last phase of the program, several approaches were analyzed, designed, and tested to provide a signal-to-

noise enhancement to the FTIR to solve issues relative to diffuse reflectance measurements from asphalt surfaces.

Positive accomplishments for the ASAP program included the development of a working ruggedized FTIR spectrometer from the smallest component up to a full working system. This FTIR has demonstrated absolute repeatability in its performing high-resolution spectral measurements throughout the infrared band in the transmission mode. Substantial research into FTIR technical issues and many design challenges were addressed to evolve the initial FTIR design to a reliable working system. Among many technical areas and issues, these challenges included the intricacies of the moving corner-cube mirror using a unique "porch swing" mechanism to ensure tight control of the mirror during scans. The approach to using the HeNe sinusoidal fringe patterns as a precise reference for sampling the infrared interferogram according to the optical path difference regardless of minor perturbations in the mirror velocity was a significant accomplishment. To create high-fidelity spectral measurements using the FTIR instrument, the spatial points of reference for sampling had to correspond exactly with the peaks and valleys and zero crossings for the HeNe laser reference signal. The dual quadrant detector was successful in supporting the tight control loop for the moving mirror. Development of the DRIFTS rotary optical arms were very successful in that these arms allowed transfer of the collimated FTIR output down through the van floor to the end-effector near the asphalt surface. The collimation and directivity were held very precisely over many different rotary movements and configurations. The nitrogen purging and hermetic seals of the FTIR were demonstrated to work well as observed by the reduction of CO_2 and H_2O absorptions as the purging continued.

The software developed in the National Instruments LabView^{tm} environment was completely designed and developed for the ASAP program. It has provided very specialized signal processing to support the fundamental measurement and analysis capability required for FTIR operation. The front panel display provide the operator with very easy GUI menus to collect, process, and analyze interferograms and FFT-transformed spectral signature data. The software has a suite of digital filtering tools and data windowing functions required by the FTIR signal processing. Overall the FTIR has worked well in the transmission mode and has demonstrated very repeatable operation in detecting known signatures for atmospheric molecules as well as high-density polyethylene materials. Additional information regarding the design and functionality of the FTIR hardware and software design is provided in the main body of our Final Report.

A major challenge that occurred in the program came when attempts were made to take direct measurements of asphalt surfaces with the DRIFTS end-effector device. Upon initial delivery of the FTIR from PLX to Innova Engineering indicated good performance in the transmission mode and showed such absorption phenomena as the absorption curves for HDPE films as well as CO_2 and H_2O. When an asphalt sample was placed at the end-effector aperture, no signal was detected. This was the first indication that a problem with diffuse reflectance accessories would occur for asphalt surfaces. It was apparent that alternative designs for the end effector or other aspects of the FTIR

design would have to occur. Immediately various design options to improve the signal-to-noise performance of the FTIR were explored. Basically the design options included an end-to-end assessment which centered upon improvements to the IR source, improvements to the IR detector, and improvements to the intervening optics between the source and the detector. These design alternatives and the efforts to identify various solutions within each of the these options are presented in the main body of the Final Report. While some of the optical design alternatives provided incremental improvements, it was apparent that the need for orders-of-magnitude improvements would be needed to solve the asphalt measurement problem for diffuse reflectance measurements. Procurement of the HgCdTe detector with a 77K cooler engine had the potential to offer the required orders-of-magnitude improvements over the ThermoElectric-cooled HgCdTe detector originally delivered with then system. Early testing of the FTIR with the more sensitive detector showed substantially greater signals when operated in the specular mode. Once the FTIR was tested in a diffuse reflectance mode with the asphalt binder slide sample inserted in the end effector optical path, a strong spectral signature was observed for the asphalt binder material. These signals have been analyzed and attempts to interpret the signatures are on-going. The results were significantly worse for a direct measure of an asphalt core sample, and the resultant signature was very low and noisy. Additional tests have been run, but it appears that direct measurement from an asphalt surface will be problematic. We are also investigating an alternative receive-only configuration using the HgCdTe 77K detector to see if direct spectral measurements from actual asphalt surfaces can be collected. Although the contract period is complete, Innova Engineering is continuing to work with the FTIR spectrometer to conduct these experiments at no costs to attempt to prove the concept may viable in detecting carbonyl content in roadway asphalt surfaces.

The Final Report will address the development of the FTIR spectrometer and the final design of the system. Additionally the van design and modifications will be presented along with a suite of test planning, test conduct, and post-test analysis tools that were developed to aid in the measurements process. A design for adapting the FTIR to an airborne telescope receive-only configuration is presented. All of the quarterly progress reports presented during the execution of the project provide additional insight into some of the design challenges, tradeoffs, down-selections, and decisions that occurred over the life of this effort. Given the limited test results that were collected for direct diffuse reflectance measurement on asphalt surfaces, the Final Report primarily addresses the work that was performed to get to a working FTIR system, the van modification and integration accomplishments, and the design for an airborne version of the FTIR spectrometer operating from a Cessna aircraft.

The organization of the Final Report begins with Section 1.0 Introduction that describes the purpose and scope, system overview, design constraints, future contingencies, document organization, points of contact, and project references. Section 2.0 System Architecture provides an overview of the hardware and software architecture for the ASAP program. Section 3.0 provides a detailed presentation of the overall H Detailed Hardware Design. Similarly Section 4.0 presents the Detailed Software Design.

ASAP System Design

1. 0 INTRODUCTION

1.1 Purpose and Scope

The purpose of the Asphalt Surface Aging Prediction (ASAP) program is to develop a field-capable non-contact system to quantitatively determine surface-aging properties of asphalt roadways. The America Society of Civil Engineers estimates that our nation's roadway and infrastructure are in need of $2.2 trillion of near-term repair and improvements to sustain our economic potential. To mitigate this cost impact, the ASAP program is focused on providing a predictive means to quantify asphalt surface aging so that less-costly surface-treatment rejuvenators can be preemptively applied before micro-cracking and micro-fissures develop. These conditions are the beginning of breakdown in hot-mix asphalt concrete (HMAC) roadway surfaces.

Western Research Institute (WRI) has performed extensive laboratory research to demonstrate a repeatable linear relationship between the log of shear modulus (log G*) of the asphalt and the asphalt's carbonyl (C=O) content. Various laboratory Fourier Transform Infrared (FTIR) spectrometers and accessories have been used to determine carbonyl content in differing asphalt samples. The carbonyl content of various asphalt samples has been shown to strongly correlate with log G* measurements for these samples under varying temperature and moisture conditions. The repeatability of this fundamental relationship between carbonyl content and log G* have proven that asphalt surface aging can be measured indirectly using FTIR spectrometer instruments.

Based on this asphalt-aging research and findings using laboratory FTIR spectrometers, the ASAP program has been established to develop a ruggedized FTIR spectrometer with the objective of measuring carbonyl content in asphalt surfaces in the field. Under this program, ASAP's overarching goal was to replicate the asphalt aging-prediction capability that has been demonstrated in WRI's laboratory to a field-capable system using a non-contact remote-sensing FTIR spectrometer. Operationally the field-ready ASAP FTIR would be used to gather asphalt road-surface data at the specific regions of the spectrum that exhibit carbonyl-absorption signature phenomenology. Carbonyl-content measurements would be made at various locations along a selected asphalt roadway to indirectly determine the shear modulus of the binder. With two or more measurements, a prediction of the rate of change in G* increase could also be determined. Based on this data, the proposed concept of operation would have the ASAP van or aircraft gather data at pre-determined locations on U.S. highways. This data would be processed to determine a Carbonyl-content Index (CI) that would subsequently be used to determine optimum times to apply surface rejuvenators to significantly prolong the integrity of asphalt surfaces. In addition to the multi-billion dollar savings this capability could provide, it would also preserve the surface quality of the roadway systems for improved surface vehicle usage.

The scope of this Final Report is to provide a detailed description of the systems engineering tasks and hardware/software encompassed in the ASAP program development phase. Additional details regarding the carbonyl signature phenomenology and its relationship to complex modulus of the asphalt binder is deferred to the WRI final report discussion.

1.2 Project Executive Summary

System Overview

The ASAP system comprises the following subsystems that have been developed or investigated under the subject contract:

- ASAP FTIR spectrometer with associated detector and optical accessory configurations
- ASAP van and associated equipment, instrumentation, and operator station
- ASAP aircraft configuration for remote sensing investigation and plan

The ASAP system design centers on development of the ruggedized FTIR spectrometer instrument. The FTIR spectrometer is designed to collect high-resolution (4 cm^{-1}) infrared-absorption spectral data over a broad infrared band ranging from 800 cm^{-1} (~12m) to 5000 cm^{-1} (~2m). The primary carbonyl absorption bands of interest are around 1700 cm^{-1} and between 1150 cm^{-1} and 1250 cm^{-1}. Figure 1.2-1 presents an absorbance plot for a spectral range of 2000 cm^{-1} to 600 cm^{-1}. The regions where carbonyl absorption occurs are indicated in this data.

In addition to these regions of interest for carbonyl, a means to normalize the carbonyl measurement has been developed that uses a Carbonyl Index (CI) factor rather than absorbance units for carbonyl alone. The CI provides a simple basis for comparing carbonyl concentration regardless of asphalt content in the laboratory-sampling accessory. The carbonyl band area and the carbon-hydrogen (CH) stretch band (2800–3050 cm^{-1}) area are ratioed to provide the CI value. Basically the amount of carbonyl measured in an asphalt sample could vary based on how much asphalt binder existed in the sample. The amount of asphalt in a sample can vary over wide ranges. Therefore, a ratio of the *presence of carbonyl* to the *presence of asphalt* is needed. The Carbonyl Index provides a normalizing index for asphalt surface aging prediction.

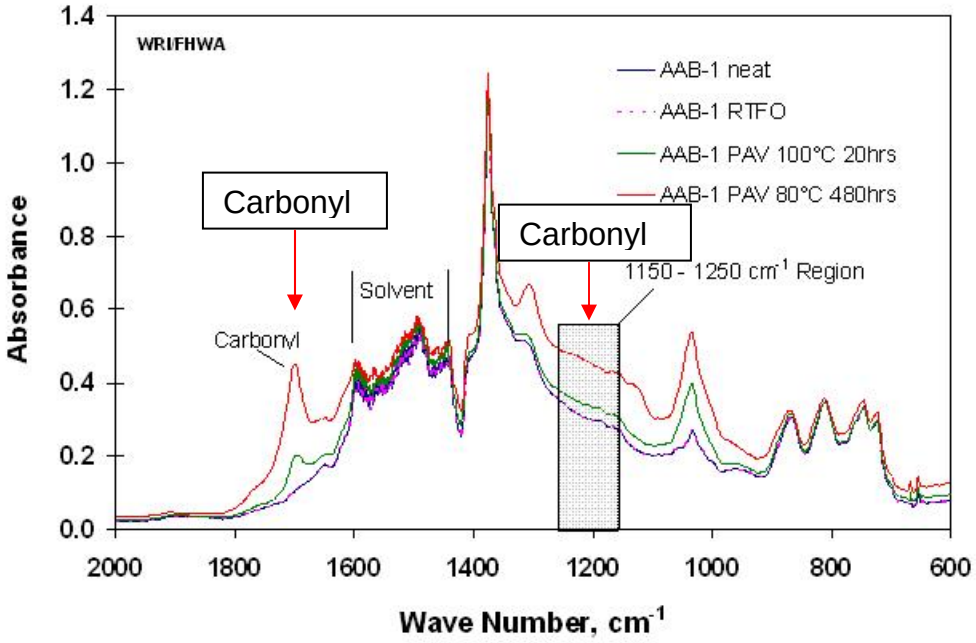

Figure 1.2-1 Absorbance Spectra for Several Asphalt Sample
Indicating the Primary Regions of Interest for Carbonyl Detection

Design Constraints

The primary design constraint was that the ASAP FTIR spectrometer had to operate in a remote-sensing, or non-contact, mode of operation. Many spectrometer require that the sample under test be contacted under normal operation. As one example, the attenuated total reflectance (ATR) accessory on a spectrometer requires that pressure be applied against the sample under test. In more cases, the sample are ground up and mixed with an inert host material (e.g., KBr) , contained in a vessel for gases or liquids, or other means of spectroscopic measurement that requires manipulation of the sample material for the preparation process. For the ASAP program, since there is no contact with the asphalt sample under test, then other means have been pursued to enable non-contact spectrographic measurement of asphalt surfaces for aging prediction. Additional details of the approach to this design problem are contained within this Final Report Document. Other design constraints included the need for the FTIR to be ruggedized, and had to fit inside the aft cargo compartment of a van and enable a look-down viewing port to observe the asphalt below, and also plan for integration into a Cessna aircraft.

Future Contingencies

The primary challenge of the ASAP FTIR development project was the requirement to produce infrared spectra from asphalt surfaces in a non-contact or remote-sensing scenario. For the initial laboratory and van testing, a modulated infrared beam had to be directed toward the asphalt surface—and after interaction with the asphalt binder material on the surface of the asphalt pavement—collect the diffusely reflected infrared energy scattered toward the detector optics and produce a signal that could be transformed into an infrared spectrum. This is the most challenging FTIR measurement scenario relative to other approaches due the limited energy being scattered from the asphalt diffuse surface. Recognizing these low-signal challenges, several design contingencies included increasing the source IR energy, increasing the size of the intervening optics in the spectrometer, and/or increasing the sensitivity of the IR detector. Under this best effort research contract, these contingencies were pursued and are described in the Final Report.

1.3 Document Organization

Section 1 (this section) of this Final Report provides the Purpose and Scope of the ASAP project, and the Project Executive Summary including system overview, design constraints, and future contingencies, points of contact, and project references. Section 2 summarizes the System Hardware Architecture and System Software Architecture. The Final Report then progresses to the Detailed Design which includes Section 3 describing the Hardware Detailed Design to include the ASAP FTIR Design, Van Integration, and Aircraft Design Plan. Section 4 presents the System Software for the ASAP software that was developed using the National Instruments LabView prototyping software. While the LabView software is proprietary, any code developed using this prototyping tool may be saved as an .exe program and can operate without licensing from National Instruments.

1.4 Points of Contact

- Western Research Institute, Inc., Laramie, WY: Mr. Fred Turner, Principal Investigator (PI) for the ASAP contract, fturner@uwyo.edu
- Innova Engineering LLC, Navarre, FL : Mr. Greg Fountain and Mr. Dan Matthews, co-PI for the ASAP development, greg@innova-llc.com, dan@innova-llc.com
- PLX, Inc., Deer Park, NY : FTIR development subcontractor, agjacobson@gmail.com
- Simwright, Inc., Navarre, FL : Mr. Paul Doughty and Mr. Chris Casey, software support, paul.doughty@simwright.com; chris.casey@simwright.com

1.5 Project References

1. Fourier Transform Infrared Spectrometry. Peter R. Griffiths, James A de Haseth
2. Remote Sensing by Fourier Transform Spectroscopy, Reinhard Beer
3. Fundamentals of Fourier Transform Infrared Spectroscopy, Brain C. Smith
4. Fourier Transform Spectrometry, Sumner P. Davis, Mark C. Abrams, James W. Brault
5. Introduction to Imaging Spectrometers, William L. Wolfe
6. Modern Optical Engineering, Warren J. Smith
7. Optical Scattering, John C. Stover
8. TSMADS Hyperspectral Requirements Report, USAF Report, Gregory V. Fountain

2.0 SYSTEM ARCHITECTURE

This section provides a brief description for the ASAP system architecture. This section concisely describes the System Hardware Architecture and System Software Architecture. The ASAP system and software are described in considerable detail in Section 3.

2.1 System Hardware Architecture

A very simplified layout of the ASAP FTIR architecture is presented in Figure 2.1-1. The PC controls the FTIR unit and provides data acquisition, processing, and computation of the IR spectrum for a selected asphalt test sample measurement. Two National Instruments PC cards—the Motion Controller card and the Data Acquisition card—are inserted into the PC main system bus and provides connectors on the back-side of the PC unit. The Motion Controller provides hardware control of the FTIR moving mirror through a complex closed-loop software design. The Data Acquisition card acquires the five detector signals to include the IR detector output signal, the two HeNe laser interferograms sinusoidal analog signals from the quadrature detectors, and two square-wave signals produced via threshold comparators to provide digital counts offset by 90 degrees to control the moving mirror. The DRIFTS includes the two optical arms and end-effector unit that is used to produce spectrum from the asphalt samples. The FTIR design is expanded in considerable more detail in the next section.

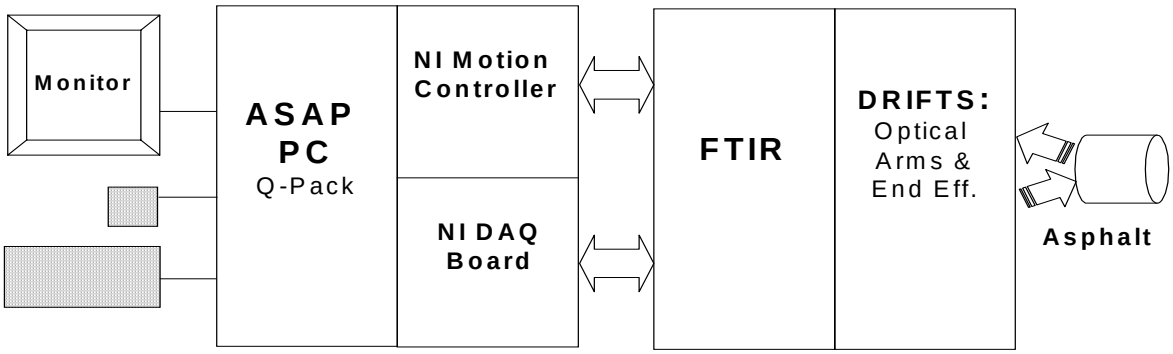

Figure 2.1-1 Very Simplified Diagram of the ASAP FTIR System

A very simplified layout of the van functional design is presented in Figure 2.1-2. The van power is depicted to the right of this diagram and provides 12 VDC to the van equipment including the FTIR and the safety lighting equipment. Two 115 VAC buses are powered by two pure-sine-wave power inverters that convert the direct current power from the battery bank to alternating current. The gel-cell battery bank includes four deep-cycle gel-cell marine batteries configured in parallel electrically. The FTIR is shown to the left with the DRIFTS optical arms and end-effecter assembly designed specifically for the van configuration. The N_2 gas provides purging of the FTIR instruments as needed to eliminate the influences of CO_2 and H_2O inside the FTIR unit.

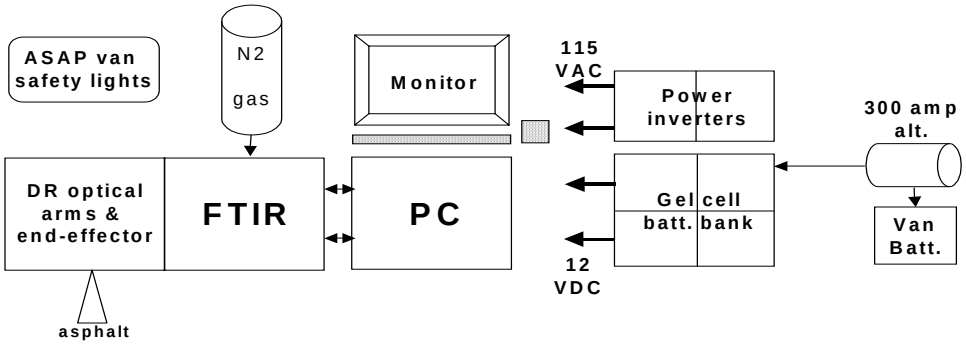

Figure 2.1-2 Very Simplified Diagram for ASAP Van Architecture

2.2 System Software Architecture

The ASAP software is based on National Instruments LabView development software tools. Basically LabView uses a graphical programming language that uses icons instead of lines of text to create applications involving dataflow programming. The software is controlled from a user interface known as the front panel. LabView programs are called virtual instruments (.vi's) because these graphical modules imitate various instrument functions that process data in a defined way. The Vis have three components:

- **Front panel**—Serves as the user interface
- **Block Diagram**—contains the graphical source code that defines the functionality of the VI

- **Icon and Connector Pane**—identifies the interface to the VI so that you can use the VI in another VI (called a subVI) and is analogous to a subroutine in text-based programming languages.

The VIs comprising the ASAP software is presented below. Section 4, Software Design, describes the VIs in additional detail and also presents the graphical design of the software VIs used to collect and process the ASAP FTIR spectrometer data. The VIs are:

- FTRX Applications Rev 11.vi
- Processing Interferogram
- Minimax
- ZeroPadder
- Pad to…
- Get Interferogram
- IR Sampler- Interpolator
- Zero Phase Filter
- Decimate by 1-2-4-8
- Reference Subsampler
- Peaks and Valleys
- Subsample Indexer
- Is Even
- ZX Detector
- Threshold Detector with Hysteresis
- Configure DAQmx Read Parameters
- Configure, Load, Enable, and Wire Breakpoint
- Configure motion and move to startpoint
- Config Analog Input Channels
- Config FTIR Scan Parameters

ASAP DETAILED DESIGN

3.0 Hardware Detailed Design

This section provides detailed design description for the Asphalt Surface Aging Prediction (ASAP) system hardware development. The major hardware design components of the ASAP system include:

- FTIR Design
- Van Design
- Aircraft Design Concept

The following sections describe the current system hardware design.

3.1 ASAP FTIR Spectrometer Design

Before describing the specific hardware design for the FTIR spectrometer, a few basic fundamentals of FTIR operations are discussed to provide a better understanding of the specific design for this program. Figure 3.1-1 presents an elementary version of the Michelson interferometer that is the optical basis for the FTIR spectrometer. It bears a very close resemblance to the actual design for the ASAP FTIR spectrometer. To the left of this figure is the infrared "point" source that provides the IR energy source for the spectrometer. The IR source light is then collimated and directed toward a beamsplitter. The beamsplitter redirects half the light to a moving mirror and half of the light to a fixed mirror. Both signals are reflected from these mirrors back to the beamsplitter where they are recombined. However, the IR energy is "modulated" by the variation in optical path difference created by the moving mirror relative to the fixed mirror. The recombined collimated light is then directed toward a collector optic that focuses the modulated IR light onto a detector element to capture the optical interference signal. Note that net effect of the moving mirror velocity **V** cm/s on the input frequency **n** cm^{-1} results in an output frequency in the audio frequency range. For example, a 4000 cm^{-1} input frequency and a mirror velocity of 1 cm/s would result in an output frequency of 8000 Hz.

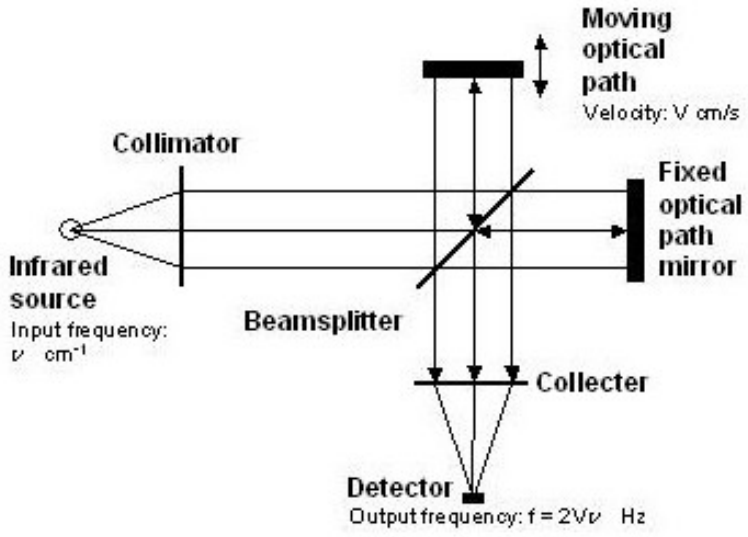

Figure 3.1-1. Elementary Diagram of Michelson Interferometer

Using this simplified discussion from above, we now will expound upon the spectrometer fundamentals. A Michelson-interferometer FTIR spectrometer operates by creating simultaneous *constructive* and *destructive* interference of all electromagnetic wavelengths contained within a selected infrared band. To create the optical mechanism for these varying interference conditions, a beam-splitter is used to divide the incoming light into two different optical paths. Typically, 50% of the light is transmitted through the beam-splitter, and 50% is reflected along an alternate path (at a 45-degree angle to the beam-splitter surface). Along one optical path, a fixed mirror is placed to reflect the light back toward the beam-splitter. The optical path distance remains constant along the round-trip path from the beam-splitter to the mirror and back to the beam-splitter. Along the other optical path, a moving mirror translates inward and outward along this optical path. The optical path distance varies along the round-trip path proportional to the instantaneous position of the mirror during the mirror scan cycle.

Through this process, the two "split" beams recombine back at the beam-splitter. Due to the moving mirror's changing optical path distance during its scan motion, the recombined beam is modulated such that varying constructive and destructive interference conditions are created by the relative phase differences for all wavelengths comprising the spectral band. The scanning mirror motion therefore creates a dynamically changing interference condition such that at any given scan instant, a unique optical path difference (OPD) exists for that mirror position value with a corresponding composite interference-signal amplitude value comprising all wavelengths' interference contributions in the spectral band for that unique OPD instance.

We will now introduce the compensator optical plate used to "balance" the optical paths. Figure 3.1-2 presents a simplified diagram of the basic Michelson interferometer showing the beam-splitter, fixed mirror (M1), moving mirror (M2), and source and

detector layout. Note that the reflective path indicated in the diagram passes through the refractive plate twice enroute to the M2 mirror, and once again through the refractive plate enroute to the detector, i.e., a total of three passes through the refractive material. For the transmitted path indicated in the diagram, the source light would only pass through the refractive plate once enroute to the M1 mirror, and then reflected from the beamsplitter backside to the detector, i.e., a total of one pass through the refractive plate. To compensate for the refractive differences, a compensator plate is added to the transmitted path for an additional two passes through the refractive plate to equal the three passes through the translating-mirror path. The compensator plate appears to the right of the beamsplitter in the diagram below.

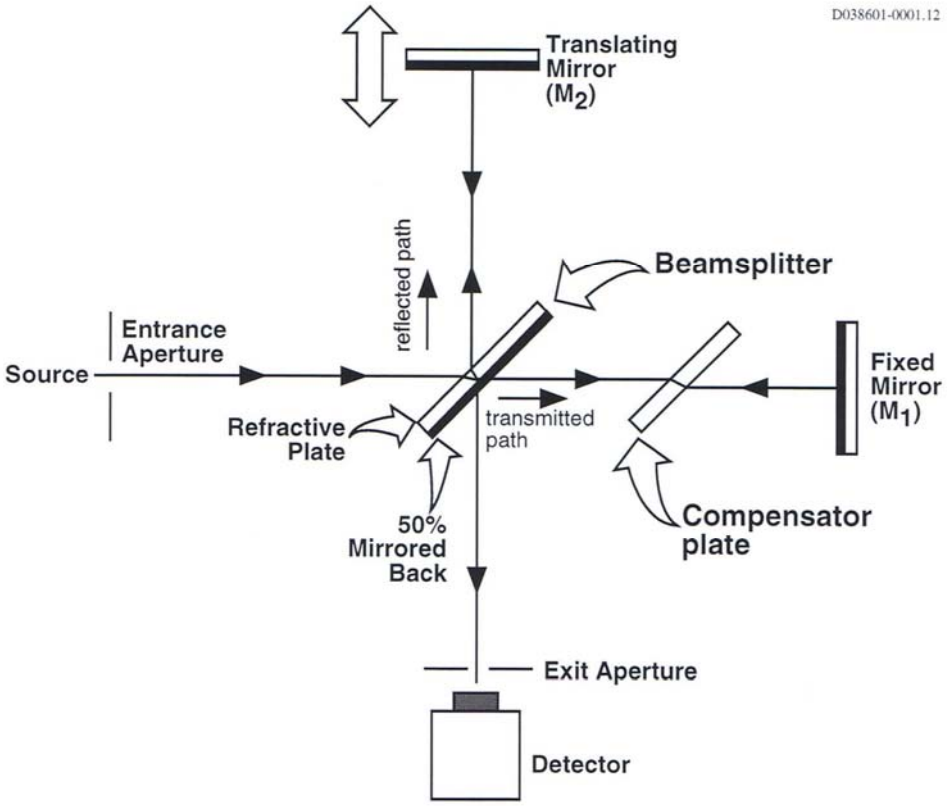

Figure 3.1-2. Simplified Diagram Showing the Basic Michelson Interferometer with the Compensator Plate in the Fixed Mirror Optical Path

For a FTIR spectrometer, the infrared detector output is sampled during each mirror scan cycle. A single-scan dataset collected during the scan has OPD units (cm) on the x-axis and the composite light-intensity amplitude variations on the y-axis. This two-dimensional dataset is referred to as an *interferogram*, and is the fundamental measurement output of the FTIR spectrometer. An example of an interferogram is presented in Figure 3.1-3. The actual spectrum is derived by computing the Fourier

Transform from the measured (and preprocessed) interferogram dataset as depicted in the figure.

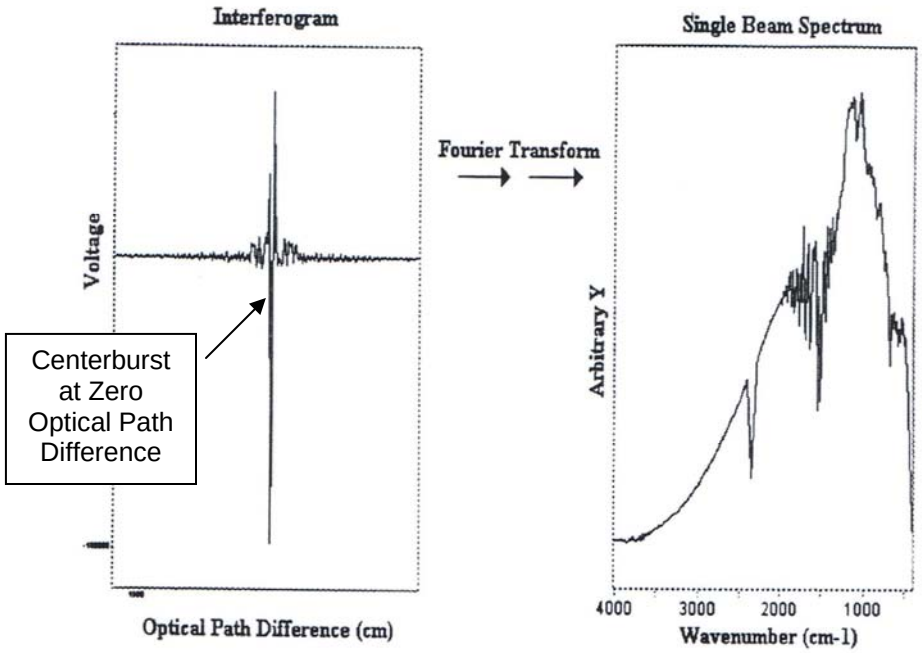

Figure 3.1-3 Example of an Interferogram and Showing the Centerburst at Zero OPD Value and a Characteristic Fourier Transform to Compute a Spectrum

For the ASAP program, the fundamental objective is to use WRI's laboratory results for spectrometer measurements of a Carbonyl Index for various asphalt samples, and replicate these results "in the field" using similar FTIR spectrometer technology. However, the difference between the laboratory and roadway environments poses significant challenges the ASAP FTIR design. Many laboratory spectrometers are relatively delicate instruments that have many sensitive adjustments for the various optical components encompassed in the Michelson-interferometer FTIR spectrometer design. The harshness of the roadway environment requires that a ruggedized ASAP FTIR spectrometer be developed.

The most critical design aspect of any Michelson-interferometer FTIR spectrometer is the interferometer design itself. Extreme precision in the relative positions and orientation of the various optical components must be maintained to small fractions of a wavelength. The angular relationship between the beam-splitter plate and the compensator plate—since they are the primary refractive components in a spectrometer—have to be maintained to a parallelism that is an extremely small fraction of the wavelength, and have to remain invariant to external conditions of temperature, vibration, etc. Additionally, the mirror surfaces have to be extremely flat and their orientation to the optical path must be precisely aligned, and have to remain invariant as well.

It is for this reason that the new monolithic optical block interferometer was selected for ASAP FTIR development. The proprietary technique patented by PLX, Inc., for aligning and adhering the optical "glass" component into a single integrated unit was a foremost requirement for this development. Another design consideration is the low thermal coefficient of expansion for the "glass" materials used in the interferometer and the concomitant insensitivity to temperature variations. A simplified diagram of the monolithic optical block interferometer is presented in Figure 3.1-4.

Figure 3.1-5 shows a photograph of the monolithic interferometer block used in the ASAP FTIR. This photograph shows the top glass "slab" of the interferometer and locations where the beamsplitter, compensator, fixed mirror (M1) and second fixed mirror (M2) are located under the top slab. Adhesive points appear as light blue spots areas in the photograph. The M2 mirror is optically coupled with the corner-cube retroreflector moving mirror to create the optical path difference during scans. This configuration provides an improved scan efficiency since 1 unit of mirror displacement yields 4 units of OPD displacement.

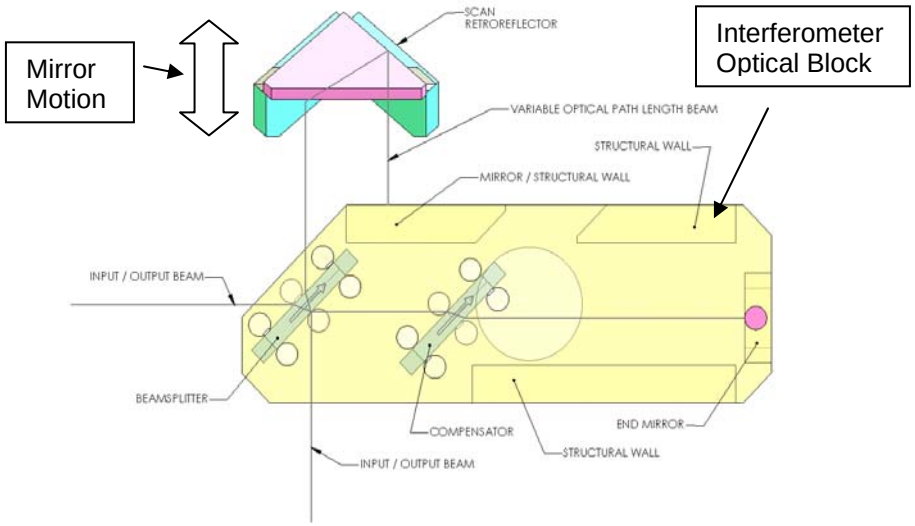

Figure 3.1-4 Diagram of Monolithic Optical Block Technology for the ASAP Interferometer

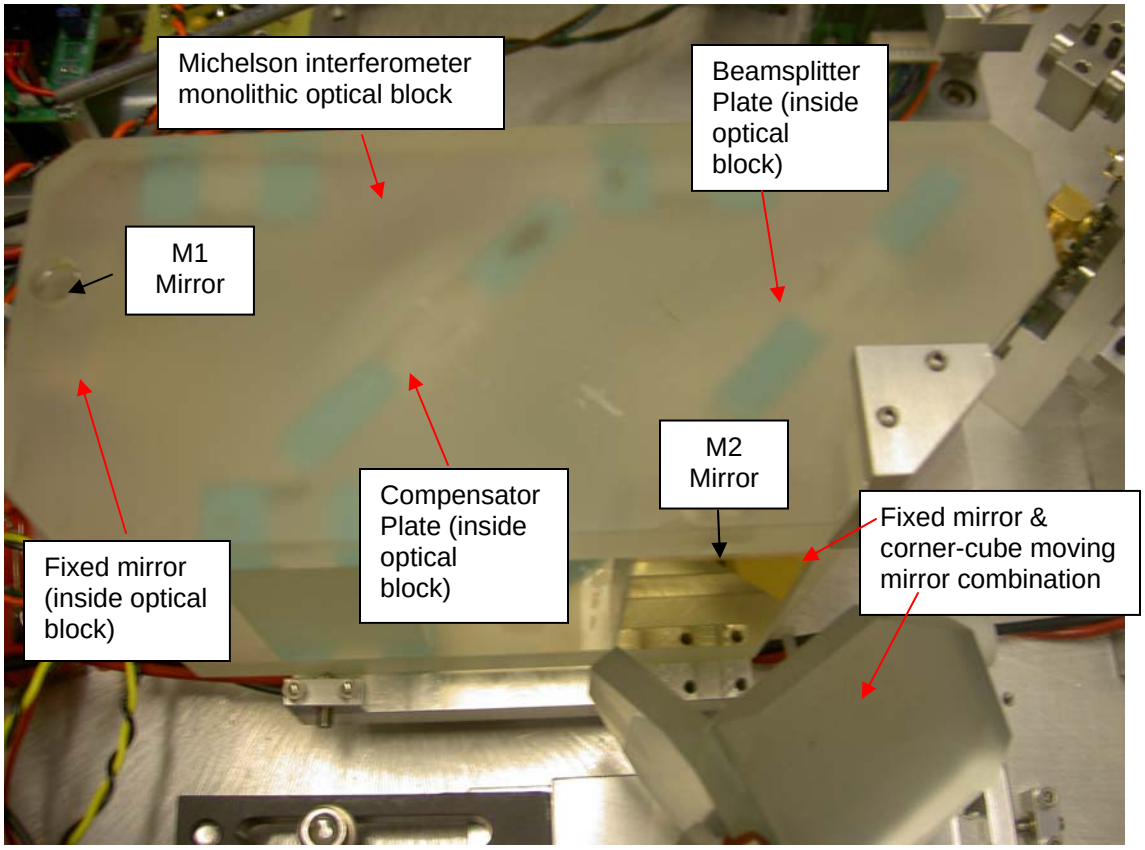

Figure 3.1-5. Photograph of the Monolithic Optical Block Interferometer

Figure 3.1-6 shows the relative acceleration power spectra that IE collected using an inertial measurement unit (IMU) to collect the data during various van and aircraft maneuvers. Performed early in the ASAP contract, this exercise provided quantitative characterization of the vibration environment to aid in further design and development of the ASAP FTIR including mechanical isolation mounting design.

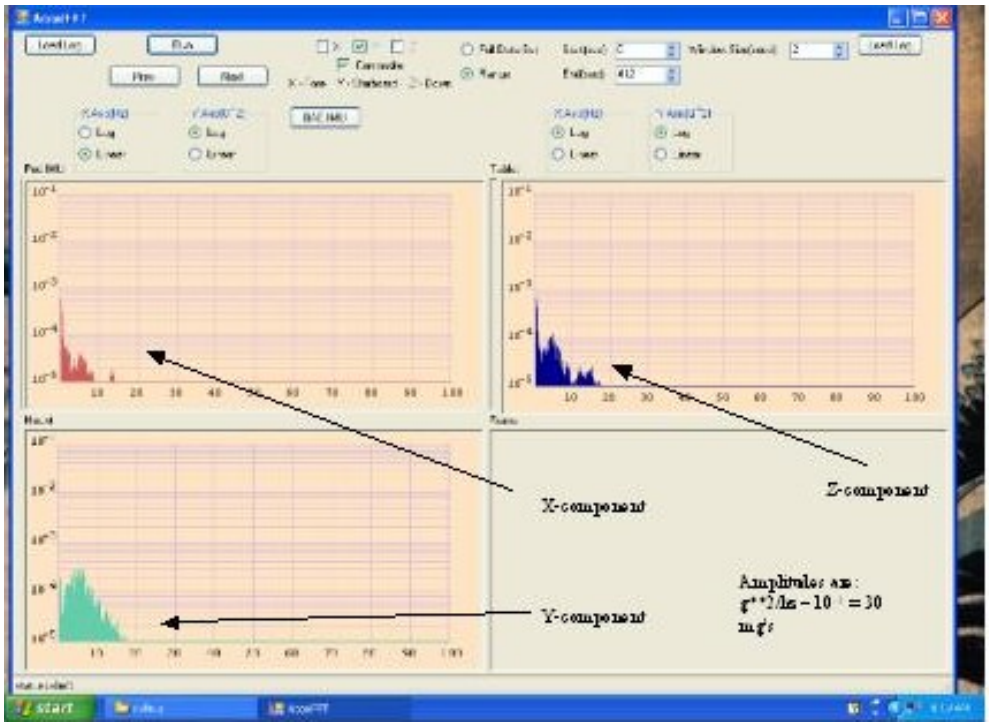

Figure 3.1-6 Acceleration Power Spectrum Data Collected in Van Environment

Our approach to describing the hardware design for the FTIR will address the *interior* (interferometer) design of the FTIR unit first, and then describe the *external* (accessories) units that are attached to the basic FTIR unit. The internal FTIR design accomplishes all functions necessary for the spectrometer to collect an interferogram over a broad infrared spectrum (2-12m). The exterior design includes an IR source and an optical arm and diffuse-reflectance (DR) end-effector accessory. Figure 3.1-7a presents a 3-D CAD drawing of the overall FTIR system showing the basic spectrometer unit and interior design, and the external units that include the IR source and the DRIFTS front-end optics unit. The overall FTIR system is shown with four shock mounts attached to the special mounting plate for the van floor aperture used to measure the asphalt below the surface. Figure 3.1-7b shows the FTIR and supporting computer and instrumentation in the ASAP development and test laboratory at Innnova Engineering.

These exterior components may be replaced with other accessories and components for different applications. For example, the current IR source may be replaced with a 77K-cooled HgCdTe detector, and the current optical-arm/end-effector components may be replaced with another accessory type, a 90 deg off-axis parabola mirror, or with a collection telescope optic for long-range FTIR spectroscopy measurements. Other source and accessory combinations may be used. The exterior units will be referred to as source or accessory components in subsequent discussions.

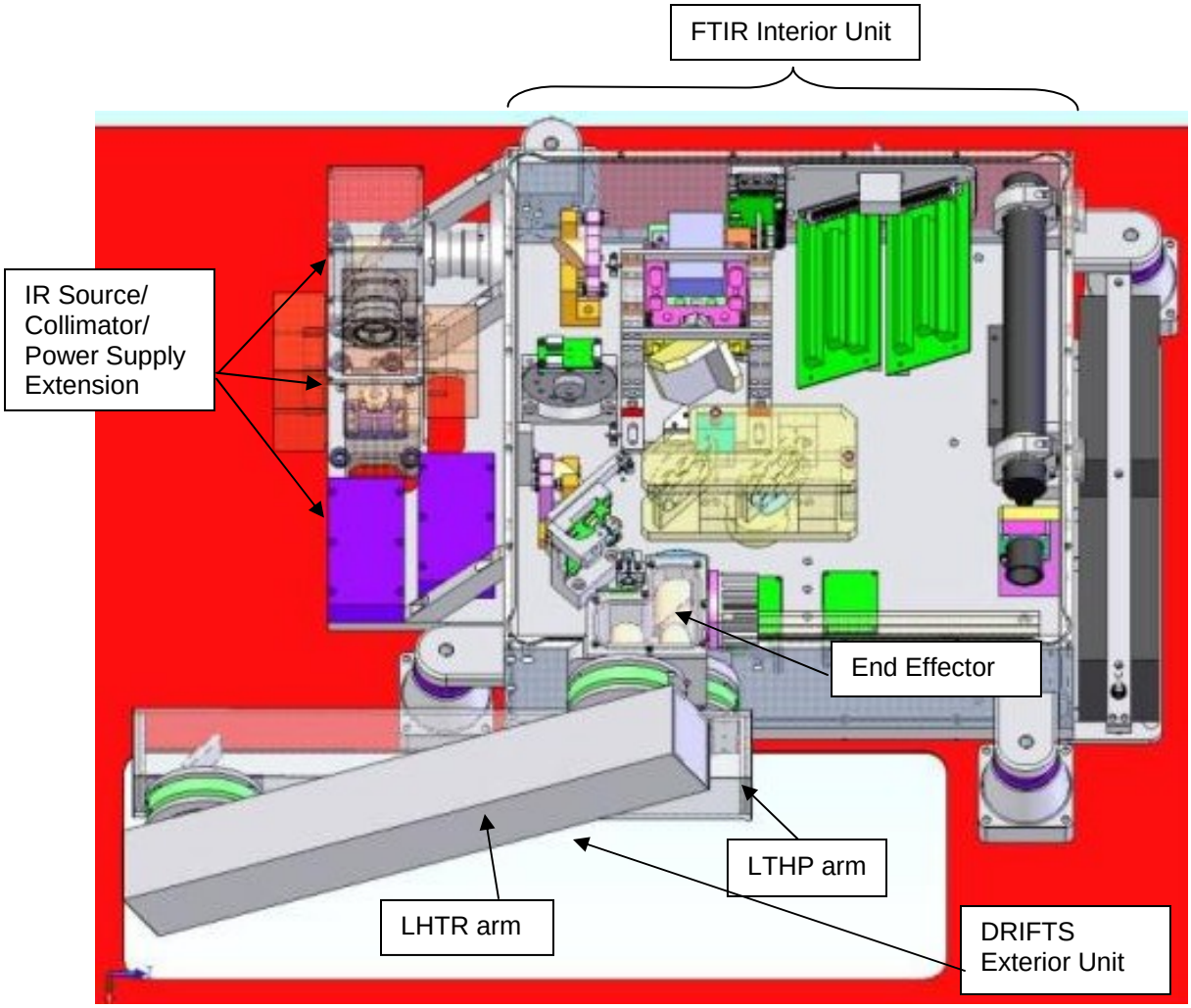

Figure 3.1-7a ASAP FTIR 3-D CAD Drawing Showing Basic Interior Design and Exterior Units – For van Configuration Data Collection

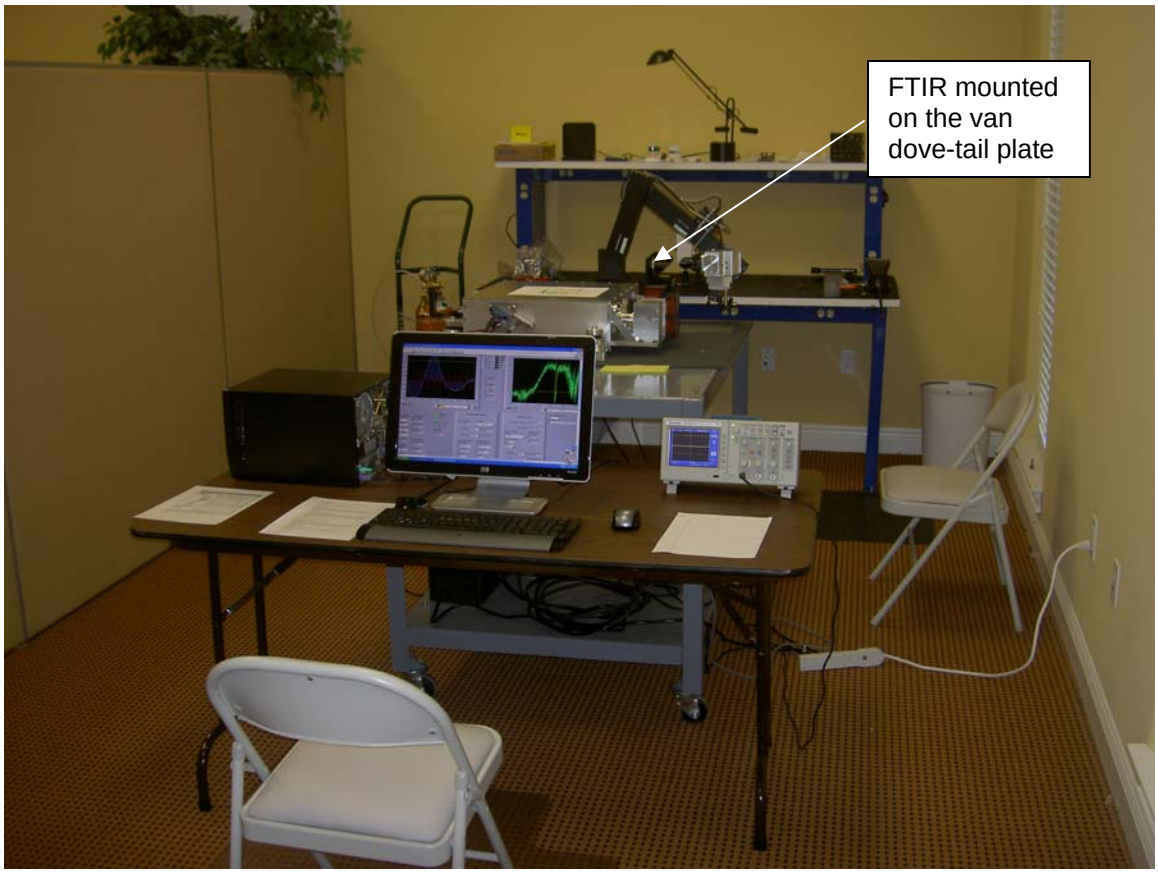

Figure 3.1-7b ASAP FTIR and Associated Computer and Instrumentation in the ASAP Development and Test Laboratory at Innova Engineering

3.1.2 ASAP FTIR Spectrometer Optical Design – Interior (Interferometer)

FTIR Housing

A two-dimensional CAD representation of the ASAP FTIR interior hardware design is presented in Figure 3.1-8a. The ASAP FTIR housing dimensions are 18" x 18" x 9". Future designs could reduce the FTIR footprint to ½ this size. The FTIR housing is constructed of aluminum plates that are bolted together with Allen-head machine screws. The base chassis is a ¾-inch-thick aluminum plate that provides substantial rigidity and strength for the FTIR optics mounting. The ruggedness of housing is extended to the sides which are comprised of ½-inch-thick aluminum plates. The side plates also are used for optical and equipment mounting in the current design. The FTIR top cover is a 3/16-

inch-thick aluminum plate to complete the enclosure of the FTIR unit. At each of the intersecting plates, an o-ring-like gasket and groove provide hermetic sealing of the FTIR for nitrogen gas purging as required. For vibration isolation, four shock mounts (Figure 3.1-9) are fastened at each corner of the FTIR side-plate appendages, and to the van dove-tail plate that is used for quickly mounting the FTIR in the van or aircraft. The design description for the dove-tail plate is presented in the Section 3.2, Van Integration.

Figure 3.1-8 also shows the apertures for the FTIR on the left-hand side of the figure (Aperture 1) and at the bottom of the figure (Aperture 2). The inside diameters of the apertures are 1 inch. The apertures also have flanges and fittings that provide for a hermitic seal to enable N_2 gas purging of the interior FTIR space. The IR source and collimator, and the DRIFTS accessory couple to the aperture fittings. A photograph of the FTIR internal components corresponding to the 2-D CAD drawing is presented in Figure 3.1-8b on the following page.

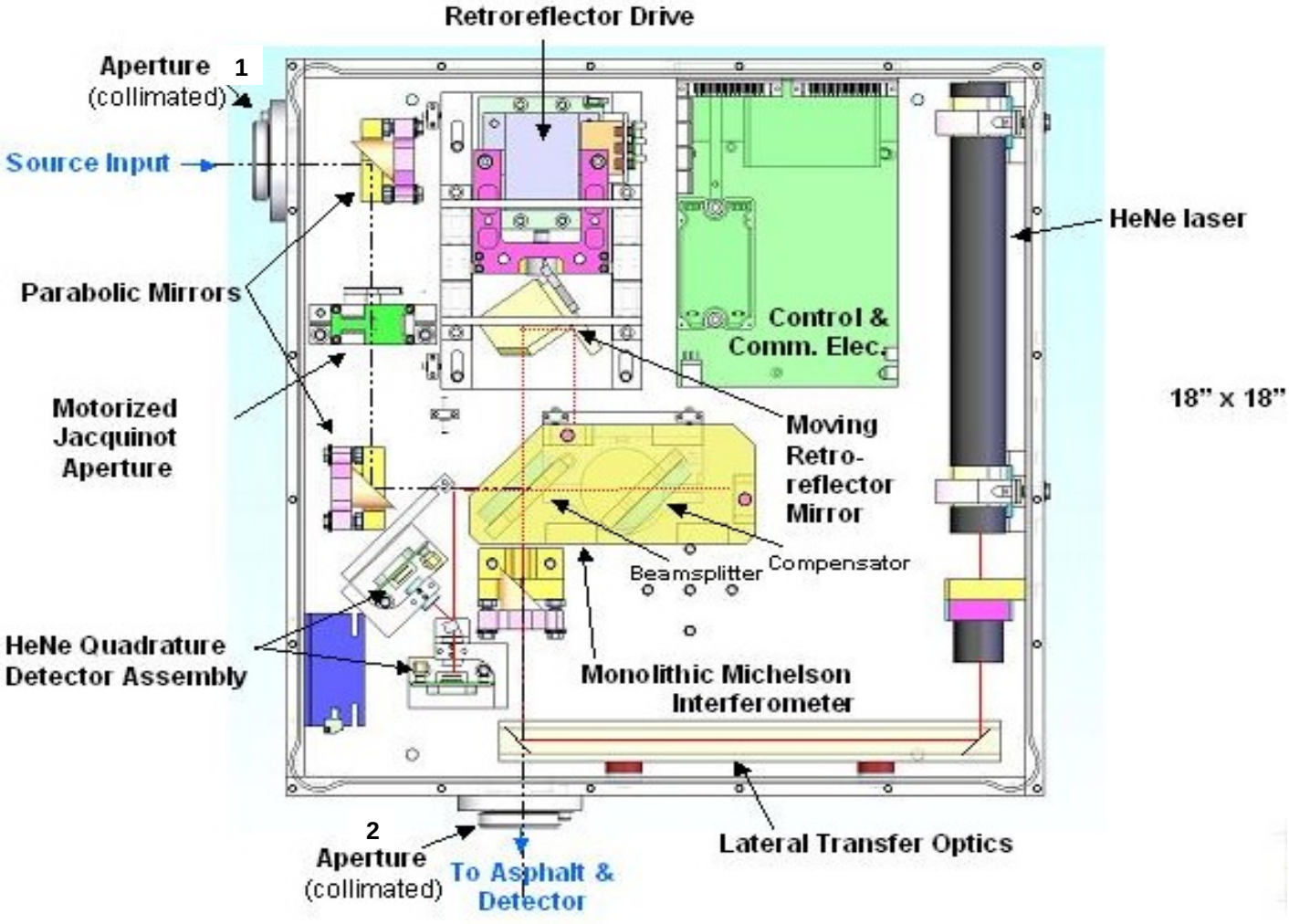

Figure 3.1-8a. ASAP FTIR Housing and Primary Internal Components – 2-D CAD View

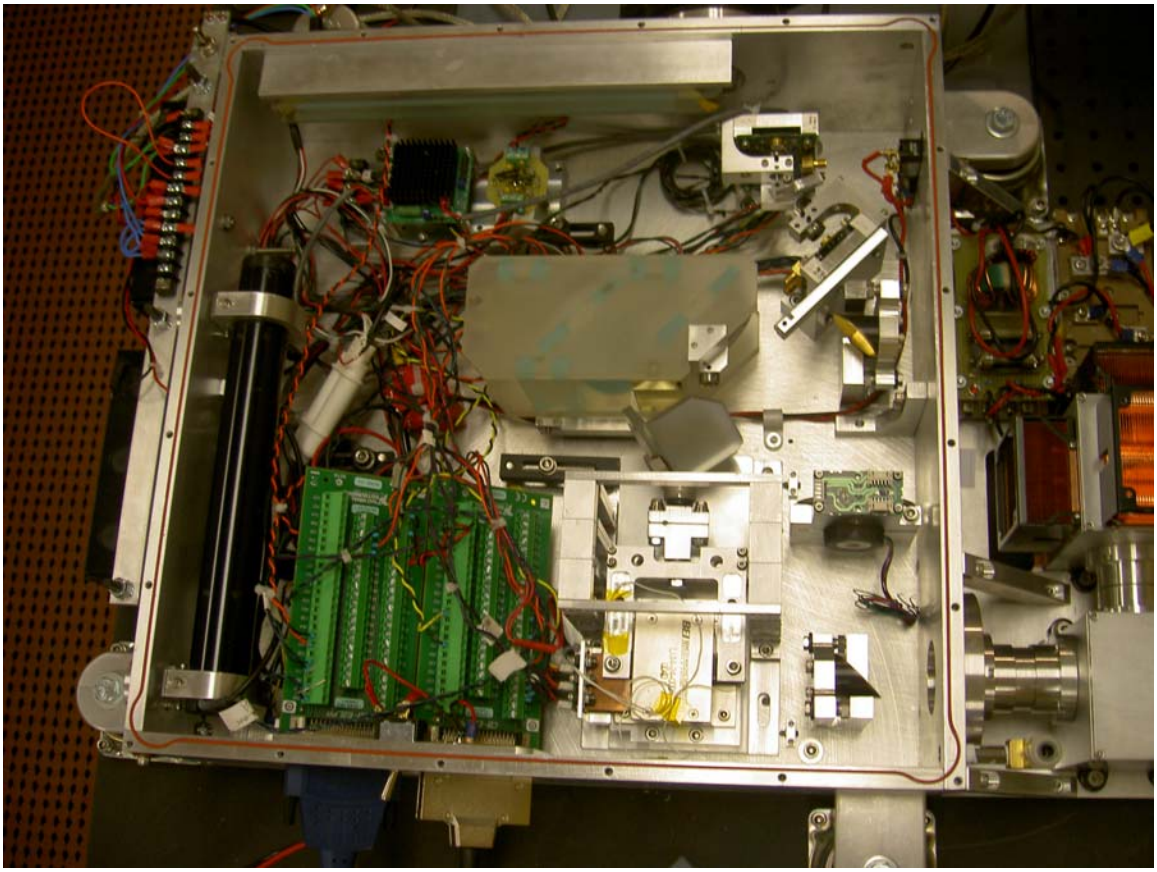

Figure 3.1-8b ASAP FTIR With Top Removed To Show the Interior Design for the Interferometer Components and Function

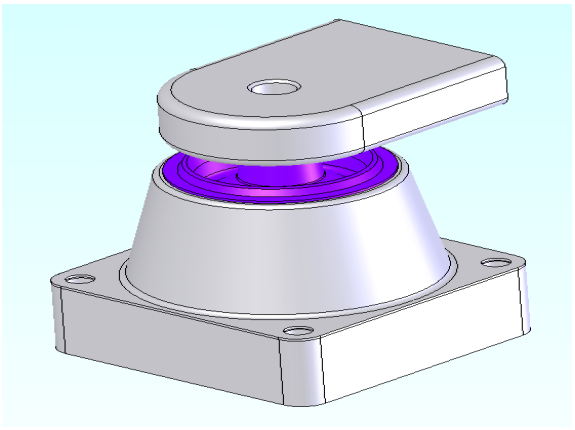

Figure 3.1-9 ASAP FTIR Housing Shock Mount CAD Design

FTIR Optical Design

There are two "channels" internal to the FTIR optical operation that provide the interferogram for Fourier transformation into a spectrum:

- IR Signal Channel
- HeNe Laser Reference Channel

IR Signal Channel

This section addresses the IR signal channel that ultimately produces an interferogram prior to Fourier transformation to a IR spectra. The Michelson interferometer is the heart of the IR channel operation. The interferometer provides the optical mechanism for broad-band "modulation" of the incoming IR source spectrum by varying the optical path difference (OPD) created via the moving mirror displacement over a scan interval. An interferogram is produced from this modulation process—providing a composite interference amplitude values (y-axis) for each corresponding OPD position measurement value (x-axis) over a scan interval. Each composite amplitude value is created by an ensemble of varying degrees of *constructive* and *destructive* interference for all wavelengths comprising the spectral band at a given OPD instance.

To elucidate this optical process, the cases of single-wavelength, two-wavelength, and three-wavelength constructive and destructive interference described below. The broad-band case involving many wavelengths contained within a band is then discussed. The resultant interference signal is the interferogram.

Single Wavelength Case

If a single-wavelength light source (e.g., laser) enters the entrance aperture of a Michelson interferometer, the light will be split, travel to two mirrors, and reflect back to

the beamsplitter where they are recombined. Assume that the M1 and M2 mirrors are equally displaced optically from the beamsplitter. The optical path difference is therefore zero. In this case, the two infrared waves travel the same distances to and from the mirrors, and arrive back at the beamsplitter with the same phase. Because the two infrared waves are in phase, then they add together and double the amplitude of the recombined infrared waves. This in-phase additive condition is know as constructive interference and is illustrated in Figure 3.1-10.

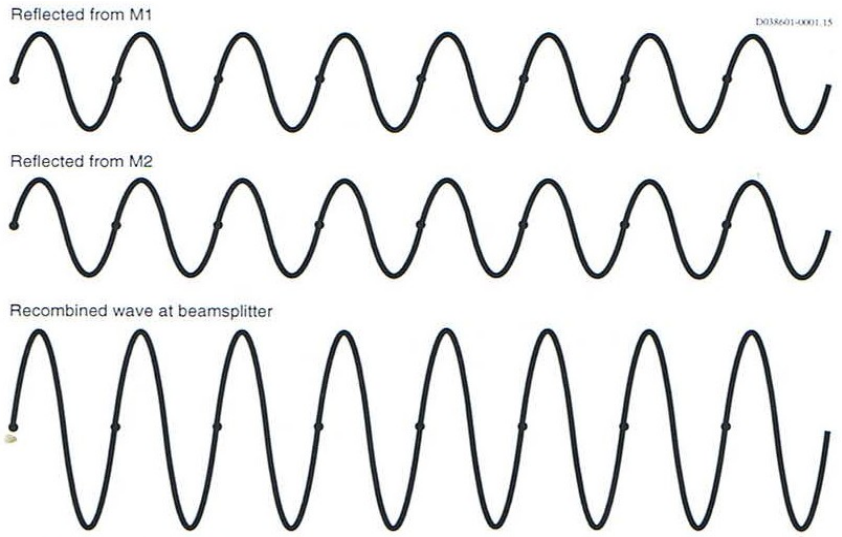

Figure 3.1-10. Single-Wavelength – Constructive Interference Example

Next we assume that the moving-mirror optical path is set at an optical path difference equal to ½ l (actual mirror physical displacement is ¼ l since light must make a round trip). In this case the two infrared waves travel to and from the respective mirrors and recombine back at the beamsplitter—except they are out of phase by 180 degrees (½ l). In this case, the waves subtract from each other and no signal emerges after recombination at the beamsplitter. This out-of-phase subtractive condition is known as destructive interference and is illustrated in Figure 3.1-11.

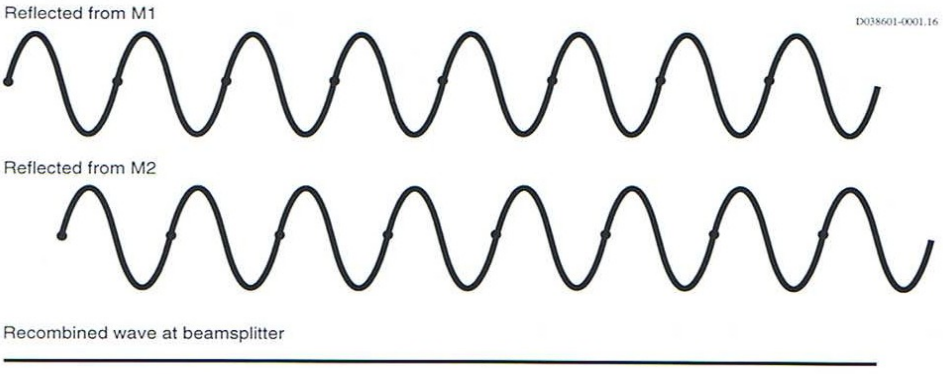

Figure 3.1-11 Single-Wavelength – Destructive Interference Example

Now if the moving mirror is free to continuously move along a linear path, then we would observe a sine-wave oscillation as the waves began at zero optical path difference (ZPD) and move through all intervening interference conditions between the totally constructive and destructive interference extremes. In the case of a single-wavelength, a sinusoidal-wave interferogram is produced with period equal to the wavelength of the light source. The single-wavelength interferogram is presented in Figure 3.1-12. While this single-wavelength example may be considered inconsequential for the broad-band IR channel operation, it is the basis of the HeNe channel (to be described later) which ultimately provides the sampling triggers for the IR channel digitization signal processing.

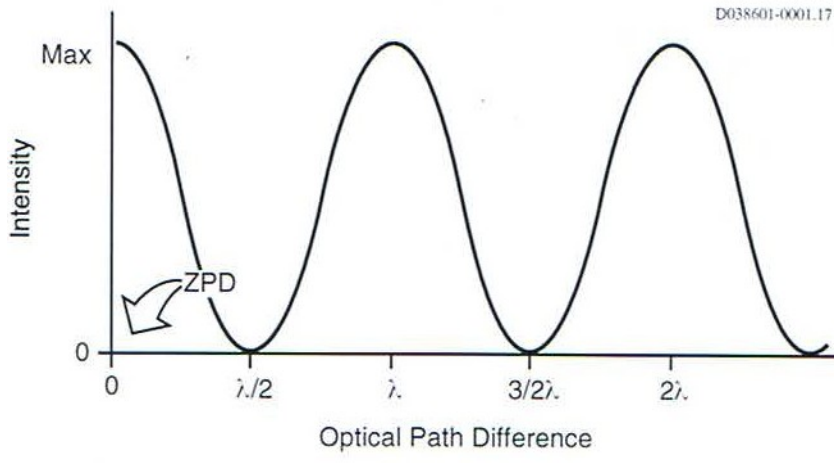

Figure 3.1-12 Output Response of a Moving Mirror and Alternating Constructive and Destructive Interference Conditions

Two-Wavelength Case

For this case, assume two different wavelength sources enter the interferometer, one with wavelength λ and one with wavelength 3λ. As the moving mirror travels from its starting position (i.e., ZPD) to its final scan limit, the λ and 3λ waves undergo constructive and destructive interference at two different optical path difference intervals. As a result, the combined interferogram will no longer appear sinusoidal. It will be the additive-and-subtractive result of the individual interferograms that would be produced by the two individual wavelengths. Figure 3.1-13 illustrates the two input wavelengths and the resulting interferogram for this two-wavelength case.

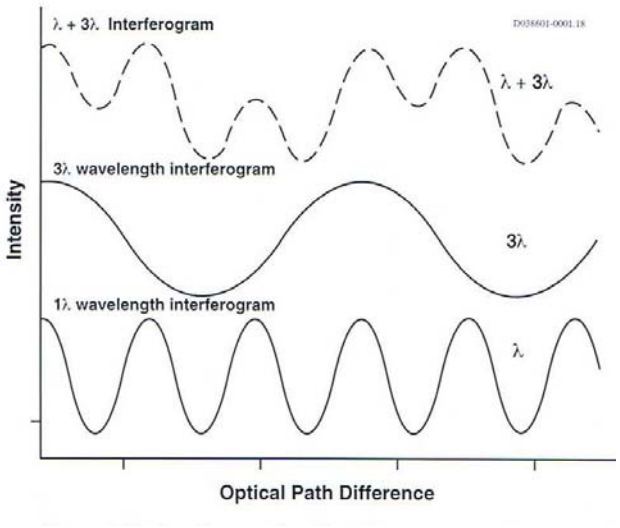

Figure 3.1-13. Interferogram for a Two-Wavelength Input Case

Three-Wavelength case

Figure 3.1-14 shows the single-wavelength interferograms for a three-wavelength (1l, 2l, 3l) input, and the resultant composite interferogram from summation of the three-wavelength input. As more wavelengths are introduced, the interferogram tends to become more complex ultimately leading to the characteristic shape presented in the Broad-Band input discussion to follow.

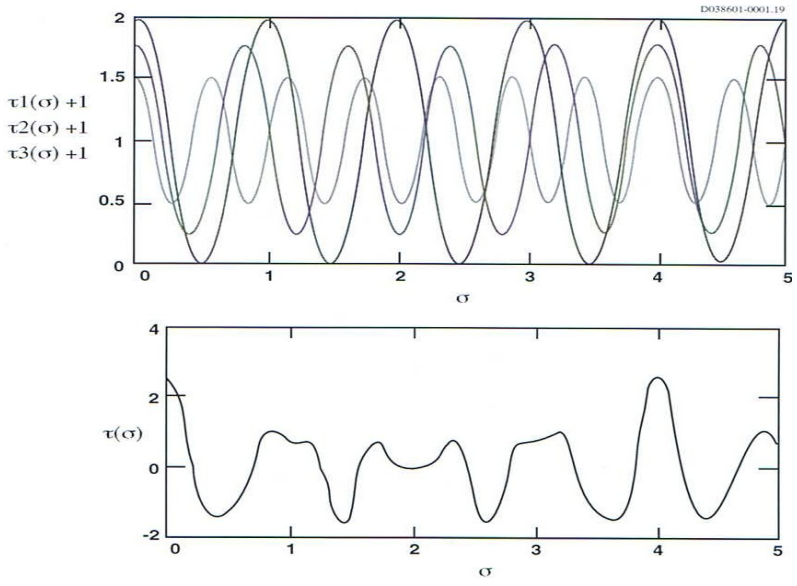

Figure 3.1-14 Three Single Interferograms (top) and the Composite Interferogram (bottom)

Broad-Band Discussion

When we replace these monochromatic light sources with a broad-band IR radiation source, then a continuum of IR wavelengths are introduced to the interferometer. In this case, the resulting interferogram at the output of the interferometer will be the summation of all the interferograms that are created for all the wavelengths within the input light source. The interferogram for broad-band IR light appears considerably more complex in structure than the monochromatic examples. Figure 3.1-15 presents an interferogram typical of broadband IR source input. The peak in the middle is known as the *centerburst*. The centerburst corresponds to the ZPD for all wavelengths comprising the band continuum. This characteristic response occurs because at the zero optical path difference, all wavelengths interfere constructively. However, as the mirror moves from the ZPD position, the destructive interference significantly influences the interferogram, and the response drops off rapidly with change for the ZPD position. The lower intensity regions of the interferogram are sometimes called the wings.

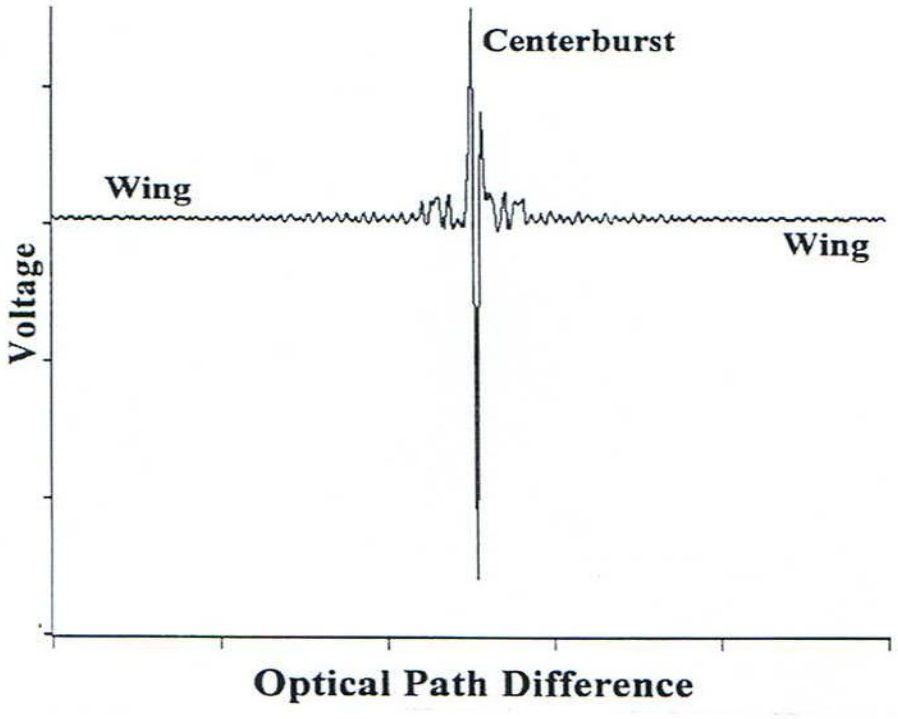

Figure 3.1-15 Interferogram Characteristic of a Broad-band IR Input Source

While the resulting interferogram appears quite unstructured, it effectively and efficiently encodes the intensity and wavelength information concurrently during a single interferometer scan motion. Therefore, the measurement occurs over the full scan interval, with all the spectral information about the source spectrum encoded in this measurement. It is apparent the interferogram provides no direct spectral data, but when processed via a Fourier Transform, it enables a recreation of the input spectral with a high degree of fidelity.

A key point regarding a FTIR spectrometer interferometric process is that all the infrared radiation passes through the interferometer and the test specimen and is received at the detector *simultaneously*. This is a major signal-to-noise advantage relative to dispersive-type spectrometers which subjects the test specimen to a narrow waveband over its scan cycle. This feature of the FTIR is referred to as the Jacquinot advantage.

We will now discuss the ASAP-specific FTIR interferometer operation referring to Figure 3.1-16 below. Beginning at the left-side aperture (Aperture 1), collimated IR light passes through the aperture and impinges on a 90-deg 1-inch-diameter parabolic mirror (4" focal length). The IR light converges to a point where a Jacquinot aperture wheel is placed. The purpose of the Jacquinot aperture is to create an optical stop at the focus between the source and the interferometer. This Jacquinot stop is used to limit the area of the light beam to the central light fringe required for higher spectral resolution (typically <1 cm^{-1}) measurements—while blocking the outer circular interference fringes (Hadinger fringes). In the ASAP FTIR design, there are actually 12 individually sized apertures on the aperture wheel to support higher resolution measurements. However, for the objective of the ASAP program for which a 4 cm^{-1} spectral resolution is used, the finer stop settings are not used.

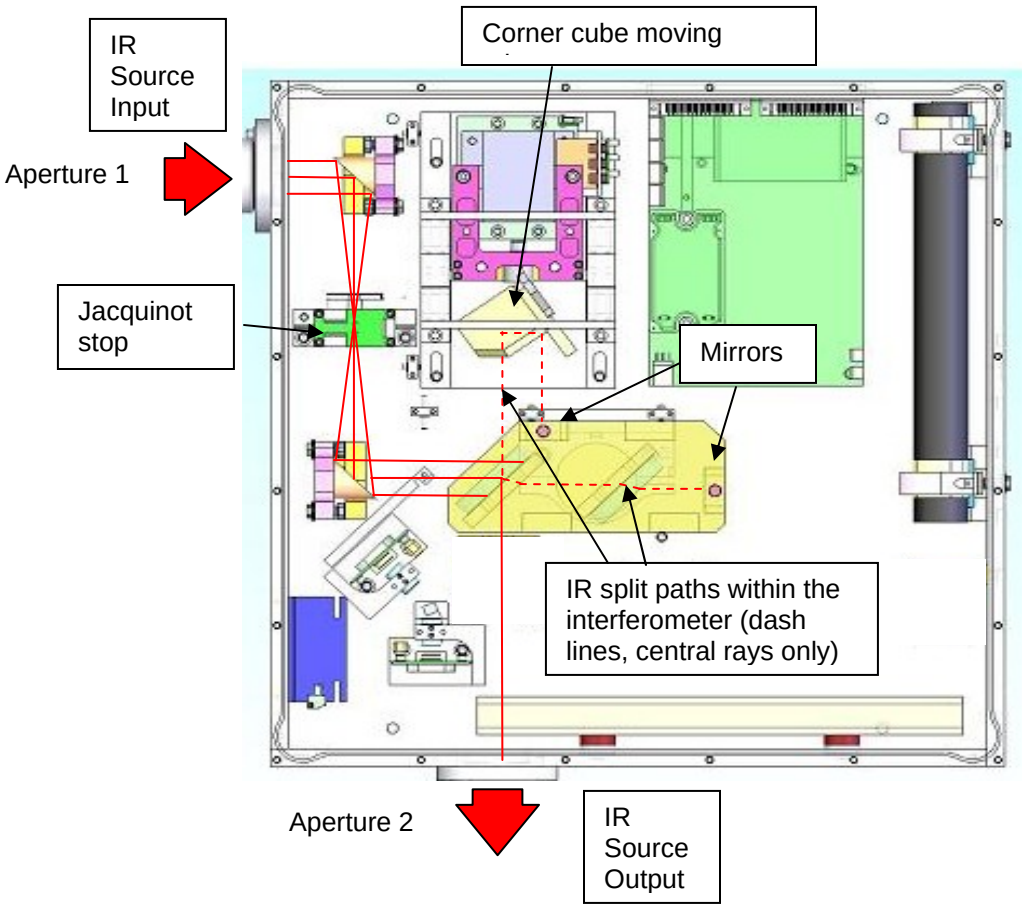

Figure 3.1-16 Optical Path for the IR Channel Within the FTIR Interferometer (Red Lines)

After the wheel aperture, the beam then diverges to impinge on another 90-deg 1-inch-diameter parabolic mirror (4" focal length) that is then directed toward the interferometer as a collimated IR light beam upon entering the interferometer.

The IR light enters the interferometer in which 50% of the radiation passes through the beamsplitter to the fixed mirror, and is reflected back toward the beamsplitter. The remaining 50% of the IR radiation is reflected at the beamsplitter surface toward the moving retro-reflector mirror and then to a fixed mirror on the side of the interferometer block. This fixed mirror is oriented at a 90-degree angle relative to the fixed mirror for the other optical path. Upon reflection from this mirror, the radiation is reflected back to the beamsplitter along the same path. The radiation from the fixed mirror path and the moving mirror path are recombined at the beamsplitter to create a composite interference amplitude value for a corresponding instantaneous OPD value (cm). The recombined radiation then passes from the interferometer as a single collimated infrared beam and exits Aperture 2 at the lower portion of Figure 3.1-16.

In the ASAP design, the output IR channel is directed to the asphalt surface, and the diffusely reflected signal is collected and directed toward an IR detector. The detector signal is acquired during the moving-mirror scan cycle and sampled at specific OPD intervals as described in the next section. This description for the IR channel path may be reversed. Aperture 2 may be the starting point, and the description of the optical processing may be reversed through the FTIR internal optics. In essence the FTIR is bi-directional in that the source and detection/accessory ends may be interchanged. This point will be expanded in a later section of this document addressing a HgCdTe detector cooled to 77 K for enhanced sensitivity.

HeNe Reference Channel

This section describes the HeNe laser reference channel. Basically this channel uses the "single wavelength" nature of the laser to provide a means to measure the position of the moving mirror at any instant in time. Moreover this signal establishes the critical sampling points for the IR channel signal digitization process. As discussed in the previous section above for the single-wavelength case, a single wavelength passing through an interferometer will produce an alternating sine wave when recombined at the beamsplitter—based on the varying optical path difference created by the scanning mirror. The sine wave will vary between extremes of constructive interference (peak signal) and destructive interference (zero signal) over an OPD difference of 2π phase difference. This sinuousoidal modulated interference pattern repeats for every 2π phase cycle (i.e., = λ wavelength) to produce a continuous sine wave over the scanning interval. The wavelength (λ) of the HeNe laser is 0.632816 μ (15802 cm^{-1}).

Since the primary purpose of the HeNe laser is precision measurement of the moving mirror position to trigger subsequent sampling of the IR channel interferogram, we will describe specifics of the moving mirror design. The design of the scanning mirror

and mechanism varies widely for all FTIR spectrometers designed over the past several decades. The various mirror designs range from flat mirrors to spherical mirrors to corner-cube mirrors—all with their respective advantages and disadvantages in performance. The mechanisms for translating the mirror inward and outward relative to the beamsplitter also vary widely—each with their unique performance capabilities and limitations as well.

The moving-mirror design for the ASAP FTIR is unique and differs significantly from previous FTIR designs. This patented design has an elasto-mechanical suspended-translating base to provide extremely smooth linear translating motion for the moving mirror support. It is commonly referred to as "porch-swing" translator due to its use of simple parts and flexure plates. A corner-cube mirror and supporting apparatus are attached to the mid-point of the porch-swing mechanism. The corner-cube mirror maintains optimum optical-alignment integrity to compensate for any off-axis mechanical misalignments in the optics elements. At the other end of the porch-swing mechanism, a voice-coil electro-mechanical drive (BEI LA14-24-000A-0040) provides oscillating translational force for the moving-mirror mechanism over the selected scanning intervals. This mirror-drive design has proven to maintain extreme measurement accuracy, precision, and repeatability over the scan period. The design is exceptionally resilient to vibration influences that are normal to the centerline of the linear motion of the mirror due to the rigidity in these axes. The software control loop is also designed with significant proportional-integral-derivative (PID) control-loop stiffness to minimize

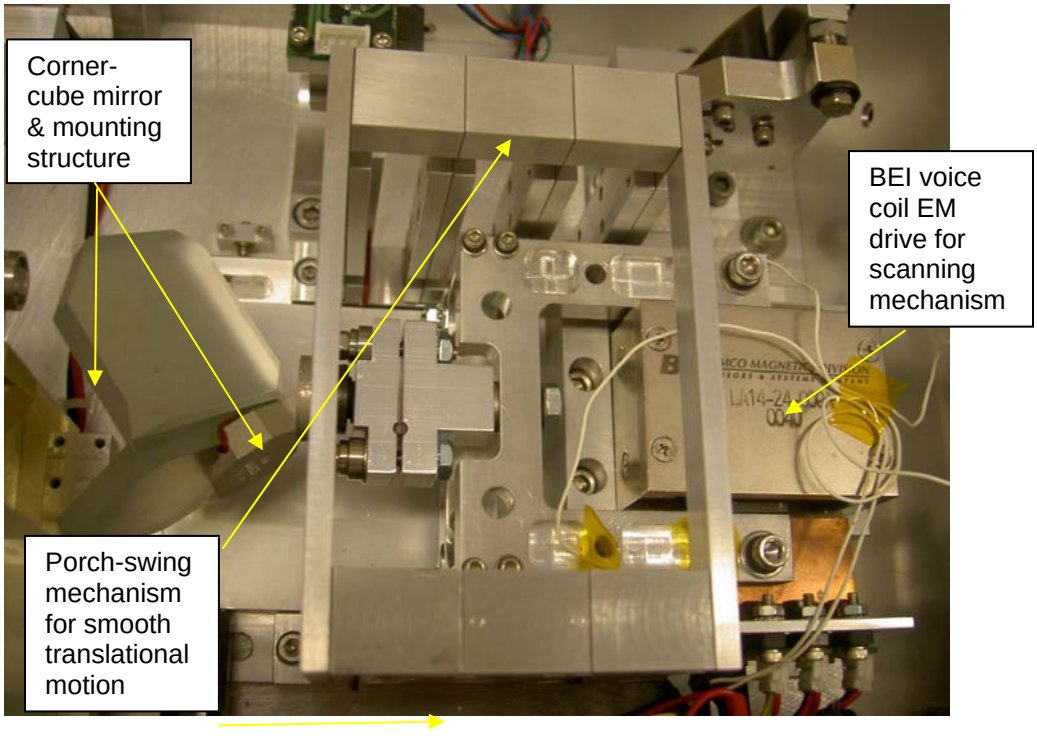

Figure 3.1-17 Scanning Mirror, Scan Mechanism, and Voice-Coil Drive

external acceleration influences along the axis of motion. Figure 3.1-17 presents a close-up photograph of the mirror, scan mechanism, and voice-coil electromagnetic drive.

As mentioned earlier, an interferogram is the basic measurement produced by the FTIR spectrometer. The interferogram measurement is a two-dimensional array OPD measurement points along the x-axis and corresponding composite interference amplitudes along the y-axis for each OPD measurement point. Given the mechanical nature of the moving mirror mechanism, the velocity cannot be maintained at a perfectly constant rate over the scan interval. In fact the mirror and associated inertia must be accelerated from a stop position to a selected mirror "constant" velocity over the scan interval, then decelerated to a stop. From this stop position, the mirror must be accelerated in the reverse direction up to the "constant" scan velocity, complete the reverse scan, and then decelerate to a stop prior to repeating the process. Using a time-based sampling technique for the interferogram would not be appropriate for producing true spectral data. Foremost is the fact that the IR channel amplitude output is directly related to the instantaneous moving mirror position *only*—regardless of any time-base measurement. In fact, the unit of measure along the x-axis are in terms of centimeters (cm) of optical path difference (OPD).

This is why the laser is used as a "ruler" for determining the position of the mirror, and why it is in a parallel optic path to the IR signal channel. The basic increment of measure is the 0.632816 m wavelength of the laser frequency. For some interferometers, this wavelength is the minimum unit of measure (resolution) for the OPD. For the ASAP FTIR spectrometer, the minimum incremental measure is ¼ of the HeNe laser wavelength (0.158204 m). This unique design of the ASAP FTIR accurately determines the "peaks" and the "valleys" and the two "zero crossings" for each HeNe interference wave cycle in the scan interval. This approach provides a higher degree of fidelity in accurately sampling the IR channel's interference signal. Furthermore, this approach is robust in that any potential mirror velocity deviations (instantaneous acceleration or jerk) inherent to the drive mechanism or from external acceleration forces are totally compensated by this HeNe sampling design. This approach may be thought of as a "spongy ruler" in this context since the "ruler" adjusts for any minute deviations from constant velocity while still providing extreme accuracy for the mirror instantaneous position. Also a time-based sampling technique would not compensate for minor mirror deviations from an ideal constant velocity.

Additional information regarding the algorithms to determine the peaks, valleys, and zero-crossings for the HeNe interference sine waves (a.k.a., fringe patterns) is discussed in the Software Detailed Design section to follow. A screen-save image of the HeNe interference wave, sampling points, and the interferogram is presented in Figure 3.1-18 below. It should be noted that this sampling approach includes a unique set of algorithms for precisely determining zero crossings and the peaks and valleys in the HeNe sinusoidal signal to enable sampling of the interferogram four times for every HeNe wavelength (0.158204 m). Many spectrometers only sample at a zero crossing, or in some cases, several zero-crossings. This algorithm design is unique to ASAP and will be discussed in more detail in the Software Design Section.

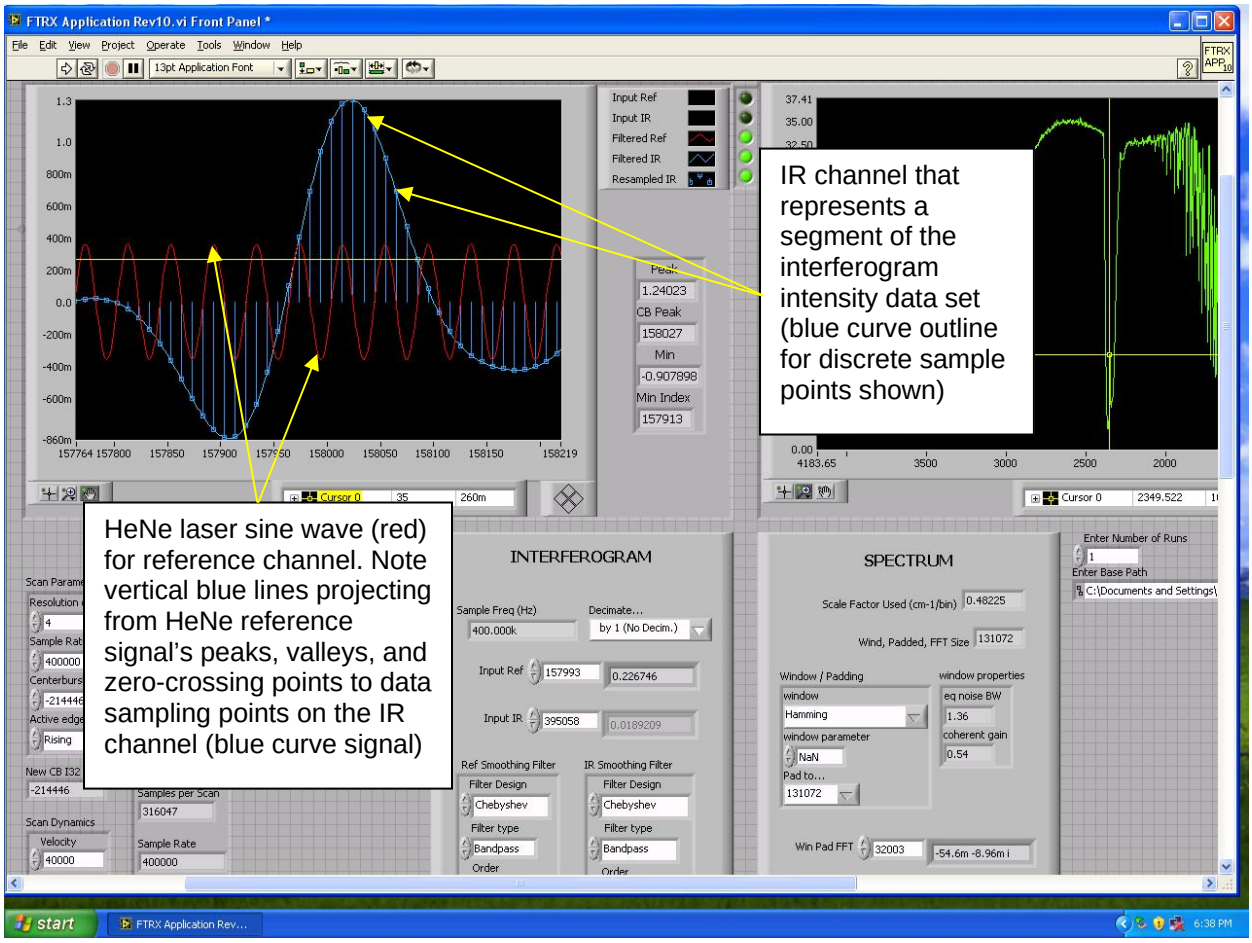

Figure 3.1-18. Screen-Save Image Showing the HeNe Laser Reference Signal (red) and the IR Channel Interferogram Signal (blue), and the Vertical Lines Representing the Sampling Points

Having discussed the role of the HeNe laser in the OPD measurement process, the following description of the HeNe optical path and detection process follows. The HeNe laser is mounted to the right-side wall of the FTIR housing as shown in Figure 3.1-19. Mechanical adjustments are provided on the mount to allow alignment of the laser beam. The output laser beam is directed toward a lateral transfer optic element mounted to the bottom-side wall of the FTIR. This element is essentially an elongated retro-reflector that re-directs the beam into the interferometer optical block as shown in the figure. This element leverages PLX's patented technology in optical mirror alignment.

The HeNe laser beam then enters the interferometer and is split at the beamsplitter in the same manner as was previously described for the IR signal channel. The laser beam is offset slightly to the top of—and parallel to—the IR channel to avoid any interference, and also allows the HeNe fringe detection to not interfere with the IR channel optical

beam. Along one path, the laser beam is reflected from the beam splitter to the fixed mirror and completes a round trip return back to the beamsplitter. The return laser interference amplitude is constant at the beamsplitter due to the fixed optical distance along this path.

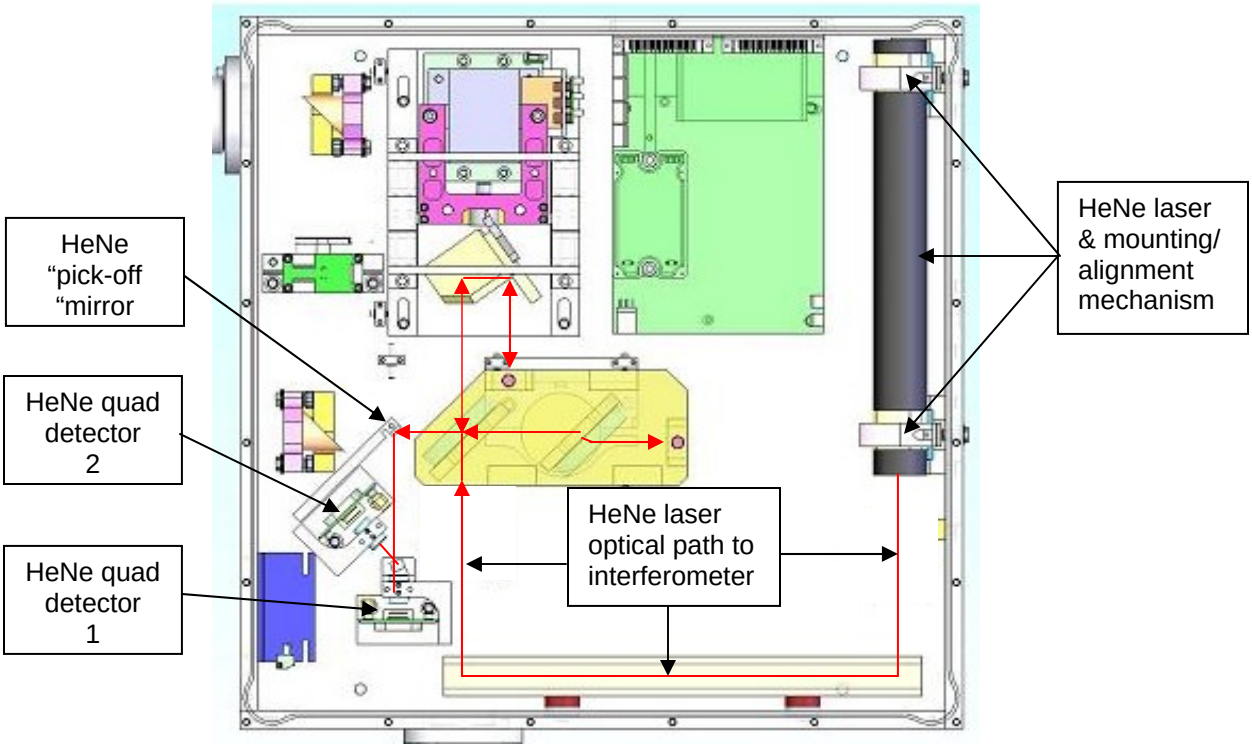

Figure 3.1-19 HeNe Laser Mounting and Adjustments to the FTIR Side-Wall Housing

Along the other path, the laser beam is transmitted through the beamsplitter and follows the round-trip path reflecting from the corner-cube mirror (two-reflections) and back toward a flat mirror on the side of the monolithic block, then backward along the same path to the beamsplitter—where it is recombined with the signal from the fixed optical path. When recombined, the signal appears as an alternating sinusoidal signal based on the scan movement of the mirror as previously described. The sinusoidal signal provides a direct observation and measurement of the instantaneous OPD position at any point in the scan interval. The recombined sinusoidal signal emerges and is directed toward a “pick-off” flat mirror on a mechanical arm. This mirror reflects the HeNe beam toward a small HeNe beamsplitter. In turn, the beamsplitter redirects the transmitted and reflected HeNe signals to the two HeNe detectors as shown in the figure.

The HeNe laser beam is polarized. While the beam is initially polarized, there is a polarization asymmetry created between the fixed and moveable arms of the Michelson interferometer. This makes the different optical paths distinguishable by polarization. As the beam travels through the moving mirror optical path, the polarization is changed relative to the polarization traveling through the fixed mirror path. A quarter-wave plate

optic and adjustment is provided in the moving mirror path for polarization phase adjustment. An additional quarter-wave plate optic is provided forward of one of the HeNe detectors. Also, forward of the two HeNe detectors are polarization optics for additional relative polarization adjustment for the two detector paths. The sum total of the polarization adjustments for the two HeNe detector paths is intended to induce a phase-quadrature relationship between the two paths in which the phase difference of the fringe pattern is 90 degrees. The two channels are analyzed separately via the two detectors, respectively, in a polarization-sensitive way. The polarization state analyzed in each channel is adjusted so that the fringe patterns generated during the scan are in phase quadrature relative to each other. Figure 3.1-20 presents the design of the HeNe quadrature detection design. Only one detector—and thus HeNe fringe signal—is actually needed for measuring the optical path difference. However, the direction of the scanning mirror would still be unknown. For this reason the second HeNe signal is offset in phase quadrature to detect the direction of the mirror scan. Basically the relative phase difference between the signals is directly related to the direction of travel of the moving mirror. When scanning in one direction, the quadrature phase difference leads the reference signal; conversely, when the scan is in the opposite direction, the quadrature phase lags the reference signal.

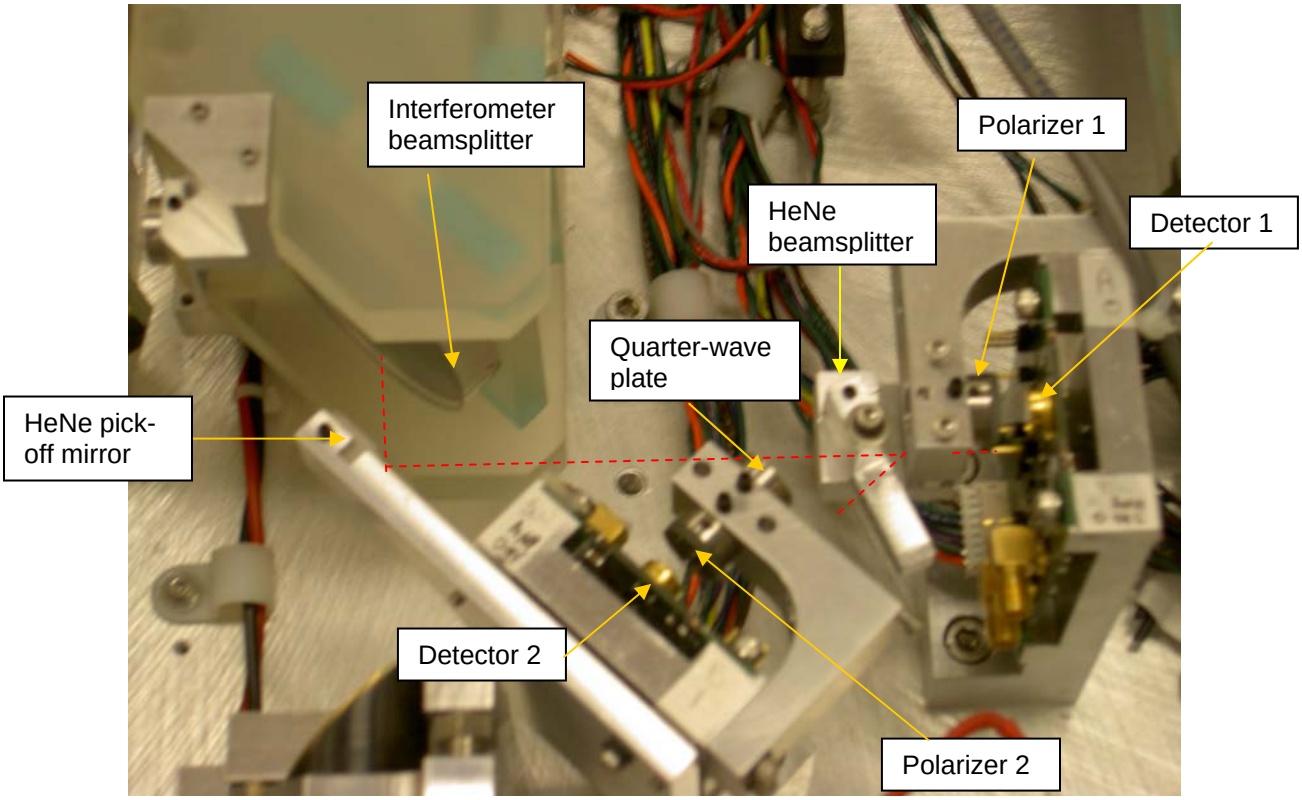

Figure 3.1-20 The HeNe Laser Optical Design for Establishing a Phase Quadrature Detection (HeNe laser beam path highlighted with red dashed line)

The HeNe detectors both receive a sinusoidal signal. After amplification, these signals are routed from the FTIR to the PC NI-PCI-6120 digital-to-analog converter (DAQ) board where they are received for subsequent processing. The sinusoidal signal is further processed as discussed earlier into 4 sampling points for each HeNe wavelength. This signal and associated sampling provides exact optical sampling intervals regardless of minor deviations in the scan mirror's scan velocities.

In addition to the sinusoidal signal processing, these signals are also converted to square waves via comparators that are also on the detector board. One signal is used for counting where the mirror is in a scan cycle, while the other is used to determine which scan direction the mirror is traveling by phase comparison with the primary HeNe square-wave signal. These square-wave signals are also routed from the FTIR to the PC DAQ board for subsequent processing. The HeNe laser fringe pattern is 15,802 wavenumbers (cm-1), meaning that 15,802 counts are detected in 1 cm of OPD travel. The system is accurate to ¼-wave of OPD at 0.632816㎛ and can scan at 250,000 waves of OPD at 632.816 nanometers per second.

Summarizing, the HeNe *sinusoidal* signal's peaks, valleys, and zero crossings are used as sampling points for the IR channel interferogram. The HeNe *square-wave* signal counts are used to determine counts, range, and direction of travel—basically the fundamental measurements used for position and control of the moving mirror.

There are five primary detector signals that are routed from the FTIR to the PC DAQ board—two HeNe sinusoidal reference signals, two HeNe square-wave reference signals, and the IR signal channel from the HgCdTe detector (described in the end-effector discussion to follow).

3.1.3 ASAP FTIR Spectrometer Optical Design – Exterior (Accessoriess)

IR Source Design

The IR source assembly is mounted on a supporting plate structure to the left side of the FTIR housing. A CAD drawing for this assembly is presented in Figure 3.1-21 below. The assembly is comprised of three components:

- Collimating optic
- IR Source
- IR Source Power Supplies

The collimating optic is a 1-inch diameter, 90-degree off-axis parabola mirror with a 4-inch focal length. The mirror is protected gold reflector. Its function is to collect the IR radiation from the IR source element (assumed as a point source) and transfer the IR radiation into the FTIR optics path in a collimated beam. This mirror is housed in an external aluminum housing with o-ring seals and cylindrical couplers for the optical path

to the FTIR, and to the IR source. A photograph of the collimating mirror assembly is presented in Figure 3.1-22 below.

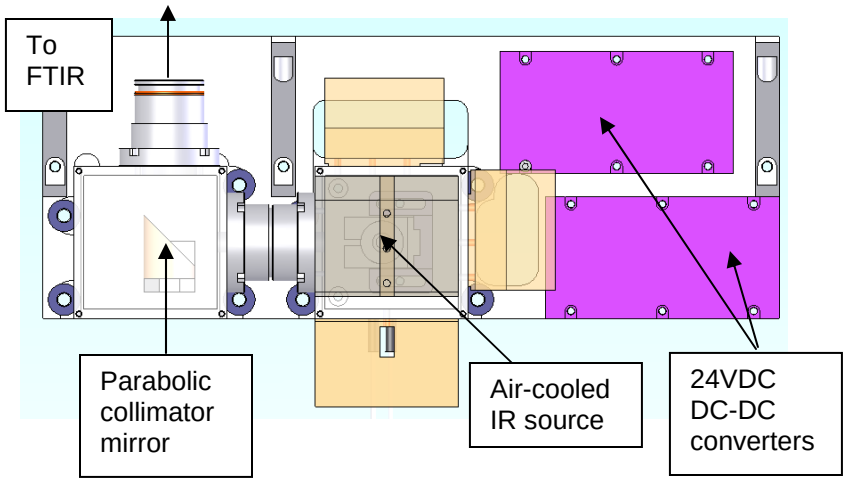

Figure 3.1-21 CAD Drawing (Top View) for External IR Source Assembly

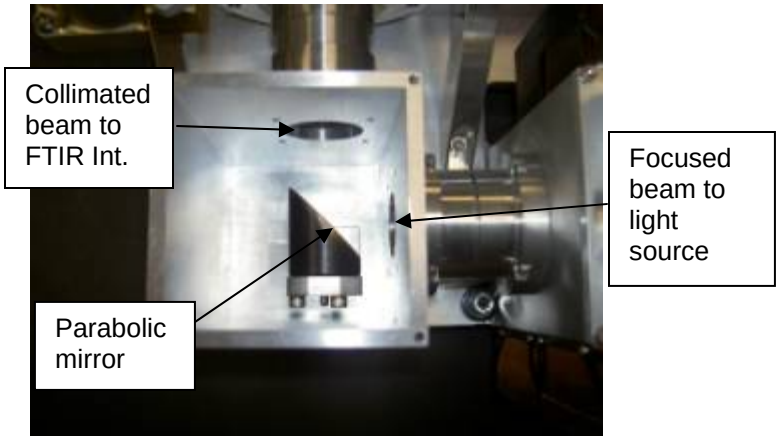

Figure 3.1-22 FTIR External Collimating Optics Assembly Photo (Lid Removed)

The IR source is a 150 W element with a source temperature of 1300K. It is a Surface Ignitor^{tm} MM100 SiC stub element with a ceramic body for holding at the lower end of the stub. This item is used in many applications including FTIR instruments. The IR element is secured as shown in Figure 3.1-23 and provides for adjustments up-down and fore-aft adjustments. The IR element is shown in the photograph as a glowing point, but is actually a stub approximately ½-inch tall. As mentioned, this IR element is considered a point source for the input optics. The source also requires a custom power source for operation.

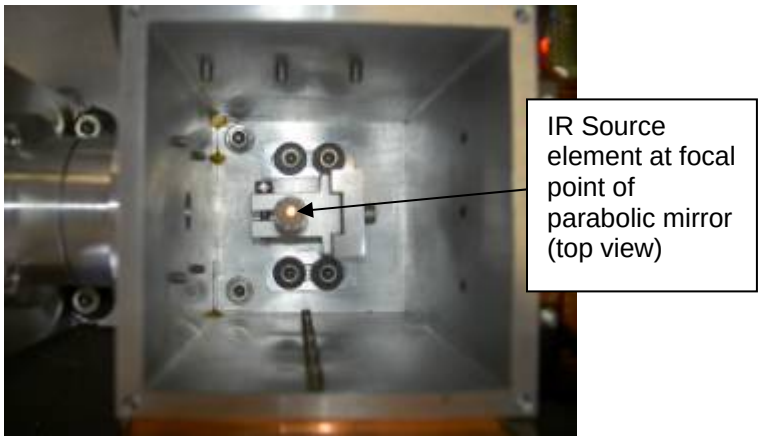

Figure 3.1-23 IR Source Housing and Active IR Element Photo (Lid Removed)

The power supply provides power for the IR source and has two 24 VDC 75W DC-DC converters that run on the main 12 VDC power bus. On the opposite side of the FTIR housing is the two medical-grade +12 VDC batteries that are used to provide basic +12VDC and –12VDC power for the FTIR operation. The application of medical-grade batteries is due to a risk mitigation design approach that minimizes the noise influences of the power source supplying the bias voltages for the HgCdTe detector (Figure 3.1-24).

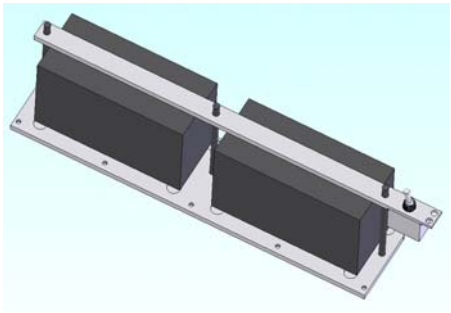

Figure 3.1-24 External Battery Pack for +12 VDC & -12 VDC Detector Bias Voltages and Other FTIR Power Needs

The general power source distribution for the FTIR in general is as follows:

- 12VDC input power: Either from a switching or linear power supply, or a series of sealed gel-cell batteries recharged by the van alternator.
- ±5V DC-DC converter from 12VDC to power transimpedance amplifiers of the HeNe detection system.
- High voltage DC-DC converter to power HeNe laser from 12VDC.
- +5VDC 1.5-amp DC-DC converter to power the detector thermoelectric cooler.
- +24VDC 5-amp DC-DC converter to power light source.
- ±12VDC independent rechargeable 7.2amp-hour battery pack to run IR detector amplifier.

FTIR Spectroscopy Measurements Technical Discussion

As a prologue to describing the DRIFTS design used for van testing, the various approaches to general FTIR spectrometer measurement techniques will be summarized. The objective of the ASAP program was to develop a means of measuring carbonyl content in surface asphalt roadway surfaces in the form of a carbonyl index, and to apply the statistically linear relationships between carbonyl and log G* to predict asphalt aging and "trigger" conditions for application of surface rejuvenators. A key design constraint is that the carbonyl measurements had to be *non-contact* in nature.

FTIR spectroscopy may be categorized according to the following techniques grouped as:

- Transmission techniques
- Reflectance techniques
- Photoacoustic spectroscopy techniques.

Within each of these measurement techniques are various methods of acquiring infrared spectral signatures as either *transmission* or *absorption* spectral data. These methods are listed below. Each of these methods may be implemented in a variety of design approaches with instrument attachments commonly referred to as *accessories* to the FTIR spectrometer instrument.

Transmission:

The test sample is placed in the optical path between the output of the FTIR and the detector. In this configuration, the "modulated" IR beam passes through the sample and the spectral absorbance (or conversely transmission) is measured.

Solids: Since the IR energy cannot pass through solids, the solids must be reduced to small particles that are suspended in an inert material such as potassium bromide (KBr). Using this approach the IR energy may interact with the particle's molecules, while the inert suspension material allows the IR energy to propagate through the sample volume to the detector side. In this case, considerable sample preparation is required for the sample vessel.

Liquids: A liquid sample may be filled in a sample vessel and the IR light propagates through the vessel to the detector.

Gases: A gas sample may be filled in a sample vessel and the IR light propagates through the vessel to the detector.

Reflectance:

DRIFTS: Diffuse Reflectance Infrared Fourier Transform Spectroscopy is a technique that uses the "modulated" IR energy from the spectrometer to illuminate a solid sample and collect the diffusely reflected IR energy from the sample and focus this energy onto the detector. This is the most challenging of all FTIR measurement techniques. There are two techniques used in DRIFTS—one involving sample preparation and one not requiring sample preparation. The former technique is used largely in pharmaceutical testing in which the drug is ground up and suspended in a sample tray. The sample is illuminated with the "modulated" IR energy and the energy is collected and focused onto the detector. In so doing, the incident IR energy interacts with the top few millimeters of the sample, and some degree of absorption takes place before the energy reemerges from and is reflected and scattered in the general direction of the detector. This phenomena is depicted in Figure 3.1-25 below. The challenge of collecting a fraction of the scattered IR energy is evident in this diagram. However, there is sufficient interaction for absorption to occur and yield a spectral signature at the detector.

In the case where sample preparation is not possible, the same mechanism is used wherein the interaction of the IR energy with the sample's surface molecules occurs even with the depth of penetration restrained to the top several microns of the material. One key design necessity for DRIFTS is the use of large illumination—and even more so the collection optics for gathering all the scattered energy and focusing it toward the detector.

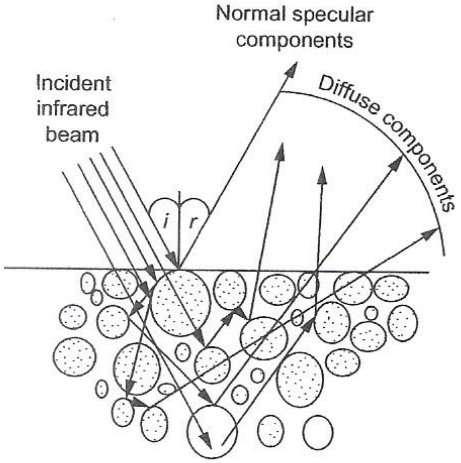

Figure 3.1-25 Graphical Illustration of the Interaction of Incident IR Energy with the Sample Molecules and Reemergence as Scattered IR Energy to the Collection Optic

Attenuated Total Reflectance: ATR is a direct sample contact technique for measuring the spectra of solids, semisolids, liquids, and thin films using an FTIR spectrometer. The key component of the ATR techniques is an IR transparent crystalline material with a high refractive index (e.g., diamond, zinc selenide, germanium). The

crystal shape is cut to mimic a waveguide cavity; however, the ends of the rectangular solid are beveled. The IR source enters one end of the crystal, and the bevel surface refracts the beam toward to top of the crystal surface where it is reflected toward the bottom of the crystal. At this point the IR energy extends several microns beyond the bottom surface and interacts with the sample below. The reflected wave is then reflected to the top of the crystal, then toward the other bevel end of the crystal, and then to the detector. Under the correct refractive index and incident angle, the radiation experiences *total internal reflectance* phenomena. While the IR energy is inside the crystal, a standing wave is created known as an *evanescent wave*. The key property of this wave is the radiation extends just beyond the surface of the crystal surface thus allowing interaction with the sample surface it is in contact with. The IR energy interaction with the sample resulting in an IR absorption that will be measured by the detector. The term *attenuated total reflectance* is related to evanescent wave attenuation at specific absorption regions. *Firm contact between the crystal and the sample surface below is critical to proper ATR measurements.* Also there are various means to influence the depth profiling using different crystal materials and other design parameters. Typically ATR accessories interact with the top 0.1 – 5 m of surface depth penetration to collect spectral data.

Specular: In this case, the incident IR energy is reflected from a mirrored surface. A sample may be placed between the incident IR energy and the detector, and a sample material applied to surface of the mirror. The IR energy passes through the sample material and is reflected to the detector.

Photoacoustic Spectroscopy (PAS)

PAS: This FTIR accessory technique detects IR absorption by an acoustical transducer process. As a sample absorbs IR energy in a contained vessel, it heats up. As the sample is irradiated at a specific FTIR OPD instance, the heat is transferred from higher temperatures to lower temperatures, meaning that the heat creates a thermal wave that moves toward the surface. Once the wave arrives at the surface, the gas above the sample is heated and then expands. Usually helium is used for the gas although air may be substituted. The gas expansion causes a pressure wave to propagate through the gas volume. At the top of the closed sample vessel is a highly sensitive microphone that produces a signal from the time-varying pressure waves that are directly related to the absorption at a given FTIR OPD instance. In fact, a plot of the microphone-signal-variation output vs the OPD position results in an interferogram. Various approaches for depth-profiling may be used. An absorption spectrum may be computed via a Fourier Transform similar to other FTIR processing approaches. The PAS does require a sample preparation process to be placed in the acoustic containment vessel, and therefore implicitly requires contact with the sample material.

WRI's laboratory testing has been performed using a Perkin-Elmer Spectrum One laboratory FTIR instrument using a transmission-mode accessory and a PAS accessory. In both cases, the asphalt samples required appropriate preparation prior to collecting spectral measurement.

Why DRIFTS?

From the foregoing discussions, we can understand that the various approaches to performing laboratory FTIR spectrometer measurements require that the sample must be prepared in some manner requiring manipulation of the sample material (e.g., grinding and mixing), or that contact with the sample material must be made, e.g., ATR. In any case these measurement techniques require contact with the sample materials. The ASAP requires that the field-capable FTIR must be non-contact or remote sensing in operation. Although DRIFTS may apply to laboratory testing for pharmaceutical and chemical analyses, it may also apply to FTIR spectrometer configurations that rely on diffuse reflectance signatures collected from a surface sample without any sample preparation.

Since the sample material—asphalt surfaces—cannot be contacted, then a means to collect the signature required illumination of the sample surface with the IR energy modulated via the spectrometer, and collection of the diffusely reflected energy by a collection mirror and focusing on a detector element. In this case, the incident IR energy interacts with the top few microns of the sample as pictured in Figure 3.1-25 above. For conducting close-in measurements from the van platform, non-contact diffuse reflectance techniques were the only solutions. DRIFTS in the context of the ASAP project therefore relates to non-contact diffuse reflectance signature collection.

Early in the program, a variety of design approaches were investigated to satisfy this requirement. From these investigations, the design approach as detailed in the following section was pursued. To this end, a means to deliver the incident IR modulated energy to the sample via an optical arm configuration, and then focus the incident energy on the sample surface, and then collect and focus the diffusely reflected energy back to a detector surface was accomplished. Basically two optical arms and an end-effector (term derived from robotics) formed the baseline design for performing the DRIFTS function.

For longer range measurements, an alternative configuration has been developed to apply a highly sensitive HgCdTe cooled to 77K to observe the sample in a different sense. In this case, the sun becomes the IR energy source, and the FTIR receives and processes the sample signature response in a passive manner. The intervening atmosphere must also be considered in the long-range measurement scenarios and attendant atmospheric perturbations attributed primarily to H_2O and CO_2 absorption. More design details regarding this technical approach will be presented a later section following the DRIFTS discussions. Figure 3.1-26 presents a notional depiction for optional IR sources (high-temperature IR element, or the sun) that may be used for illumination of the asphalt surface, and subsequent collection fo the diffusely scattered energy to an IR detector.

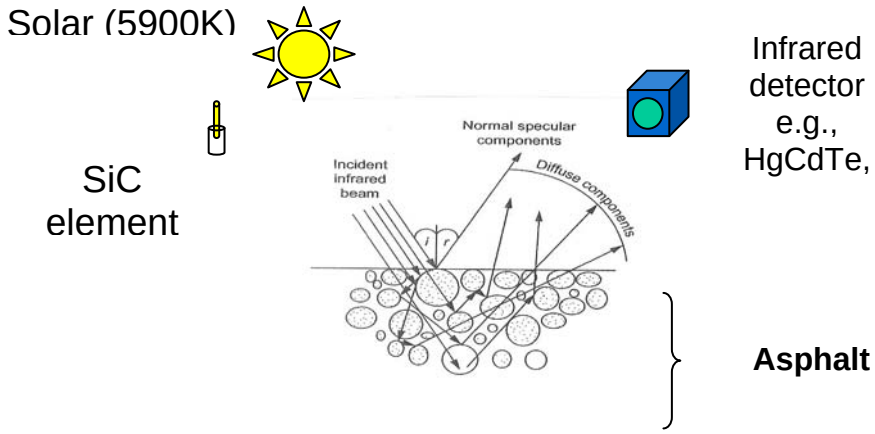

Figure 3.1-26 Two System-Level Approaches to Providing IR Illumination to the Asphalt Sample Surface – An Internal FTIR IR Source Element or Solar Illumination for Very Sensitive Detector Applications

DRIFTS Optical Arms and End Effector Design

Figure 3.1-27 shows a CAD design for the ASAP FTIR optical arms and end-effector that are used for the DRIFTS accessory unit. One key aspect of the design is the rotary gas bearing joints that allow rotary movement of the optical arms and end-effector as a single integrated mechanism, while maintaining hermetic sealing of the internal hollow optical path to support N_2 purging of the optical system. Long-term plans are to automate the articulation process to move the end-effector through the van floor toward the asphalt below. Figure 3.1-28 presents a CAD drawing for the gas bearings (RMDB-2) that were specifically designed and fabricated for the ASAP program.

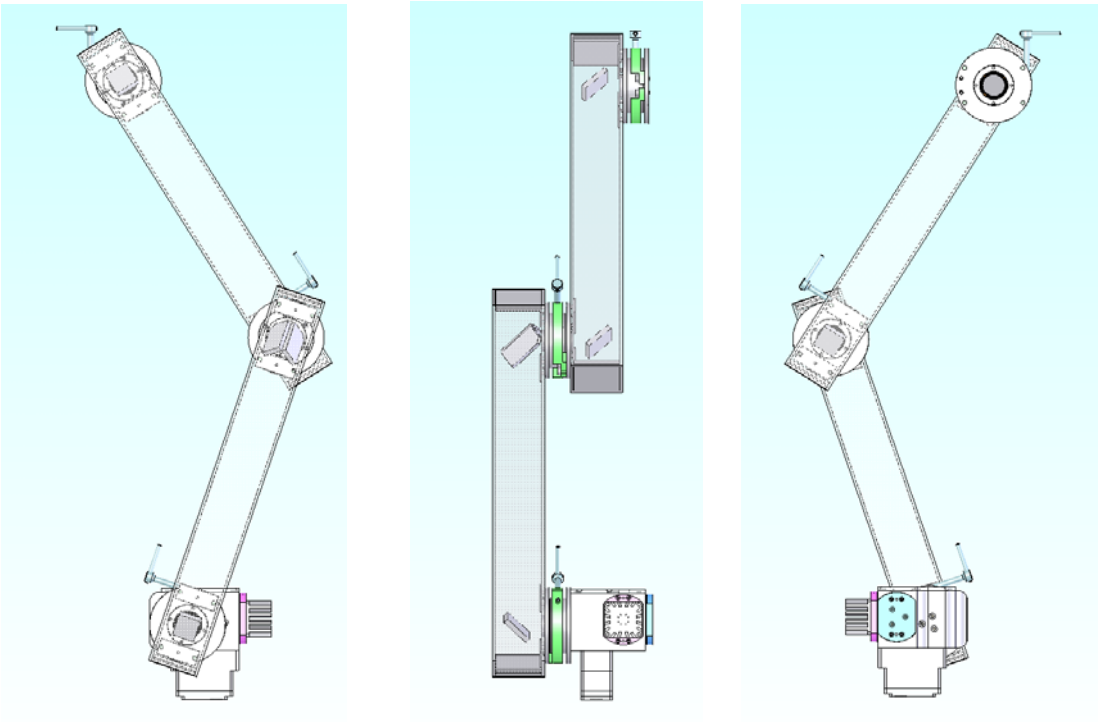

Figure 3.1-27 CAD design for the Optical Arms and End Effector Assembly

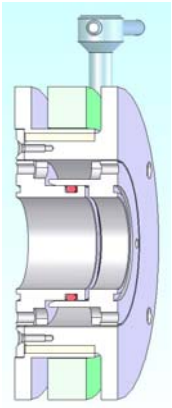

Figure 3.1-28 CAD Design (cross section) for the Gas Bearing Assembly to Couple the LHTP, LHTR, and End-Effector Assemblies

Referring to Aperture 2 in Figure 3.1-29, the gas bearing assembly couples the ASAP FTIR housing to the Lateral Hollow Transfer Periscope (LHTP). A second gas bearing couples the LHTP to a Lateral Hollow Transfer Retro-reflector (LHTR) to transfer the collimated IR light from the FTIR unit output to the end-effector optics input. The LHTR terminates at another gas bearing that couples the optical arm assembly to the

end-effector assembly. The purpose of the LHTP/LHTR optical assembly is to transfer the IR light to the end-effector with perfect fidelity in collimation for any selected rotation angular configuration from the entrance to the exit aperture of this integrated optical-arm assembly. This optical assembly allows for lowering of the end-effector through the floor of the van toward the asphalt surface below, while maintaining perfect optical fidelity up to the end-effector unit. Each gas bearing coupler has tightening mechanisms to lock the optical arms in any angular orientation for data collection operations.

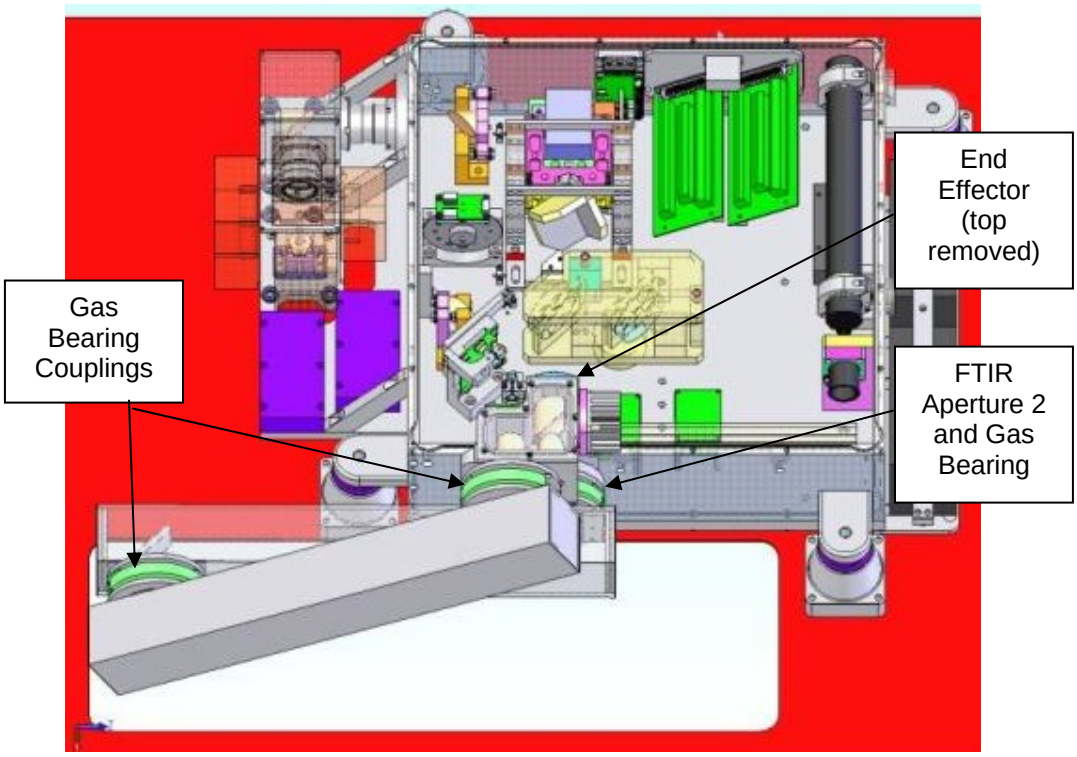

Figure 3.1-29 ASAP FTIR 3-D CAD Showing the Attachment to the FTIR Housing at Aperture 2, the Gas Bearings, Optical Arms, and End Effector

The end-effector has been designed to provide non-contact sensing of the asphalt surface to demonstrate the carbonyl signature phenomenology. Two functions are performed by the end-effector assembly. The first function is to *illuminate* the asphalt with the FTIR "modulated" IR energy during the FTIR's moving mirror scan cycle. The collimated IR light transferred via the LHTP/LHTR to the end-effector enters as a collimated beam. The collimated beam is then focused to the asphalt surface via a 101.6mm, 25.4mm clear aperture 90° off-axis parabola mirror to illuminate the asphalt surface. This beam is oriented 22.5° from normal to the asphalt surface.

The second function is to collect the diffuse reflectance IR energy and focus it on the detector. A second 101.6mm, 25.4 mm clear aperture 90° off-axis parabola mirror is

used to collect the scattered IR light (oriented normal to the asphalt surface), and the collected light is transferred as a collimated beam to a third 20.32 mm 1.5" clear aperture 90° off-axis parabola mirror to focus the infrared signal onto the detector active area.

The detector is a thermoelectric-cooled HgCdTe broadband IR detector (Teledyne Judson J15TE4:10-3GN-S01M). The photoconductive HgCdTe detector is sensitive within the IR spectrum from 2 to 12 m. The detector is mounted in a 66GE package and includes the detector, thermoelectric (TE) cooler, and thermistor for temperature feedback and control. The TE cooler refrigerates the HgCdTe detector to approximately 200 Kelvin to reduce the contributions of thermal noise thus improving the signal detection performance.

The detector receives the scattered IR energy from the detector-focusing mirror and converts the energy into an electrical signal. The detector is ac-coupled requiring a change in the incoming IR energy to produce an output. The interferogram is inherently an ac-coupled signal as the signal is continuously changing over a mirror scan cycle. Also the detector has a signal detection and amplification electronic board on the backside of the detector package, and is mounted within a custom-fabricated detector mounting with a heat sink on the reverse side. The end-effector 3-D CAD design is presented in Figure 3.1-30 below showing these various mirror elements and the detector housing. One of the key design objectives for the end-effector is to be compact so that it could be manipulated through the floor of the van in conjunction with the LHTP/LHTR optical arms. Additional information regarding this van design requirement is presented in Section 3.2 addressing the van integration design. Photographs of the end-effector internal optics are presented in Figure 3.1-31 showing the various optical components and apertures.

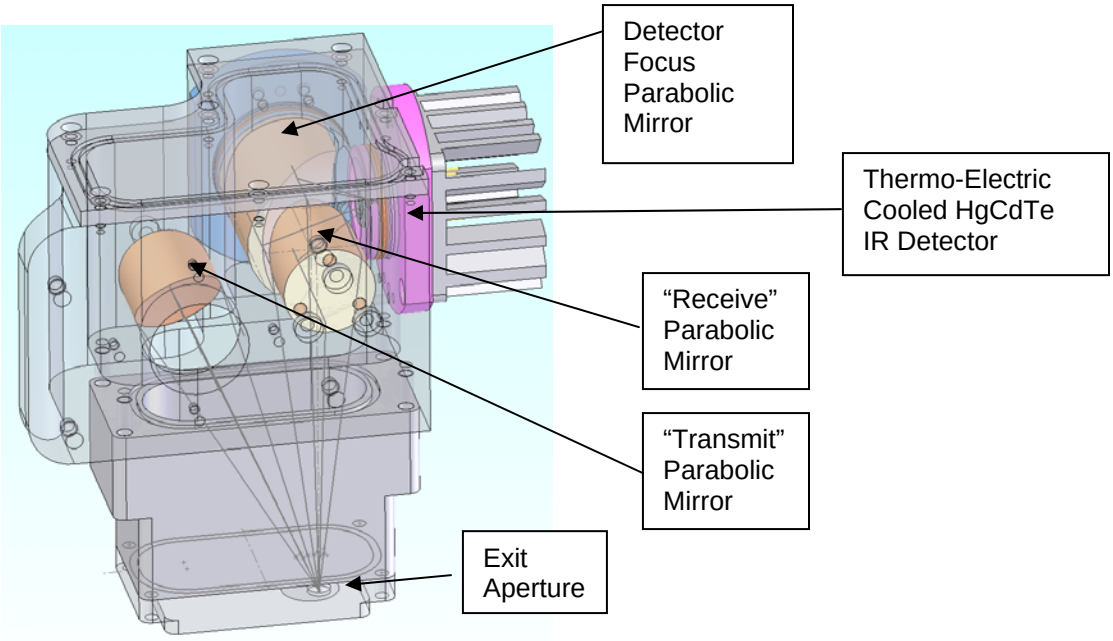

Figure 3.1-30 Original End Effector 3-D CAD Drawing with Key Components Indicated

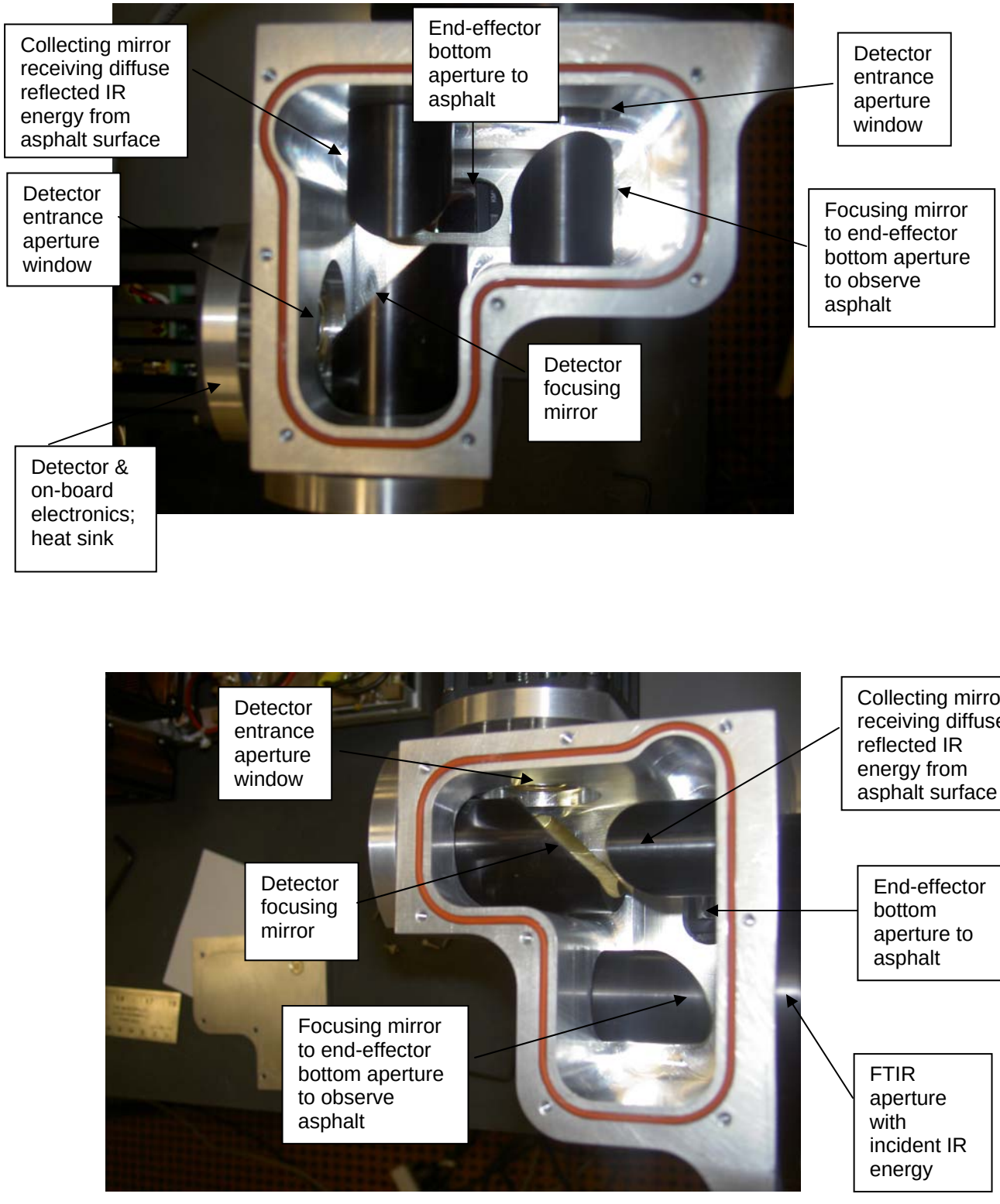

Figure 3.1-31 Photographs of Compact End-Effector Design (Top Cover Removed)

Initial Operational Testing

Many engineering developmental test events were performed during all phases of the FTIR development process. Examples included the stand-alone IR source tests, the voice coil actuation of the corner cube mirror, HeNe laser quad detector alignment and testing, stand-alone HgCdTe detector testing, etc. Also key milestones testing such as the white-light centerburst test that demonstrated and proved the core functionality of the interferogram optical process were conducted as the overall system was designed and developed. Other tests were conducted to prove significant software program capabilities and to improve performance wherever possible. As an example, PLX developed specialized techniques for processing the HeNe interferogram to precisely determine the sampling triggers (zero-crossing, peaks, valleys of sinusoidal signal) for sampling and digitization of the IR channel interferogram. These test continued at PLX development laboratory until delivery in December 2008.

Upon delivery of the FTIR, we continued to perform testing the ASAP FTIR in the Innova Engineering laboratory. Repeated testing has demonstrated that the FTIR operation was very stable and consistently produced high-resolution spectral data over the IR spectral range of the FTIR detector (2-12 micron). Test efforts to ensure the consistent capability of the FTIR were performed in the specular mode with the mirror positioned near the end effector aperture where the asphalt surface would normally be located (see Figure 3.1-32). All spectral signature reference phenomena were repeated during laboratory tests, e.g., CO_2 asymmetric stretch at 2349 cm^{-1} and other H_2O and CO_2 vibrational-mode absorption phenomenology.

Rigorous laboratory testing of the ASAP FTIR validated the fundamental technical capability of the FTIR instrument to produce stable interferograms, provide necessary processing and filtering of the interferograms, and perform Fourier Transforms of the interferogram to produce the high-resolution IR spectral data consistent with other FTIR spectrometers in general. The software remained very stable and consistently demonstrated the required operational performance during these tests. The optical arms that lowers the end-effector to near the asphalt surface has performed very well in maintaining collimation of the IR light as well as the optical alignment of the optical path centerline. The arms were tested in numerous angular positions and exhibited no optical variations in the amplitude across the aperture space.

As a FTIR transmission-mode test, a plastic film (LDPE) was inserted in the sample space (between mirror and detector) to observe the CH_2 and CH_3 bending absorption bands. The expected spectral response for the plastic material as well as standard H_2O and CO_2 absorption signatures validated that the FTIR was properly working. The optical arms and end-effector also demonstrated very consistent optical alignment and stability performance when operated in the specular mode. Optical alignment has not changed and the end-effector assembly has continued to demonstrate consistent performance.

While the FTIR works well in the specular mode—and the end-effector may also be used as a transmission-mode FTIR accessory—further testing to demonstrate the

diffuse reflectance mode for "near-field" FTIR testing in the van continues to prove problematic. Once the basic FTIR operations were demonstrated for the specular mode, the team proceeded to testing the end-effector in the diffuse reflectance mode. In this mode, an asphalt binder sample was applied to a microscope slide and the testing was resumed as before. The slide had a layer of shiny asphalt binder, and a binder that was made more diffuse by lightly applying quartz sand to the surface. Prior to this test, the FTIR was run in the specular mode to verify normal operation to produce an infrared spectrum. Upon running the FTIR in the diffuse reflectance mode with the asphalt slide samples, problems occurred in detecting an interferogram signal. We noted that diffuse reflectance FTIR spectroscopy (a.k.a., DRIFTS) normally has about a factor of 10 less signal-to-noise ratio than typical transmission mode accessories. However, multi-scan averaging is usually employed to increase the signal-to-noise ratio to comparable levels in the transmission mode. With the team observing, the tests were re-run with various tweaking of the optics and asphalt sample orientations, but the signal could not be detected. It was noted that during a PLX test meeting that a reduced interferogram signal was observed using a similar setup for asphalt sample in diffuse reflectance. Efforts continued to detect a signal, but finally the team realized that diffuse reflectance as it was currently configured had some design issues. These observed limitations appear to be related to a low signal-to-noise ratio when operated in the diffuse reflectance mode versus the specular mode with a mirror.

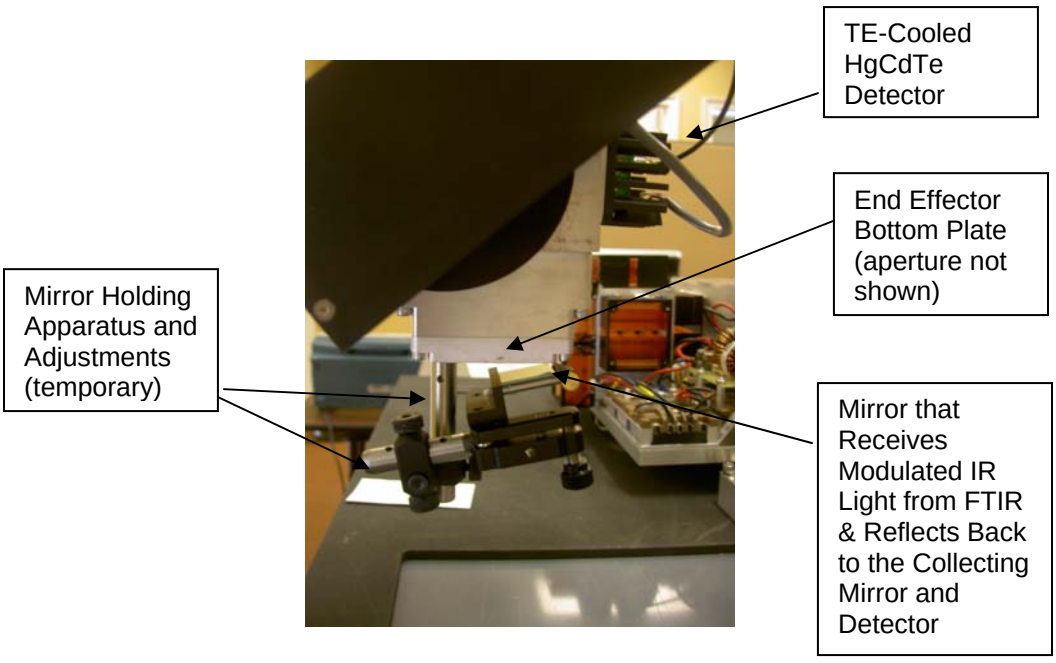

Figure 3.1-32 ASAP FTIR End-Effector With Mirror Inserted for Specular Mode Tests

Since the basic FTIR functionality and operation meets the required technical specifications—and the van integration is complete and ready for road testing—the detection of the asphalt spectrum via diffuse reflectance has been the main priority of the ASAP and best efforts to detect asphalt signatures using diffuse reflectance. Diffuse reflectance phenomenology occurs during interaction with the surface-level molecules to 5-10 micron of surface penetration—and is indicative of our objective for quantifying C=O content in asphalt surfaces.

At this stage, efforts were primarily focused on techniques to improve the overall signal-to-noise ratio performance of the ASAP FTIR. The diffuse reflectance mode is most challenging FTIR accessory operation mode relative to other types of accessories (e.g., transmission solution, ATR, PAS, etc.). Basically, the engineering options for signal-to-noise improvements that were available included focusing on the high-level design areas of the FTIR, namely:

- IR Source
- Intervening Optics
- IR Detector

For the IR source options, options included increasing the IR element temperature and therefore the energy within the IR band, or enhance the existing IR source throughput by adding reflective optics to focus back-side IR source energy forward to the FTIR entrance along with the forward IR source energy.

For the intervening optics, the constraints were that the 1-inch diameter aperture and internal parabola mirrors remain unchanged, and that the interferometer optics design remains unchanged. Furthermore, there was little to benefit from attempting to alter the internal FTIR components. The most promising design options were to increase the optics size relating to focusing the IR energy incident upon the asphalt surface, and moreover the optics associated with collecting the diffusely reflected IR energy and focusing the energy onto the detector active surface area.

For the detector, the primary option was to improve the sensitivity of the IR detector component. The only design option was to advance to the next higher level beyond the TE-cooled HgCdTe detector sensitivity to a HgCdTe detector that was cooled to the temperature (77K) of liquid nitrogen (LN_2). Since use of LN_2 outside of a controlled laboratory environment is not practical, the detector required to be cooled by a cryogenic engine (refrigerator). This option provides a quantum step in sensitivity by potentially 400x over the TE-cooled detector and offers the highest probability in solving the diffuse reflectance issue.

One additional option included adding a scan-averaging software function that basically improves the signal-to-noise by a factor of the square root of the number of scans averaged.

IR Source Design Option

An engineering research and design analysis was conducted to investigate the feasibility of substituting a high-temperature black body source for the SiC IR element currently in the FTIR. After substantial research, none of the black bodies were identified that were practical for fitment in place of the current IR source. Also the temperature increases were considered to not offer substantial solutions to the diffuse reflectance problem. A second approach involved research and experimentation with a back-side spherical mirror reflector to direct back-side IR energy to near the focal point of the collimating FTIR input mirror. In the original design this energy was lost. Through the use of a back-side mirror in addition to the energy directed toward the FTIR, the input signal should be increased. This option was partially successful in that a back-side mirror design increased the energy input into the FTIR by approximately 30%. The back-side mirror design has been implemented in the FTIR thus providing some improvement in overall signal-to-noise ratio. Additional information regarding the design, tests, and implementation of this approach was presented in the quarterly report for the seventh quarter.

Intervening Optics Design Options

The next set of signal-to-noise improvements are involved in a common set of design changes alternatives and experiments.

3) Increase illumination mirror size
4) Increase collecting mirror size
5) Optimize both mirror's optical path angles relative to the asphalt surface
6) Increase detector-focusing mirror size

A key parameter in the original end-effector design was driven by the need to move the optical arms and end-effector through the opening in the floor of the van downward towards to pavement surface, but not contacting the surface. This design parameter required that the end-effector be a small compact assembly to pass through the floor-opening dimensions. PLX designed and built an end-effector that was compact to include 1-inch diameter mirror optics primarily oriented in relatively steep angles (22.5 deg relative to illuminate and receive mirrors) as depicted in Figure 3.1-33. Additionally the HgCdTe detector had to be relatively small to allow the end-effector assembly to be compact. This drove the design to a thermo-electric (TE) cooled detector unit. While this detector selection was small, the TE-cooled detectors—while being true quantum detectors—are cooled to –60 deg C (4-stage TE). The degree of detector cooling has a direct relationship to the sensitivity performance—or detectivity (D*)—of the detector. For many applications, TE-cooled HgCdTe detector assemblies are adequate. However, when pressed for optimum detector performance, many remote-sensing applications use HgCdTe detectors that are cooled to 77 Kelvin (K) (~ -200 deg C), which is the temperature representing nitrogen's liquid state. More information regarding the detector is presented in a subsequent paragraph addressing Task 7.

In this series of aforementioned tasks, all mirrors in the original end-effector design were increased to 2-inch diameter mirrors. The optical configuration was changed slightly to ensure the larger mirrors would still be capable of fitting in a modified, somewhat larger housing that would pass through the floor opening. The illumination and collection mirrors have 3-inch focal lengths, while the detector-focusing mirror has a 2-inch focal length leading to the TE-cooled detector.

The mirrors have been configured to run a series of optical tests that will parametrically determine the optimum angular relationship for maximizing the signal in the diffuse reflectance mode relative to the asphalt surface. These mirrors have been configured in the ASAP laboratory and are continuing testing to determine the final optimum angles for re-design of the end effector assembly. Figure 3.1-34 shows the special optical configuration that is being tested.

Test results proved the basic optical design for the new mirror configuration. We moved the optical prototype to the FTIR optical arms assembly to conduct testing with the original end-effector replaced by the optical prototype assembly. Testing then proceeded with the FTIR in the loop with the prototype optics. We have been able to test the performance improvements achieved by the foregoing

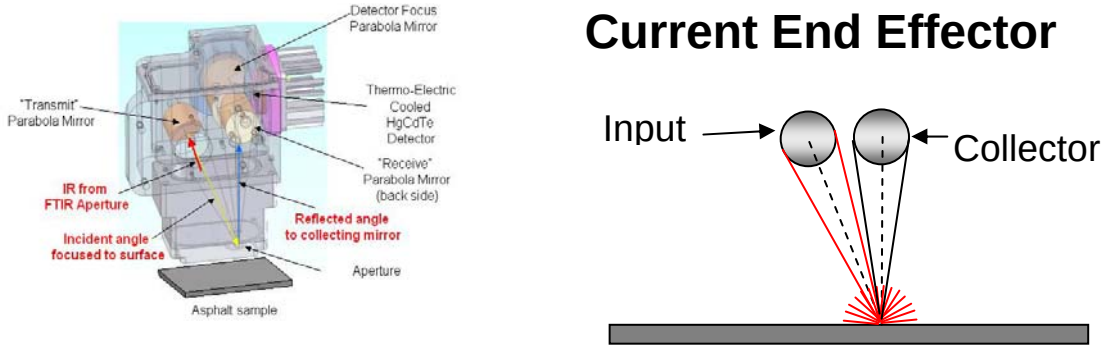

Figure 3.1-33. 3-D CAD Drawing of Current End Effector Showing Incident and Reflected Angles (above); Notional Sketch of Current End Effector Angles at 22.5 Degrees (upper right); Revised End Effector Angles and Increased Mirror Collection Area Currently Being Investigated (lower right)

design changes, i.e., increased mirror sizes with the illumination and collecting mirrors' relative angular orientations at 100, 80, 60, and 40 degrees to determine optimum performance. The asphalt slide samples will be inserted in place of the flat mirror (Fig. 3.1-34 yellow arrow) to test the diffuse reflectance mode at the selected angular relationship via new end-effector prototype optics.

The original end-effector is not affected, except that the TE-cooled detector will be swapped temporarily to the new end-effector experimental design for parametric testing. The net increase enabled by the IR source back-side mirror and the alternative end-effector design at selected relative angular orientations will be quantified by these tests.

Red Arrows Showing Optical Paths

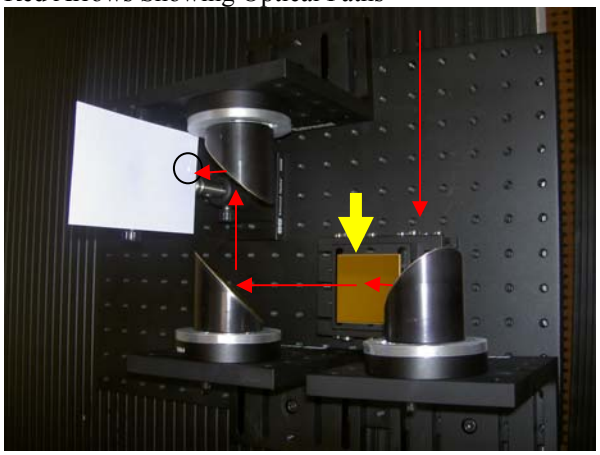

3-D Perspective of Optics

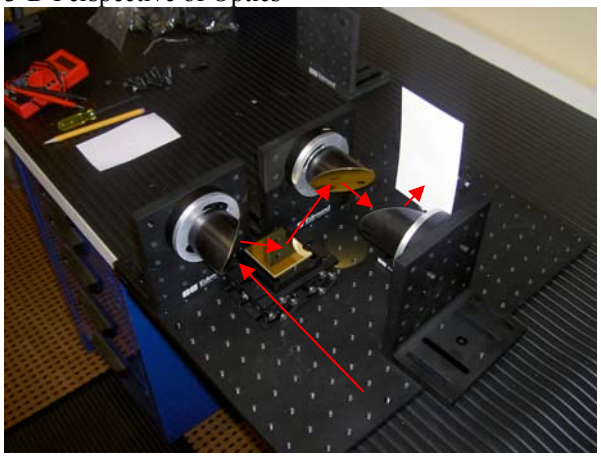

Focus at Detector Plane

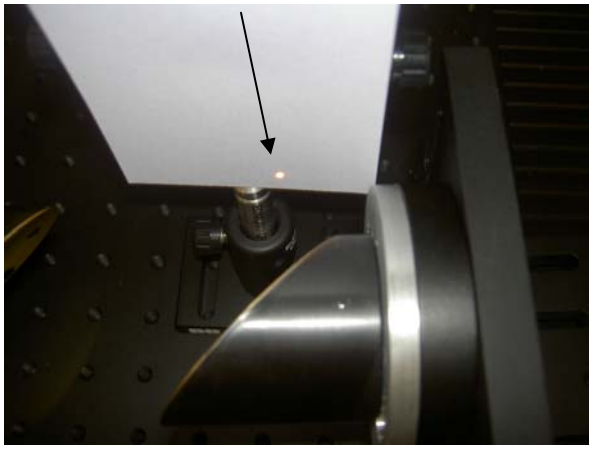

Figure 3.1-34. Optical Investigation of Incident and Collecting Angles Ongoing in Laboratory to Revise End Effector Design; Proof of Optical Design using Visible Source (red arrows added for clarity)

Detector Design Options

IE implemented a back-up plan to procure and test a 77K-cooled HgCdTe detector to provide a third—and more promising— technical approach to improving the S/N performance for the ASAP FTIR. This type of detector provides potentially *400 times higher* detectivity (D*) relative to the TE-cooled detector (based on peak detectivity). This new detector will provide substantial improvement in the sensitivity of the FTIR system. It will also enable longer-range sensing via the FTIR. Considerable research was performed on many past and current remote-sensing FTIR applications (ground, air, space), and virtually all systems' designs have cryogenic cooled detectors.

Initially the new high-sensitivity HgCdTe detector was used in the same focal point as the less-sensitive TE-cooled HgCdTe detector that was tested early in the program. Substantial bench testing of the new detector was performed prior to this effort to ensure that the new detector was working properly. Afterwards the TE-Cooled detector was removed and the new 77K-cooled detector was placed in the same position. A 3-axis adjustment table was used to align the detector field-of-view to best receive the modulated IR coming from the end-effector collection parabola mirror. Initially the new detector was tested in the specular mode whereby a mirror was placed at the end-effector aperture as shown in Figure 3.1-32. The signal-to-noise improvement using the new detector was substantially greater than we had previously observed with the TE-cooled detector. For previous testing, the preamp was set to the x1000 amplification to observe the signal. With the new detector, this amplification saturated the preamplifier output necessitating a change to the x100 amplification. The signal was substantially higher which enabled our tests to determine if a spectrum could be obtained from the asphalt slide sample (binder material).

The asphalt slide was inserted where the mirror was normally operated at the end-effector aperture as shown in Figure 3.1-32 earlier. Previously we were not able to detect a spectrum using the asphalt slide. However, using the new detector we are able to acquire a substantially stronger signal for the interferogram data collection, which once processed via the Fourier transform, produced a very much improved spectral signature for the asphalt slide sample. This experiment was very successful in that a very significant improvement in the signal-to-noise ratio was observed. For the first time we were able to collect a spectrum from the asphalt slide that could be processed relative to the instrument baseline spectrum to derive a difference signal representing the absorption graph over the infrared spectrum. Figure 3.1-35a presents the interferogram and spectrum that was collected with the new 77K-cooled HgCdTe detector using the specular mode, and represents the instrument baseline spectrum. Figure 3.1-35b presents the spectrum that was collected using the asphalt slide in place of the mirror to collect a diffuse reflectance spectrum for the asphalt binder material. The corresponding interferogram and transformed spectrum show a very distinct characteristic for the asphalt sample. The spectrum displayed in the figure was not obtainable using the previous TE-cooled HgCdTe detector. With these collections, we then executed the differencing program which allowed the absorbance data graphic to be produced showing the absorption of the asphalt slide over the 4500-400 cm^{-1} infrared spectrum. This absorption plot is presented

in Figure 3.1-35c. This data is undergoing final interpretation to determine any exploitable phenomenology at select sub-regions that will support determination of carbonyl content in the asphalt binder material.

As an alternative design approach for the ASAP van testing, the FTIR optional mode of operation will be reversed so that the FTIR is employed in a receive-only mode of remote-sensing operation. In this configuration, the IR source is replaced by the 77K-cooled HgCdTe detector. The end- effector will be removed to enable an exit aperture for receive-only detection of infrared spectral data. The sun will be used as the IR illuminator as it has been used in many other remote-sensing FTIR systems. A flat surface mirror will initially be used for close-in observations and data collection. Then a parabolic mirror directed at nadir will be used to collect data from an extended asphalt sample surface. A simplistic design of the new configuration is depicted in Figure 3.1-36 to illustrate the reverse receive-only application of the FTIR. Figure 3.1-37 shows photographs of the new HgCdTe detector and the X-Y-Z adjustor platform. The detector active area will be adjusted to the exact location of the focal of the collimating mirror leading into the FTIR aperture. The detector area is 1 mm square and is the same size as the TE-cooled HgCdTe detector, which minimizes risks in integrating the new detector. Figure 3.1-38 shows the IR detector curves for detectivity as a function of wavelength, with the peak detectivity for the original and new detector indicated by the red and blue arrows, respectively.

Our efforts have included working out a number of mechanical integration issues that include the integration of the HgCdTe detector onto an X-Y-Z adjustment table, and minor modifications to the "outrigger" table that currently supports the IR source and power supplies. An ortho-perspective 3-D CAD drawing of the 77K HgCdTe detector is presented in Figure 3.1-39. An L-bracket was custom machined for the fitment of the detector module on the X-Y-Z adjuster mechanism.

The new HgCdTe 77K detector is being integrated and tested with the FTIR at Innova for the receive-only configuration during December. The new configuration will be the primary means of potentially performing the van tests at Florida DOT State materials Office (SMO), and other sites as possible. This design approach offers orders of magnitude improvement in signal-to-noise performance and has the highest performance for observing the asphalt signal phenomenology for the ASAP program. Since the primary interferometer spectrometer function is sound, the improved detector performance will achieve ASAP program objectives.

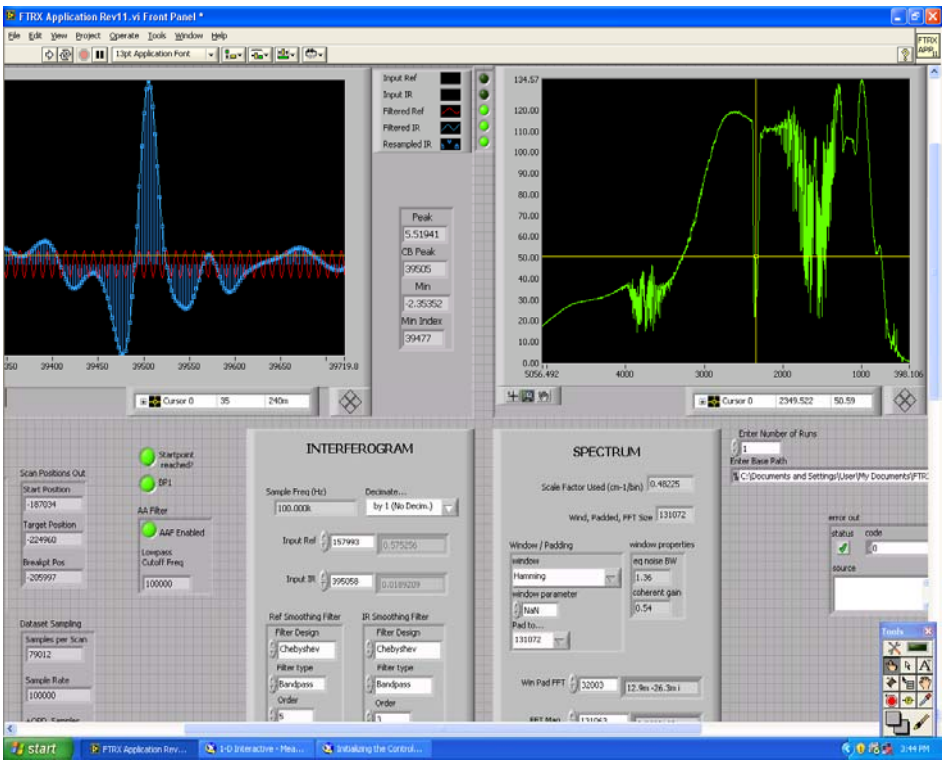

Figure 3.1-35a FTIR Baseline Spectrum for Instrument Response Function

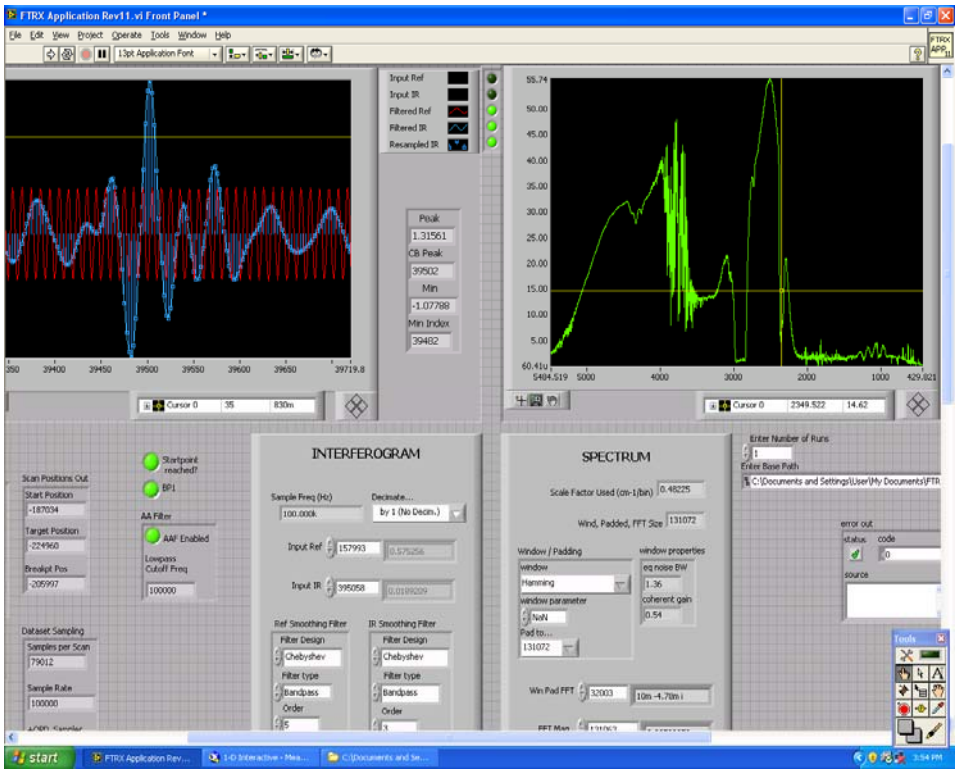

Figure 3.1-35b FTIR Asphalt Slide (Binder) Spectrum Data Collection

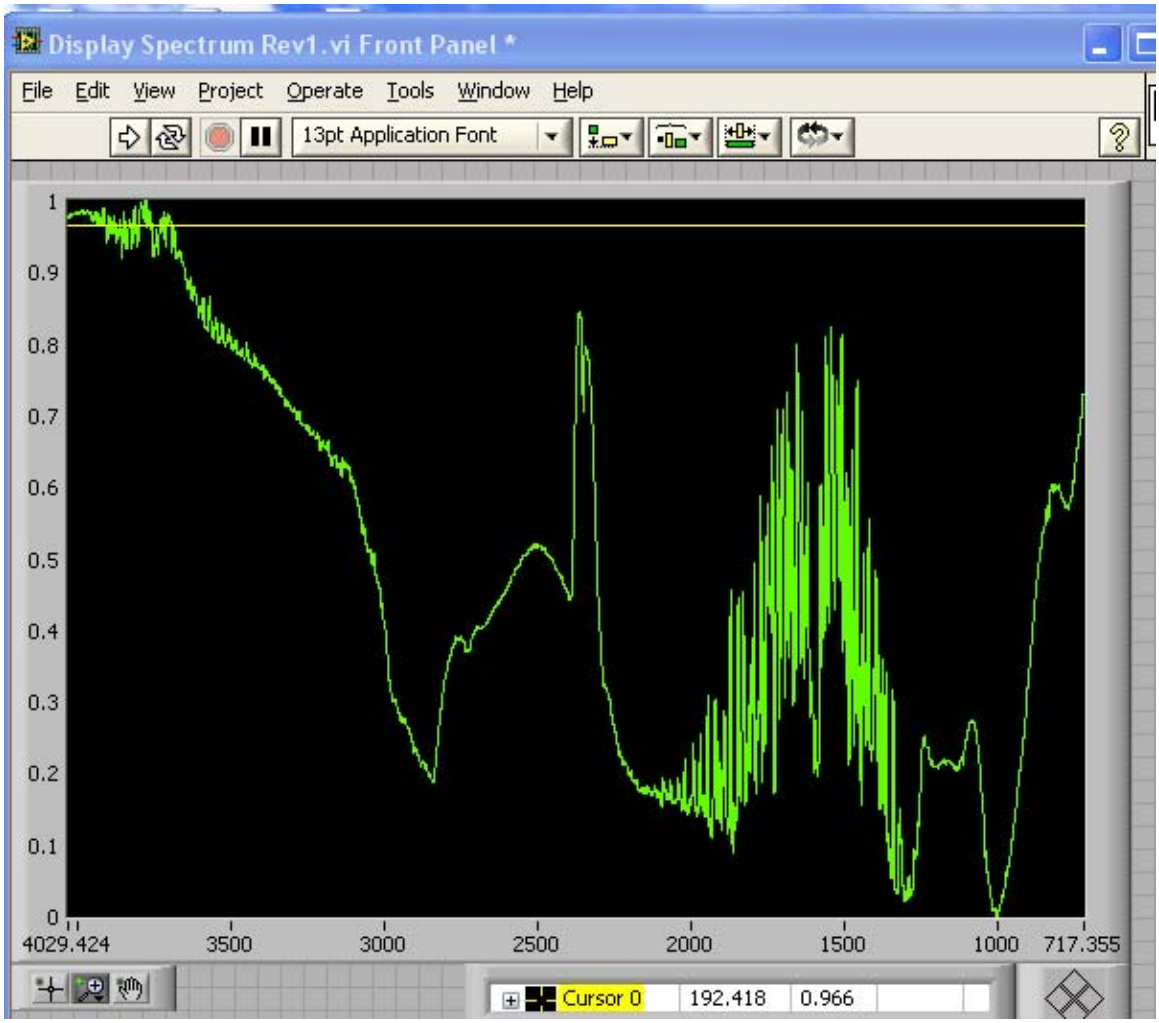

Figure 3.1-35c Absorbance Spectrum (1→0) for the Asphalt Slide Spectrum Binder Material on Slide (Baseline spectrum minus Asphalt Slide Spectrum

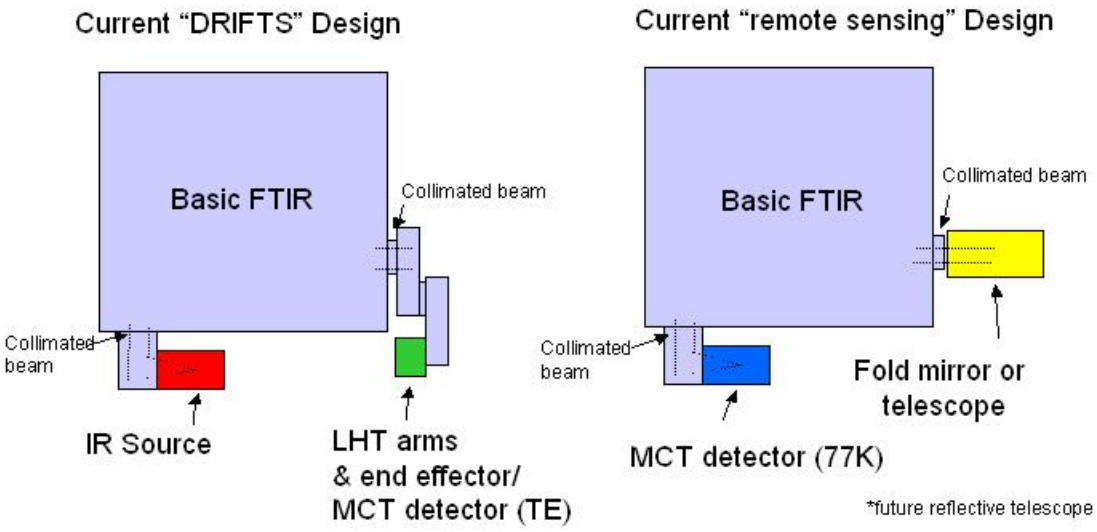

Figure 3.1-36 Reverse Optical Configuration for New HgCdTe (MCT) Detector (77K)

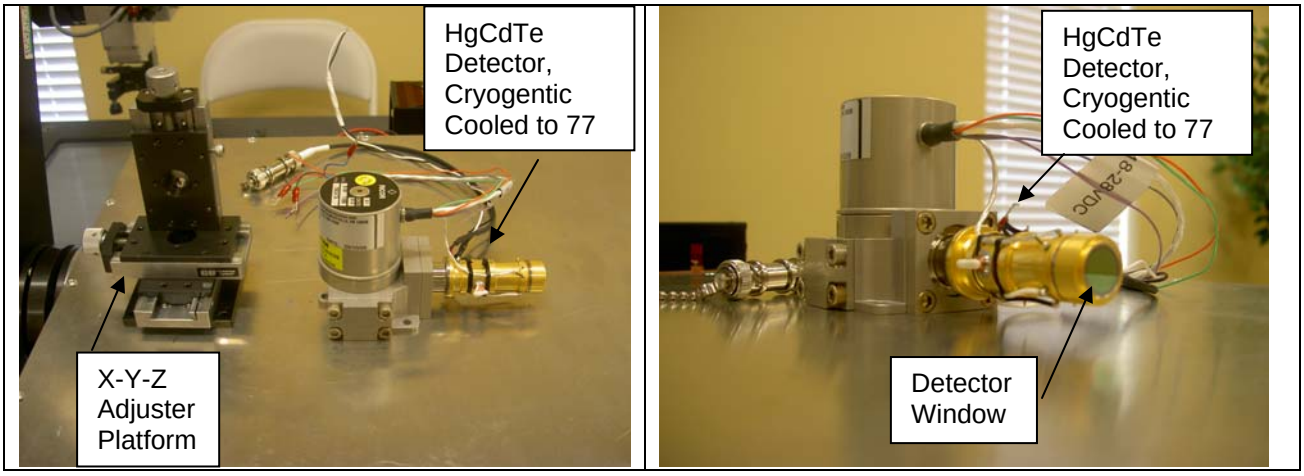

Figure 3.1-37. Photographs of New HgCdTe IR Detector with 77K Cryogenic Cooler and the XYZ Adjustment Table

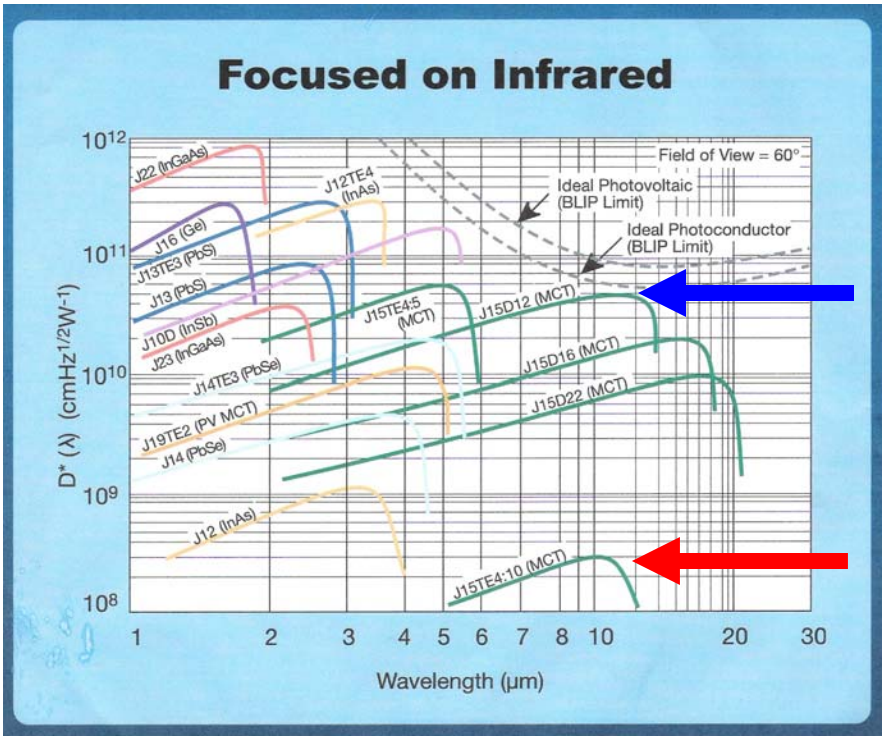

Figure 3.1-38 IR Detector D* Curves as a Function of Wavelength Showing Increased Sensitivity from the TE-Cooled to Cryogenically-Cooled HgCdTe Detectors

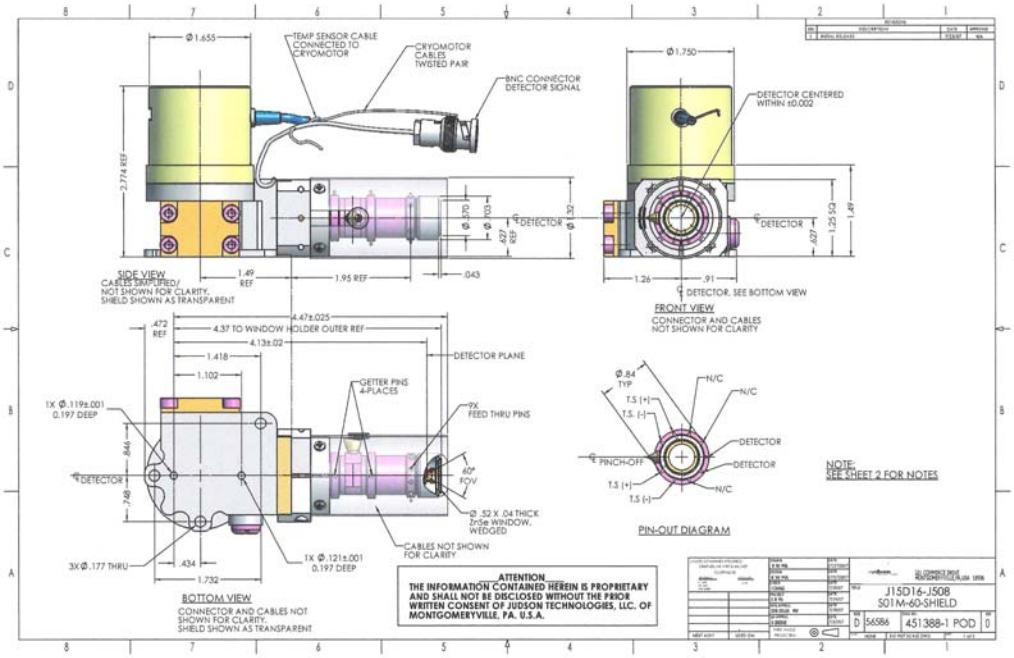

Figure 3.1-39 3-D CAD Drawing for the 77K-Cooled HgCdTe IR Detector

ASAP Computer

The ASAP system is controlled by a PC computer that controls all functions performed by the FTIR Data Control Computer to include the FTIR Data Capture & Control functionality, as well as, the Camera and Navigation system functionality for the supporting camera and navigation control system developed to support test operations. The PC is configured in a Q-Pack configuration that was chosen to fit the compact slide-out drawers design for the van operator console. The custom Data Control Computer design has been assembled with the following components:

- APEVIA X-QPACK case with 420W ATX power supply
- GIGABYTE GA-MA69GM-S2H motherboard
- AMD Athlon X2 Dual-Core BE-2350 processor 2100MHZ
- Crucial 2GB PC2-6400 DDR2 RAM
- Seagate Barracuda 750GB SATA hard drive
- Sony AD-7191A DVD/CD RW drive
- Microsoft Windows XP Professional

Figure 3.1-40 illustrates the completed system that was specified, purchased, and assembled. The computer system also provides for the inclusion of the National Instrument (NI) PCI boards that are necessary to control and capture data from the FTIR device. NI's Labview software is used for processing of all FTIR signals and controls. Customized C code has been developed to support the image and navigation processing software to support mission operations.

Figure 3.1-40 ASAP Data Control Computer Photograph (Front Panel Shown)

A simplified view of the primary interfaces is shown in Figure 3.1-41 below. The two primary National Instruments interface boards are shown with their primary functions performed within the FTIR instrument.

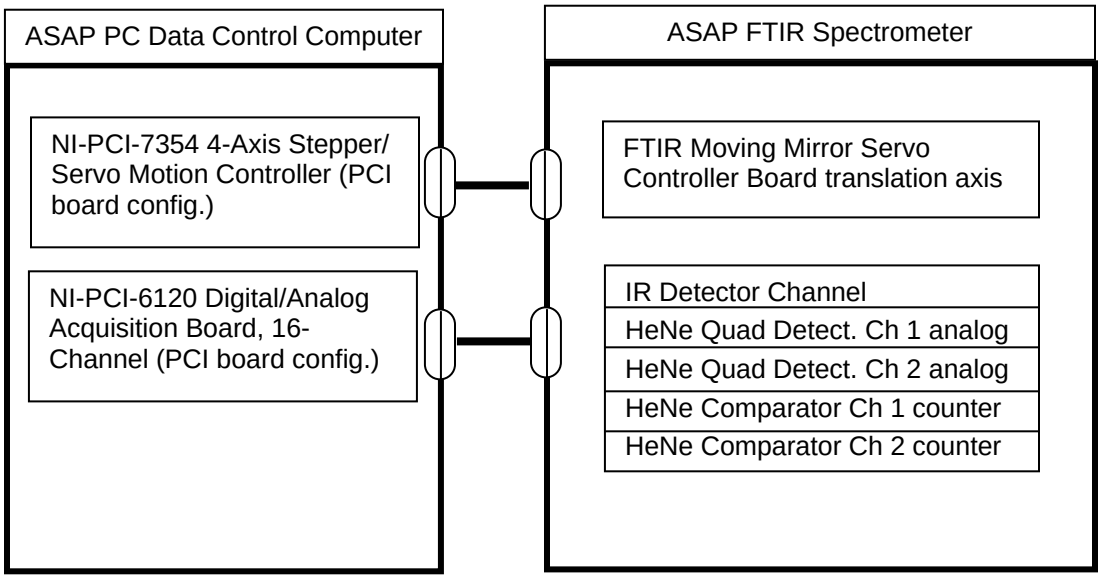

Figure 3.1-41 Simplified Diagram Showing Main Interfaces between the System PC and the FTIR Principal Functions

Two National Instruments interconnection cards are fastened to a removable back panel. These facilitate the connection of the digitizer and motion control card to internal components. The 12 VDC main power enters through the red/black plugs and is controlled by a toggle switch. There is a star ground bus bar in the lower right hand corner. Figure 3.1-42 presents the interconnect board.

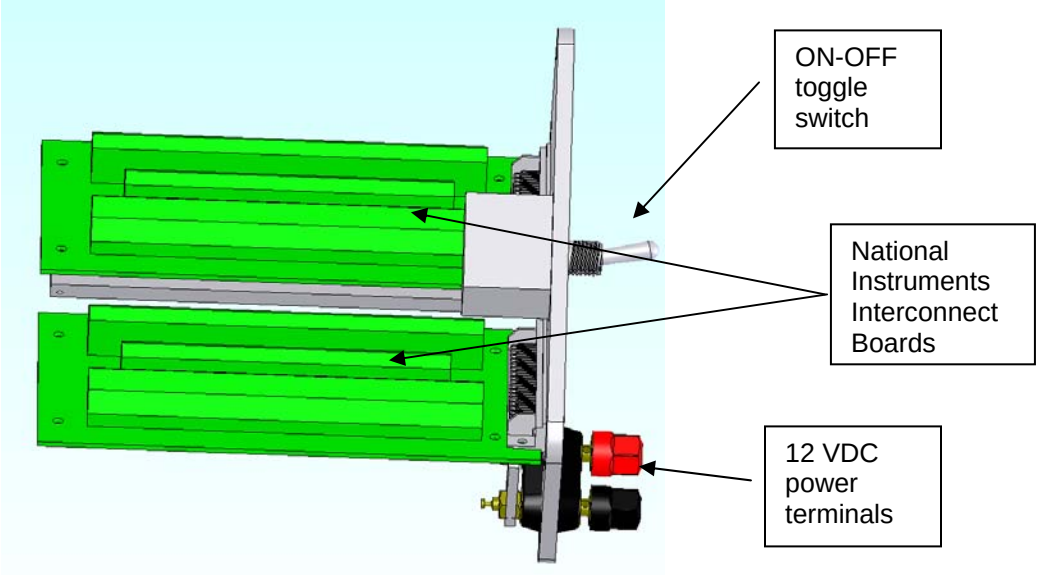

Figure 3.1-42 NI Interconnect Boards Used to Plug In Interface Cables to the System PC Backplane Connectors to NI Interface PCI Boards

The NI-PCI-7354 4-axis stepper/servo motion controller (68-pin VHDCI cable) is presented in Figure 3.1-43. The board fits into one of the PC I/O slots with the connector ready for plug in on the back-side of the PC. The board supports 64-bits of digital I/O and 16-channels of analog I/O for feedback in a 1-slot 3U PCI configuration.

Figure 3.1-43 ASAP NI-PCI-7354 4-Axis Stepper/Servo Motion Controller

The NI-PCI-6120 Digital/Analog Acquisition Board (16-bit) is presented in Figure 3.1-44. The board fits into one of the PC I/O slots with the connector ready for plug in on the back side of the PC. The board has a number of general-purpose applications including analog and digital I/O. Its primary function in the DAQ board is for the ASAP FTIR is to acquire the HgCdTe detector output for collecting the scan interferograms, the HeNe silicon detector outputs for the two quadrature detection channels, and the two square-wave HeNe detectors outputs from the comparator circuits which feed into the board's counter function to provide scan position and direction measurements and control.

Figure 3.1-44 ASAP NI-PCI-6120 Digital/Analog Acquisition Board

3.2 Van Integration

Innova Engineering procured and developed an instrumented vehicle-mounted test-bed specifically designed for the ASAP FTIR system development program. The ASAP van addressed the test objective of performing roadway asphalt surface aging data collections to assess the feasibility and effectiveness of the ASAP prediction capability. Demonstration of the FTIR in a roadway van environment was a prerequisite to attempting longer range airborne testing with the FTIR and supporting instrumentation.

Innova conducted a comprehensive investigation of different types of vans for the ASAP mobile test-bed. Our candidate U.S. van types were: Chevrolet's Astro, Express, Venture, and Uplander cargo vans; Dodge's caravan cargo van; Ford's Econoline and Freestar cargo van; and GMC's Safari and Savana cargo van. We also conducted several site visits to van dealers to investigate feasibility of mounting the requisite instrumentation and equipment in the vans. These inspections have included dimensional measurements and photographs of proposed equipment locations. Based on price, performance, volumetric capacity, and rear door opening designs, the 2008 Chevrolet Express cargo van was selected for full-scale integration of the ASAP system. A photograph of the Express van is presented in Figure 3.2-1.

One of the key selection criteria is the feasibility of designing an opening in the bottom of the van to allow the FTIR front-end DRIFTS optics to pass through to the road surface below. This was not feasible in most of the vans we surveyed. The Chevrolet Express van had an open space where the spare tire is mounted underneath and aft of the rear axle that satisfied the opening requirements. Two key design selections were the relative ease of providing the aperture opening through the van floor for collecting data from the asphalt surface below, and quick release for the FTIR spectrometer from the van for storage in a conditioned and secure building.

Figure 3.2-1 Chevrolet Express Van For ASAP Vehicle-Mounted System

IE worked on various mechanical designs to support mounting and articulation of the FTIR optics arms in the van. Key design objectives were to provide adequate structural integrity to withstand the various translational and rotational forces that will be experienced in standard road conditions. Vibration isolation design approaches were also being explored and shock mounts designed and implemented for the FTIR.

Alternative designs for the FTIR mounting requirements were analyzed to derive the best operational design approach that would be most suitable for the ASAP vehicle-mounted system requirements. The Chevy Express van chassis design provided a clear area in the vicinity of the spare tire under-mount apparatus that did not structurally impact the main chassis beams or cross members under the van. Also, our final design adapted a quick-release "dovetail plate" design that is used in modified test aircraft for instrumentation units. A rectangular sliding-door mechanism was also integrated into the stack of mounting plates to allow quick and convenient opening and closing of the FTIR aperture opening. Photographs of the FTIR mount and open- and closed-door configurations are presented in Figure 3.2-2. A series of AutoCAD files were created and supplied to the machinist for fabrication and integration in the van. The hole patterns and mounting instruction were communicated and coordinated with PLX and the machinists for mounting the FTIR.

The design for the operator table involved evaluation of several approaches to implementing the table in the van. The final design was developed in AutoCAD and provided to the machinist shop for fabrication and final integration into the van. Major design requirements were the ability to support four custom-sized gel-cell batteries and two redundant power inverters, the ASAP system PC, monitor, keyboard, printer, and mouse, and key system switches and circuit breakers for internal power distribution. Also a heavy-duty 300 amp alternator replaced the standard 100 amp alternator provided originally in the Chevy Express van (Figure 3.2-3) A broad nation-wide vendor-supply research was conducted for determination of the best approach to selecting and integrating the high-amperage alternator into the current van design. The key requirement was to significantly increase that amperage charging capacity with minimal modifications to the engine area. This change was necessary to provide ample charging capacity for the battery bank that will provide 115 VAC and 12 VDC power internally within the van. A simplified schematic of the power distribution approach for the van is presented in Figure 3.2-4.

Figure 3.2-2a. FTIR Mounting Plates with Door Closed

Figure 3.2-2b. FTIR Mounting Plates with Door Open

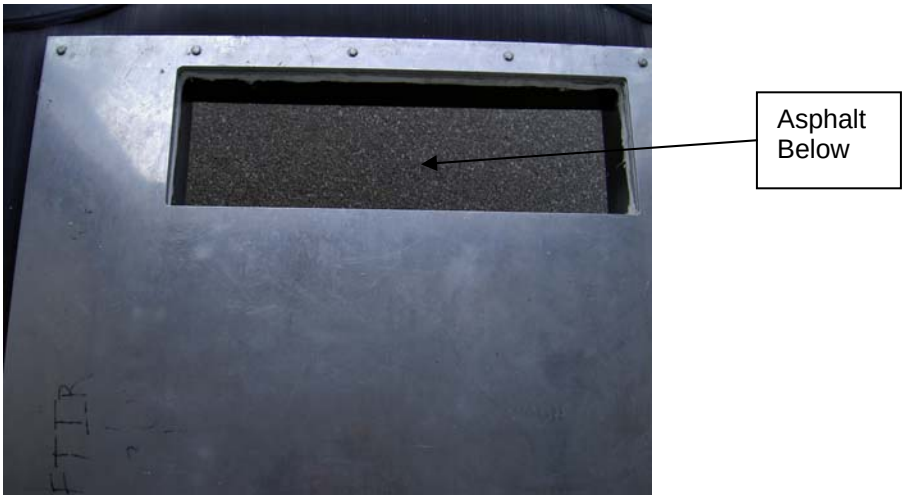

Figure 3.2-2c. Top Down View of FTIR Mount Plates with Door Open

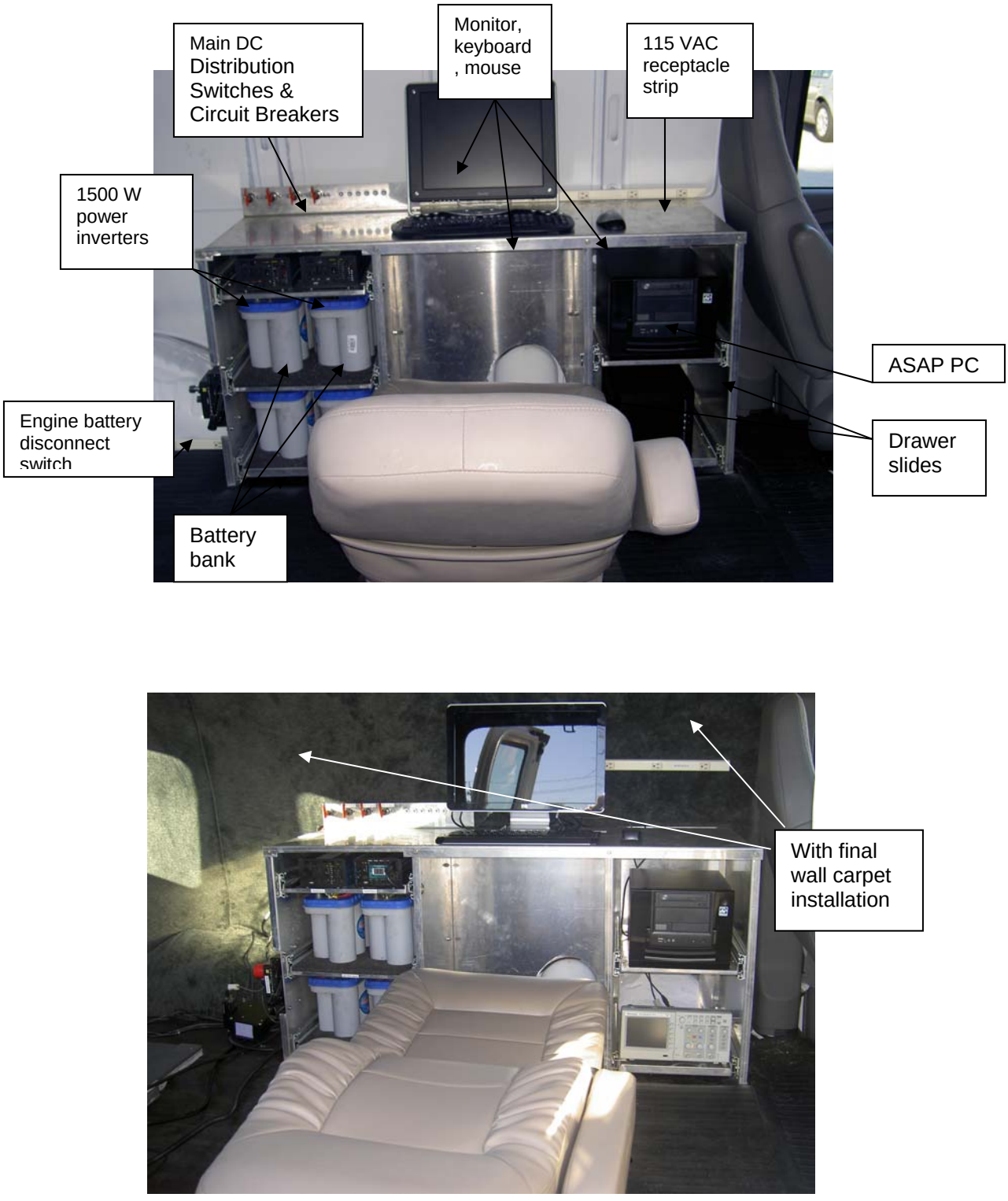

Figure 3.2-3. Interior View of the Operator's Table (chair laid back for photo)

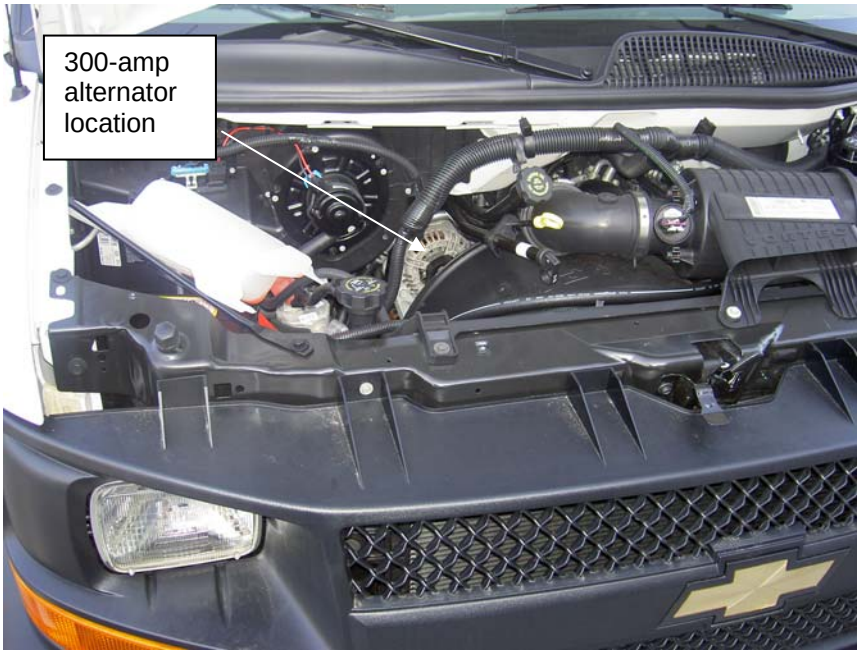

Figure 3.2-4. Integration of the 300-Amp Direct Replacement Alternator in ASAP Van

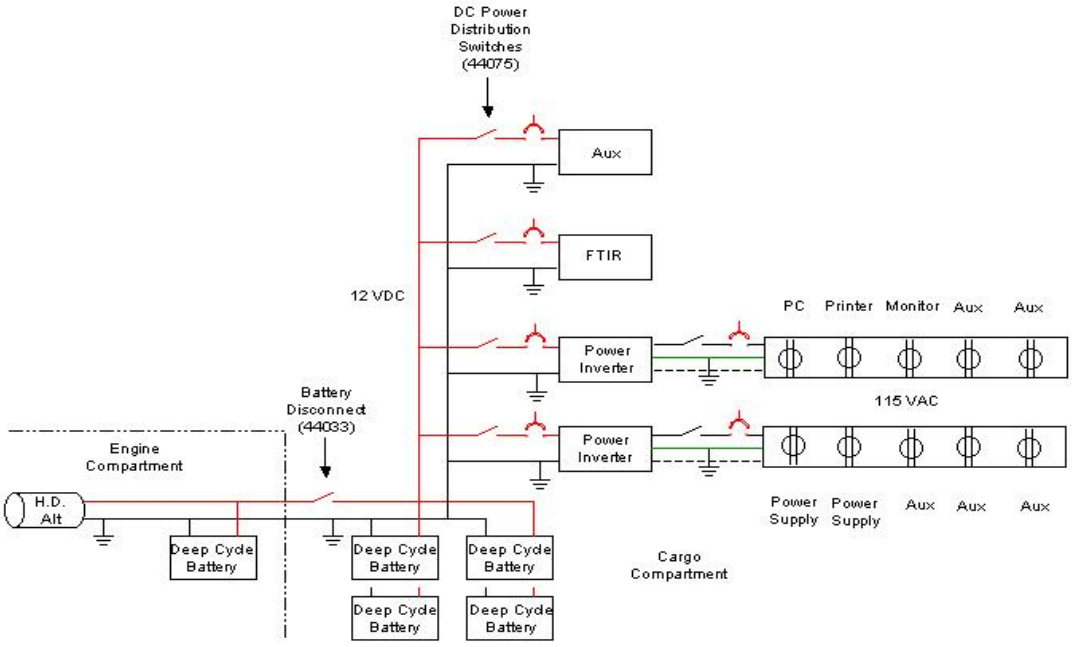

Figure 3.2-5 Simplified Schematic of ASAP Van Internal Power Distribution System

Figure 3.2-5 above shows the four-ganged 12 VDC deep-cycle battery bank supplies 12 VDC power directly to the FTIR and the auxiliary circuits. The FTIR was designed to operate form a 12VDC power source since it was destined to be operable in a van and aircraft scenario. The auxiliary circuit primarily supports the safety lights that have been installed on the van for stop-and-go data collection—in coordination with the maintenance of traffic contractor.

In addition, the 12 VDC supply bus provides power to two AIMS 1500 Watt Pure Sine Wave Power Inverters that provide 115 VAC 60 Hz power to the van. The Pure Sine Wave power invertors provide power similar to the standard electrical lines, viz-a-viz the square-wave 60Hz power that is extremely noisy in an electrical sense. One of the power inverters provides 115VAC power to the operator station which has most of the PC and peripheral equipment on this circuit. A second circuit is supplied to the back port-side wall of the van to support auxiliary equipment that requires 115VAC power such as additional power supplies. Also, the redundancy of the power inverter design helps mitigate problems that may arise with the failure of a power inverter, namely a backup source exists within the van. A photograph of the 1500W power inverters with the slide pulled out in the van's operator table is presented in Figure 3.2-6 below.

Figure 3.2-6 Photograph of Two 1500 W, 115VAC, 60 Hz Power Invertors On Equipment Slide Tray – Slide Out for Access

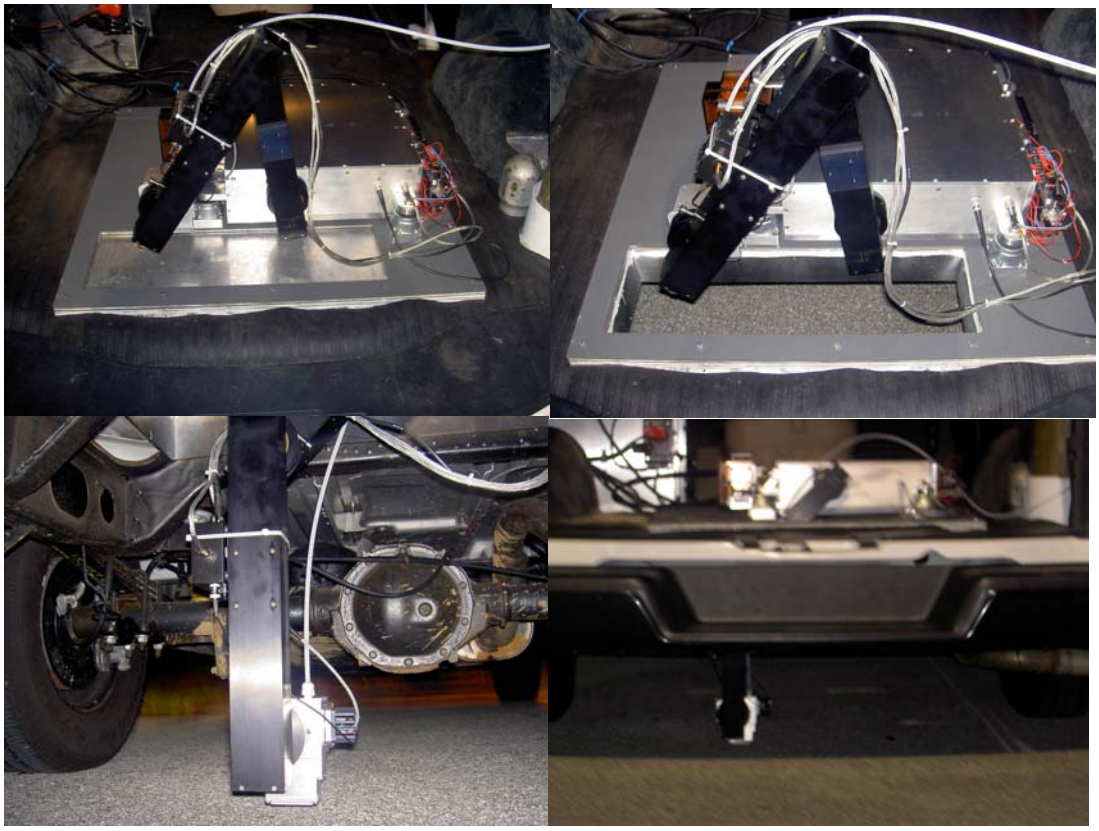

Figure 3.2-7 ASAP FTIR Installed in Van with Optical Arm Retracted and Floor Aperture Closed (upper left), Optical Arm Retracted and Floor Aperture Opened to Asphalt Below (upper right), End Effector Near Asphalt Surface for Data Collection (lower left), and Rear View of FTIR on Van Floor and Optical Arm/End Effector Extended Through Floor Aperture to Asphalt Surface in Non-Contact Configuration

Systems Concept-of-Operations (CONOPS)

The FTIR device is a component of the system that we are creating to analyze and manage the pavement condition and remediation for on-system roadways within a state DOT. The system consists of the FTIR sensor contained and managed within the ASAP system that includes other sensors and software to create a complete system for planning, executing, and analyzing the remotely sensed information developed from deploying the ASAP system.

This ASAP system has been developed for execution within a ground-based van or planned for airborne environment. The system being developed is capable of being deployed within each environment to acquire unique information about the pavement condition using this combined sensor system. The system consists of four major subsystems that are combined to provide fused sensor data that compile a record of information for a given segment of roadway and characterizes the pavement condition on that section of roadway.

- ASAP Route Planning – ASAP Mission Planner
- CleanSweep/StreetSweeper Subsystem
  - System Design
  - Camera Subsystem
  - INS (GPS + IMU + KFS)
  - FTIR
  - System Software
- Post Mission Review - CleanSweep
- FTIR Analysis Component – SpectraView

A block diagram of the system utilization is shown below. These components describe the major system elements and their connection to each other in the design of the system. With the system, data can be collected, analyzed, and archived to develop a complete description of the roadway being examined.

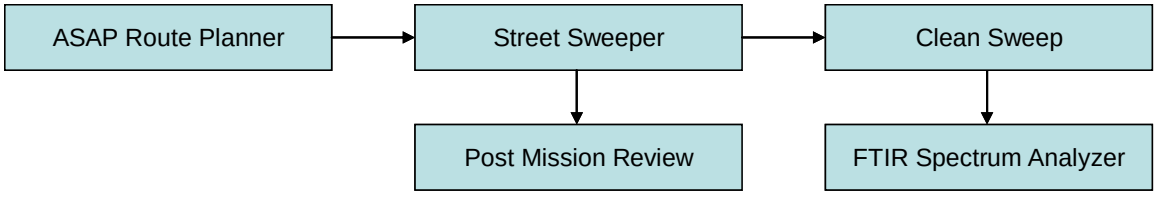

Mission Planning – ASAP Mission Planner

The system must select a roadway section on which to command the ASAP system to collect data. The current system configuration consists of a Mission Planning component from which a roadway segment can be planned for collection. Figure 3.2-8 below is a screenshot of the current design of the ASAP Mission Planner.

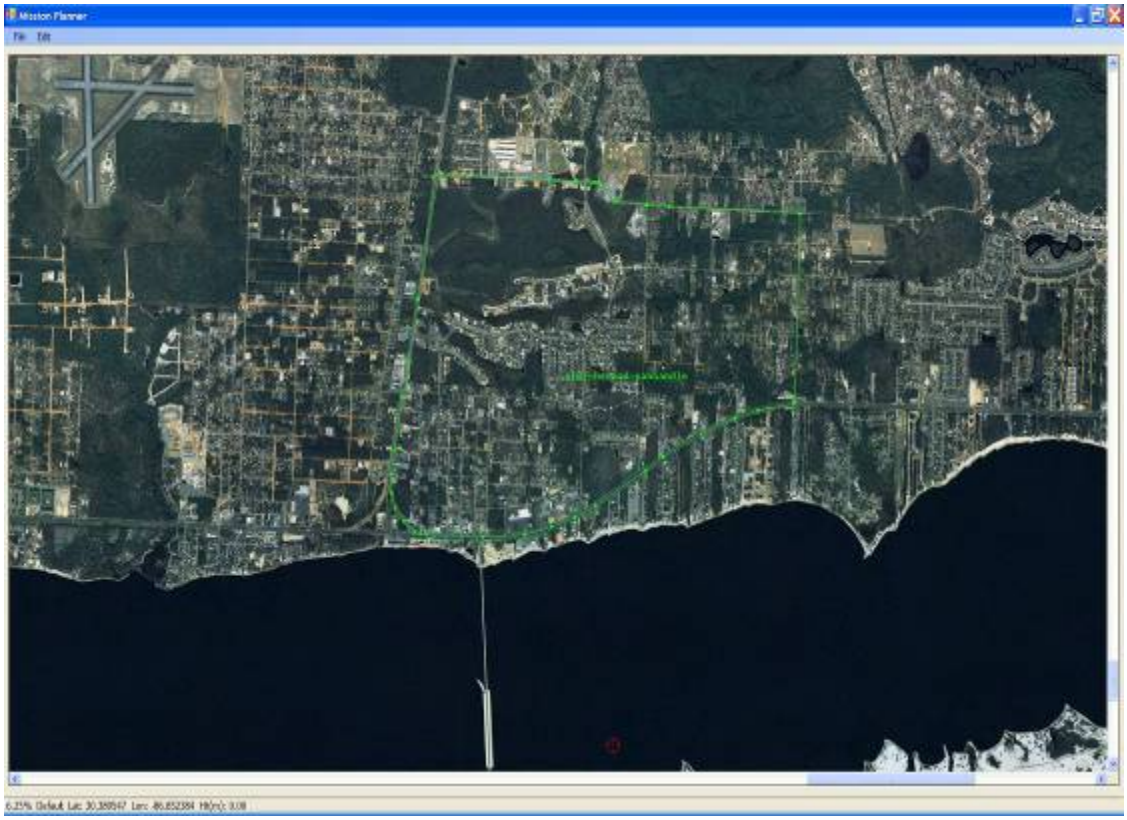

Figure 3.2-8. ASAP Mission Planner with a programmed route on a roadway segment

This software program consists of a user interface from which the user is presented with a Mosaic geo-referenced image that has been generated by a companion system called GeoSpec. The current GeoSpec sensor has been flown in a Cessna aircraft and is being commercially utilized to generate mosaics for customers in agriculture and forestry. Figure 3.2-9 below shows the current system on a Cessna located on the wheel strut.

Figure 3.2-9. Airborne Multispectral Camera System Mounted on Cessna

This system was modified to collect imagery and navigation data on a truck mount. As shown in Figure 3.2-10 below, the current system is shown mounted for testing on a truck.

Figure 3.2-10. Ground-based testing of airborne sensor on truck mount

The user interacts with the ASAP Mission Planner to select the roadway segment and the spacing of updates to command the FTIR and the Multispectral camera to collect data on the roadway. The Mission Plan is loaded into the StreetSweeper application prior to driving the

road segment. The control information is collected from the geo-referenced mosaic collected with the current airborne system.

Mission Execution – StreetSweeper

The Mission Plan created previously is loaded into the mission computer within the van. The StreetSweeper application is presented to the operator in the van and the route is driven under the command of the StreetSweeper software. As shown in Figure 3.2-11 below, the application will navigate the operator to the beginning of the road segment to be collected.

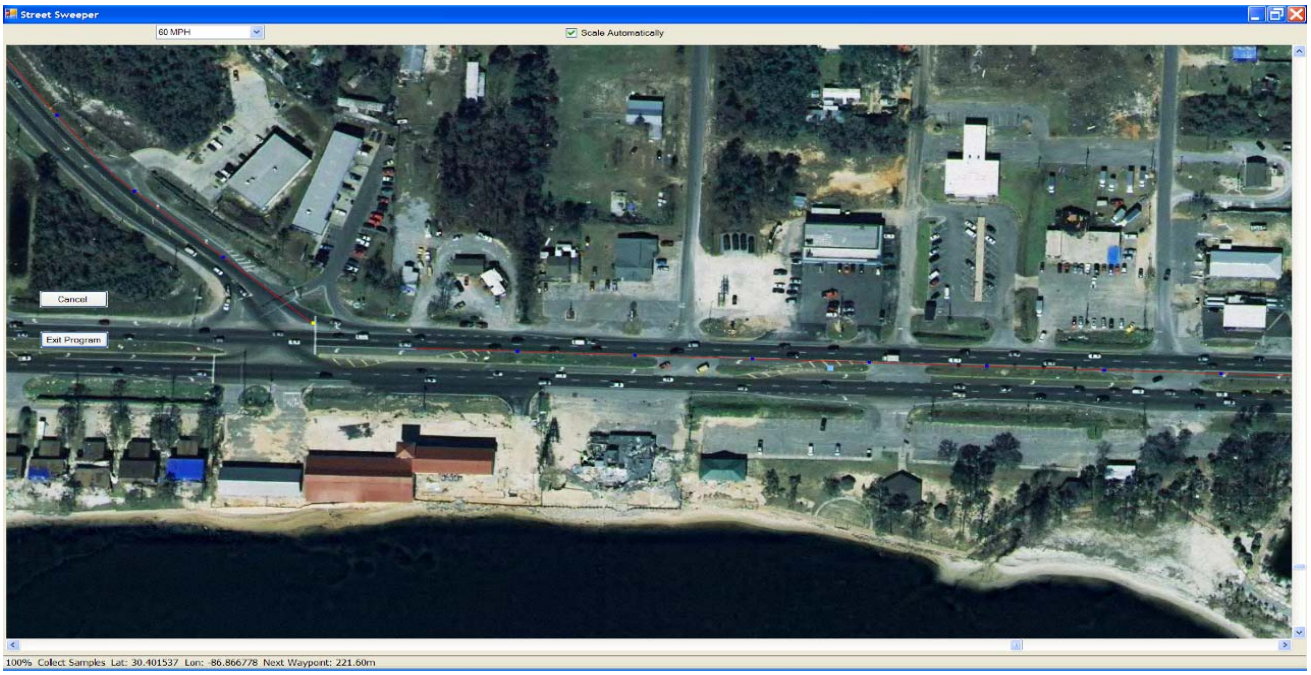

Figure 3.2-11. StreetSweeper showing the beginning of the roadway segment to be driven

The user approaches the beginning of the roadway segment. The StreetSweeper application will change the color of the designated point on the pavement to be imaged. The operator will be presented with the location of the next roadway element to be collected as he travels the section of roadway. The navigation system directs the operator and captures the data at the proper locations on the roadway section. The operator simply needs to drive the van and allow the system to perform the data collection functions.

Mission Review/Analysis – CleanSweep

The post-mission analysis of the data begins with a mission post-view analysis program called CleanSweep. This tool provides analysis functions to review the mission and analyze the success of the road segment sequence of images collected with the multispectral digital camera system.

GeoSpec System Development

The GeoSpec camera system collects visible data in the visible and NIR spectral range. The system is shown in Figure 3.2-12 below. It consists of a custom-built digital camera capture system with geo-referencing capability. The FTIR is controlled using the custom-built MicroATX that has two National Instrument special-purpose PCI-bus cards. One card is to provide the microcontroller for the FTIR system and the second card is for the digital and analog I/O channels controllers to control and capture data from the FTIR receiver.

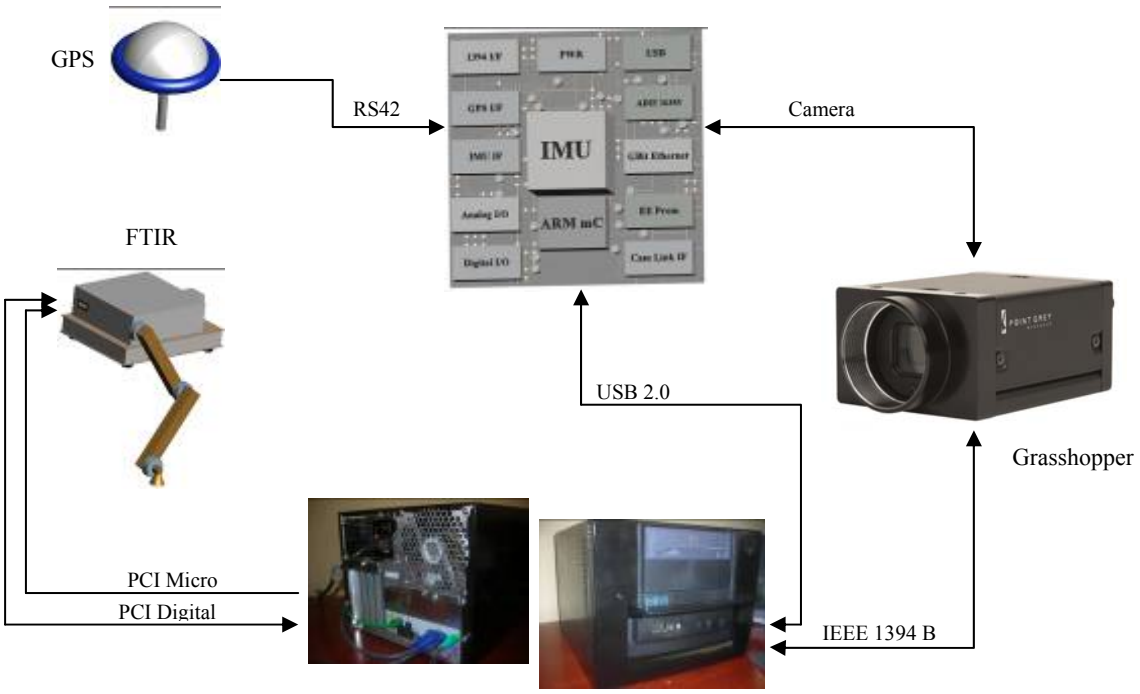

Figure 3.2-12 GeoSpec System Components

Digital Camera Design

The digital camera is a PointGrey progressive-scan camera that can provide 3-channel spectral information. It is custom-made from PointGrey and will be modified to support the proper spectral signature collect based upon the research into this spectra. The camera is shown in Figure 3.2-13 below.

Figure 3.2-13. Point Grey Digital Camera

Navigation System

The navigation system consists of a 6-channel IMU (Inertial Measurement Unit) that is currently a Honeywell HG1700. The IMU consists of 3-axis accelerometers and ring-laser gyroscopes. The modular camera system will have a 16355 MEMs-based IMU from Analog Devices. This IMU is coupled to a 12-channel GPS receiver to complete the INS system measurement devices. This INS is driven by a 33-state Kalman filter that has been custom-developed by our team in other projects. The navigation system is shown in Figure 3.2-14 below.

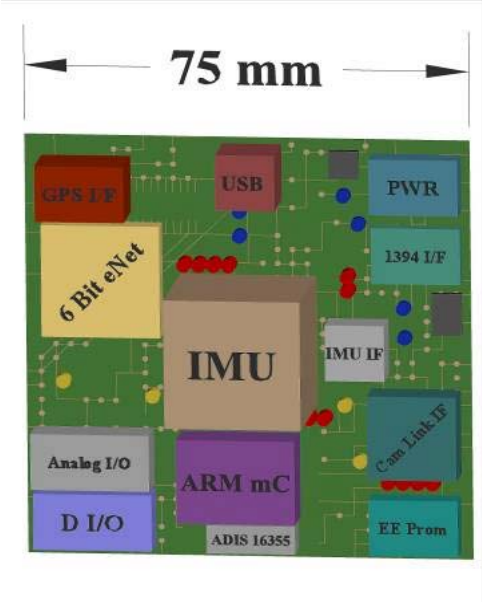

Figure 3.2-14 Navigation System Block Diagram

Data Recording System

There are two distinct data recording functions performed by the system—one for the FTIR data and one for the digital camera data with navigation-state information. The camera/navigation data recording system consists of a custom control board that performs the data pre-formatting from the GPS receiver, Inertial Measurement Unit (IMU), and the digital camera system. The system is controlled via a USB interface to the central computer and stores the data from the IMU and GPS via this interface. The block diagram of the board-level system is shown in Figure 3.2-15 below.

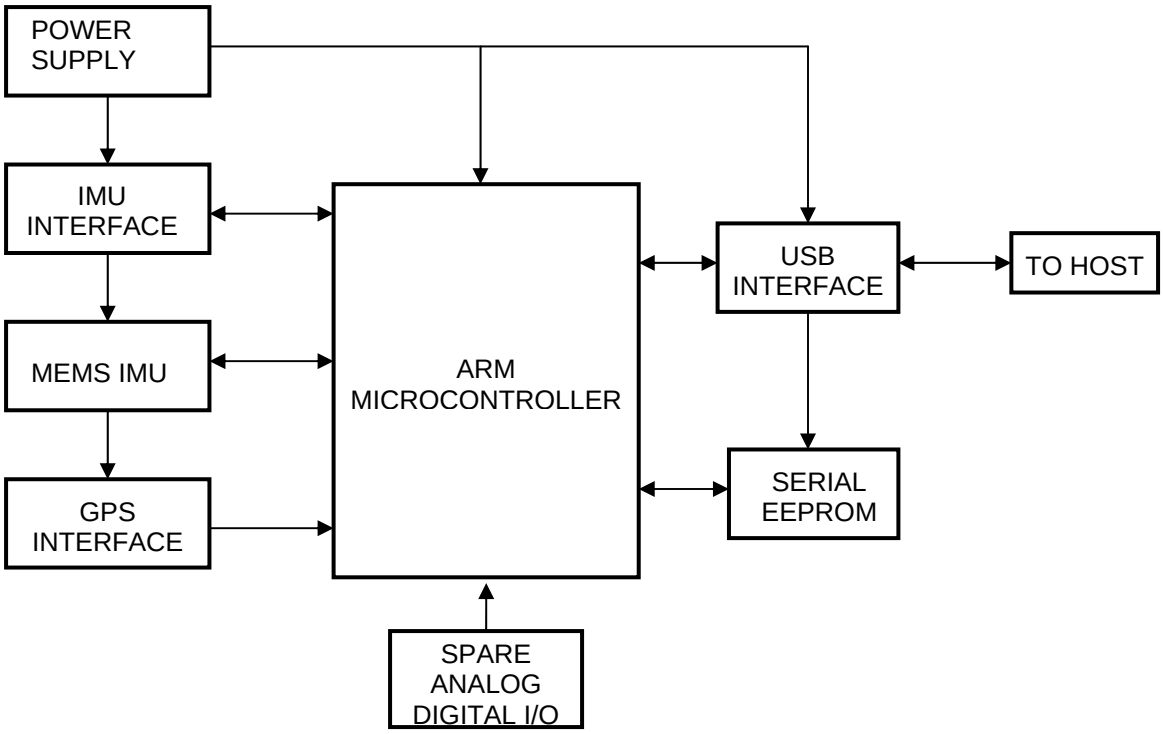

Figure 3.2-15 Block Diagram of the Navigation System

GPS/IMU Data

The photograph below (Figure 3.2-16) shows the GPS board that is integrated with a patch antenna on the reverse side.

Figure 3.2-16 Integrated GPS/Antenna Board to Support Navigation of Van for Field Testing.

3.3 Aircraft Design Study Plan

Innova conducted extensive research into identifying the technical feasibility and limitations of performing airborne measurements using a FTIR spectrometer. Basically in an airborne scenario, the aircraft is carrying the instrument and traveling in a forward direction. For ASAP, we identified a Cessna aircraft that could fly at relatively slow speed and low altitude. The selected aircraft has a hole in the lower fuselage and is covered with a conformal plate when not removed for supporting down-looking instrument usage. The ASAP FTIR spectrometer would be internally mounted (rear seat removed) and with a viewing aperture through the hole in the fuselage and pointed toward the roadway surface. A photograph of the Cessna aircraft is presented in Figure 3.3-1 below.

Figure 3.3-1 Proposed Cessna Aircraft for Airborne Tests with Down-Looking Hole Covered with Panel

For remote-sensing FTIR spectrometry, our research has revealed the need to operate in a sensor stare mode. In the stare mode, the sensor's field-of-view (FOV) footprint must maintain pointing at a specific location on the ground surface over a period of time that completes the data acquisition process. In the case of the FTIR spectrometer, this period of time could be for one spectrometer scan timeframe, or roughly one second. However, in order to improve the signal-to-noise performance of the data acquisition, multiple scans are usually collected and averaged. A typically sequence includes 32 scans, although scan sequences may be shorter or longer, with increased performance as more scans are included in the averaging process. In the case of the 32 scan sequence, the spectrometer's FOV would have to be pointed at a given spot for 30 seconds while the aircraft is in motion. Since the aircraft may have a minimum ground speed of ~100 knots, then the aircraft's ground speed may traverse ~150 feet in one second. This factor alone will likely drive how many scans will be collected in a scenario where the spectrometer is looking in near-nadir attitudes. The scans may be limited to 4 to 8 scans during a given measurement event.

In addition, the aircraft's trajectory will need to be planned for an altitude where the angular rate of change of the pointing angle (a.k.a., line of sight) does not exceed normal design performance required for stare mode tracking. A planned altitude of 2-3 kft would be feasible, but an altitude of 200-300 feet would be impractical, unless the aircraft was a helicopter or lighter-than-air vehicle. The altitude design tradeoffs also include the standoff range that will support acceptable signal-to-noise sensitivity thresholds for the FTIR spectrometer sensor. Studies are continuing on the threshold detection ranges supported by the addition of a 77 K cooled HgCdTe detector integrated into the spectrometer optical design. In the current design, the telescope's aperture is planned for to have a 4-inch diameter aperture directed by a 2-axis stabilized pointing flat mirror. As the range to the surface increases, the otherwise collimated beam will diverge and scatter to an extent that diffuses the optical integrity of the collection beam size and signal detection. These and other factors will determine the typical planned trajectory and standoff range for the aircraft flight data collections effort for asphalt aging predictions.

The stare mode requirement is driven by the need to sample a specific spot on the asphalt surface for the duration of the selected spectrometer scan intervals. Ideally the FOV would be pointed to the same exact footprint on the ground. In a dynamic scenario of changing rotational and translational forces and motion that may include various levels of buffeting, the ideal pointing of the FOV is difficult at best. However, it is critical that the same point on the asphalt surface be observed over the measurement interval. Otherwise, the intra-scan and inter-scan integrity would be degraded substantially. Since the FTIR is an amplitude-modulated optical process, any variations footprint observation area will smear the interferogram signature and subsequent processing and transformation to an IR spectrum. The stare-mode requirement is a formidable challenge to applications viewing a static point on the ground surface while in forward motion.

Our approach to developing an airborne system concept and design is depicted in Figure 3.3-2 below. This design uses an extended outrigger platform to mount the primary optics for the airborne remote-sensing configuration. Many designs were considered, and extensive research was conducted to explore various design approaches used for terrestrial, airborne, and spaceborne remote-sensing spectrometers. Our leading design candidate included using a parabola mirror similar to several that are used in the original ASAP FTIR design. The optical beam at the entrance (Aperture 2) to the spectrometer requires a collimated optics. The parabola mirror in the collimator box accomplishes that function. The mirror also focuses a divergent beam into a telescope box that is a simple Cassegrain telescope optic configuration. The focal length of this parabola mirror is 4 inches. The beam converges to a focal point and then diverges to the disk area of the small spherical convex mirror shown in the telescope box. The convex spherical mirror is placed about 8 inches from the collimating off-axis parabola mirror and is adjustable. Upon reflection, the beam diverges to the larger 4-inch diameter concave spherical mirror on the left side of the telescope box. This mirror has a hollow annular area in the center that is open for the beam coming from the FTIR collimating optics box.

The convex and concave mirrors in the telescope designed to project a 4-inch diameter collimated beam to the steering mirror shown to the right. The design allows the FTIR and supporting optics to be stationary and the flat mirror provides all steering and tracking of the target spot.

The projection of the 4-inch collimated beam onto the mirror surface would create an elliptical shape on the mirror planar surface. The mirror is an elongated octagonal shape that is slightly larger than the projected ellipse. The mirror is mounted within a metal rim frame that has two mechanical pivot pin/bearing mechanisms that are connected to the yellow azimuth gimbal ring. On the top side of the gimbal ring is the torque motor that is used to steer the mirror in the azimuth direction. A rotational position feedback transducer (e.g., optical encoder) is mounted to the opposite pivot pin/bearing mechanism on the downside of the yellow gimbal ring. The motor and encoder work in together within a PID control loop to steer the azimuth orientation of the mirror.

Orthogonal to the azimuth axis of rotation on the yellow gimbal ring is the pivot pin/bearing mechanism for the elevation axis control and pointing. A similar torque motor/encoder pair is used at the sides of the yellow ring to actuate the yellow gimbal ring to the required position for control and pointing. The latter motor/encoders are mounted to two vertical stanchions on each side of the yellow gimbal ring. The elevation motor and controller are controlled via a similar PID control loop. The azimuth and elevation control loop must be integrated in that they must work in unison to provide the necessary pointing of the flat mirror to maintain track on a selected asphalt surface area on the ground.

There are two fundamental dynamical control processes that must be implemented to effectively point the mirror and optical beam to the ground surface. One involves a tight inner control loop that must sense the external dynamics that are induced on the airframe and thus the FTIR instrument while in flight. Basically the pointing angle must be maintained to an inertially stabilized pointing angle—although the external rotational and translations perturbations typical of flight are being induced on the aircraft and FTIR structure. Regardless of these perturbations, the pointing of the flat mirror must be controlled to the same pointing as though these external perturbations were not present. Secondly, to support the stare mode while in flight, the positional pointing of the azimuth and elevation mirrors must be dynamically pointed so that the same asphalt surface area is pointed to even though the aircraft is in moving forward along its flight path. Both the inertial stabilization and pointing control loops for the azimuth and elevation axes can be designed to provide precision stable pointing of the FTIR spectrometer line of sight to the selected asphalt surface below. Various rate sensor designs have been researched for providing the necessary dynamic sensing for control processing. The current design uses a MEMS IMU, which provides the rotational rate needed for the two-axis control, plus the additional sensing of translational acceleration data in addition to the rotational rate data.

The limits of the azimuth and elevation angles will require further analysis to determine the required pointing angles for a given flight path and altitude, as constrained by the detection range limits for the spectrometer. Preliminary design analysis indicates that +/- 10 degrees of rotational displacement is sufficient for the two degree of freedom for the pointing mirror.

To reconfigure the FTIR for the airborne data collection, the optical arms and end-effector are removed from the FTIR main housing (Aperture 2). The shock mount is reconfigured to a location behind the outrigger platform. The two connectors are also reconfigured to right angles to avoid interference with the telescope components.

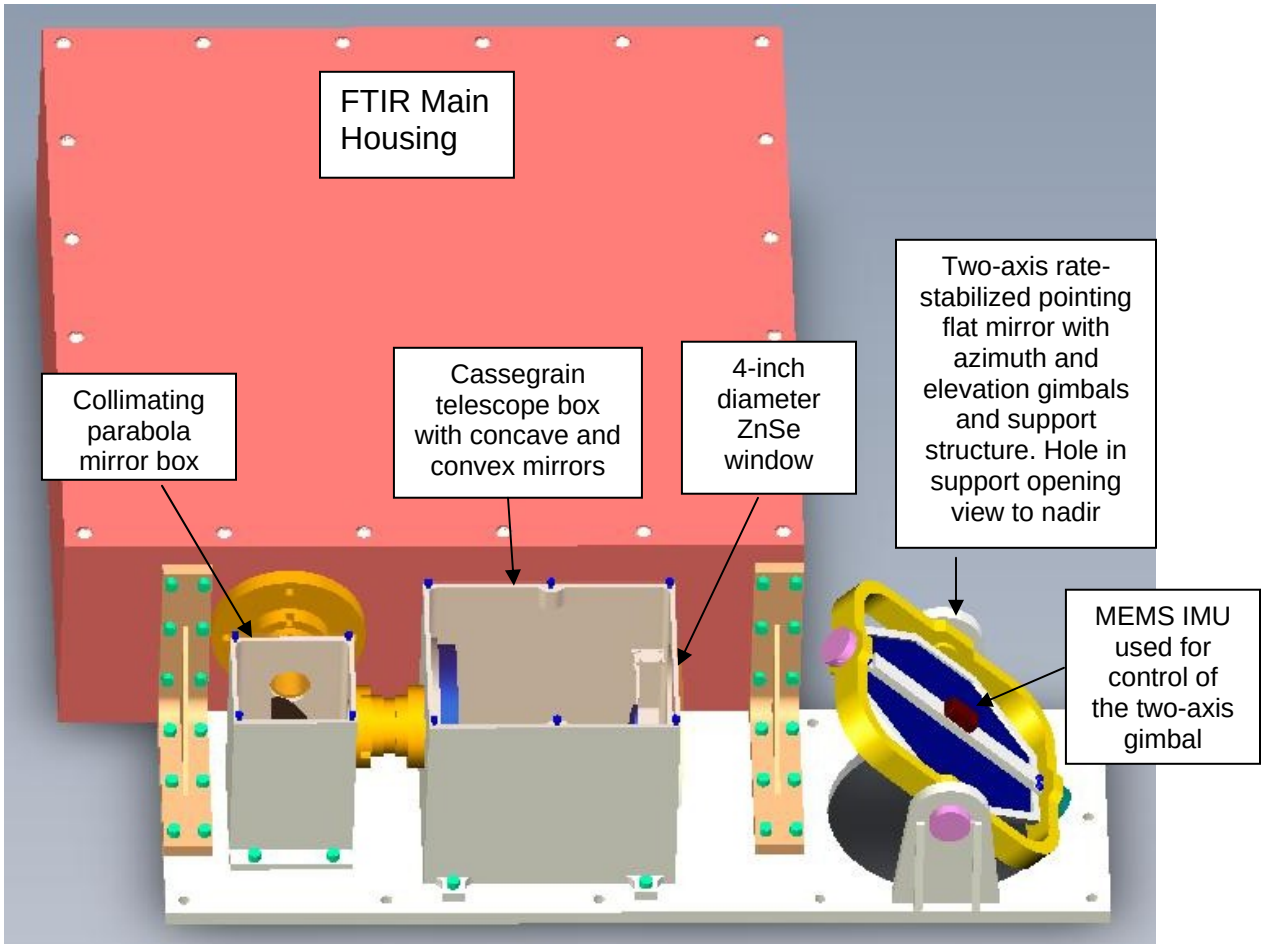

Figure 3.3-2. ASAP FTIR Design Concept Reconfigured for the Airborne Data Collection

Additional viewing perspectives of the FTIR design concept for the airborne data collection configuration are presented in Figures 3.3-3- 3.3-5.

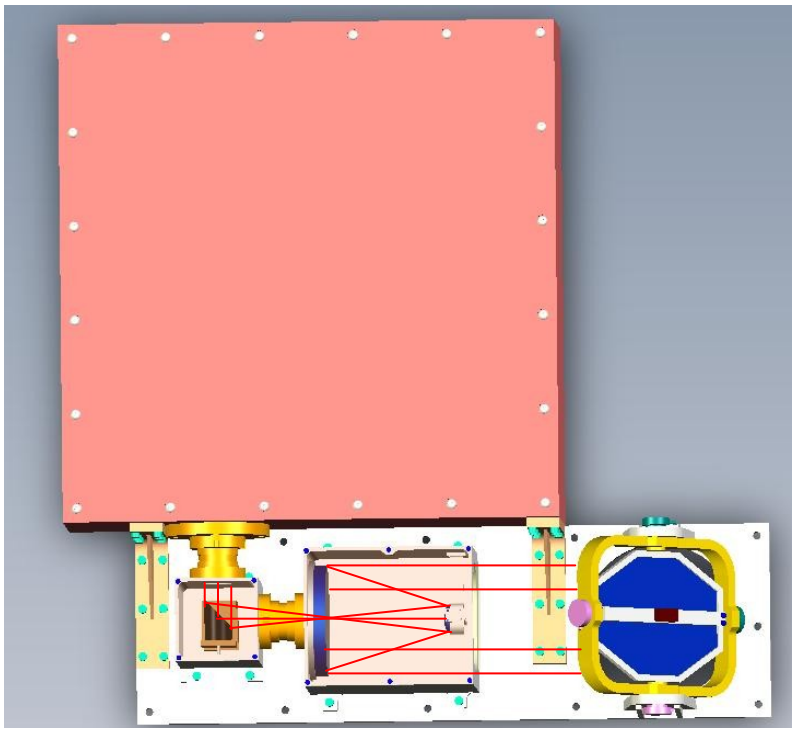

Figure 3.3-3 Top Down View of the Airborne Design Concept with Red Lines Showing Optical Beam Paths From the FTIR and Through the Telescope

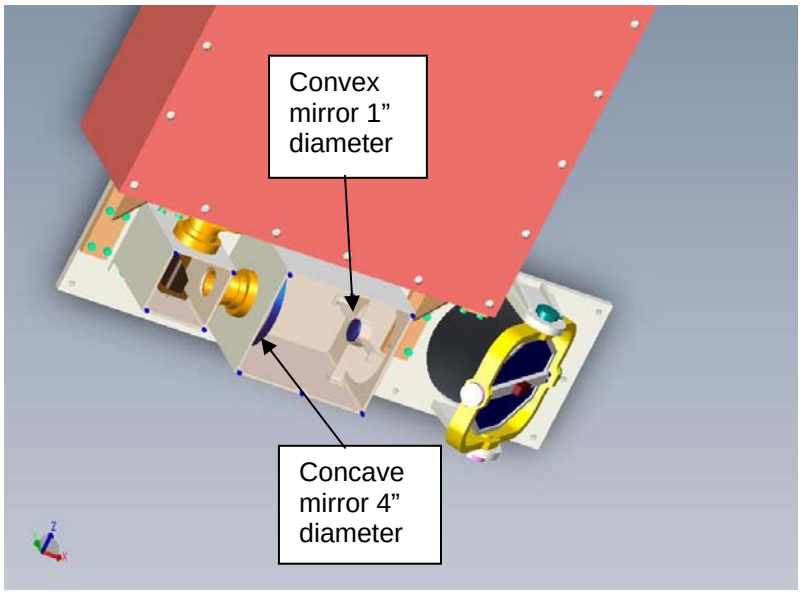

Figure 3.3-4 Backside Perspective View of the Airborne Design Concept

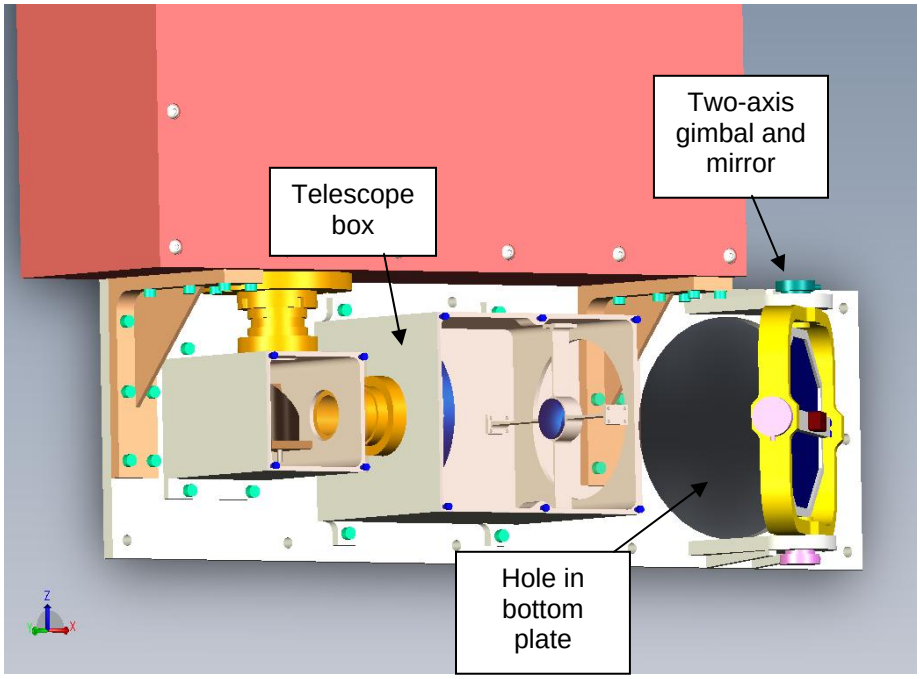

Figure 3.3-5 End–View Perspective of the Airborne Design Concept Showing Telescope and Two-Axis Gimbal Components and Hole Through Bottom Plate

Given the technical challenges posed by obtaining a fundamental asphalt spectral signature using the DRIFTS end-effector, the airborne conceptual design was basically accomplished. Various design approaches were researched and explored, and the most practical design was formulated based upon the existing FTIR instrument and the least-impact approach to developing an inertially-stabilized platform for executing a stare mode to the ground by a telescope design. This design could be developed into a prototype capability in the event additional resources could be placed on the ASAP program.

APPENDIX A

Part 2. ASAP SDD Software Design

4.0 Detailed Software Design

The ASAP software is based on National Instruments LabView development software tools. Basically LabView uses a graphical programming language that uses icons instead of lines of text to create applications involving dataflow programming. The software is controlled from a user interface known as the front panel. LabView programs are called virtual instruments (.vi's) because these graphical modules imitate various instrument functions that process data in a defined way. The Vis have three components:

- **Front panel**—Serves as the user interface
- **Block Diagram**—contains the graphical source code that defines the functionality of the VI
- **Icon and Connector Pane**—identifies the interface to the VI so that you can use the VI in another VI (called a subVI) and is analogous to a subroutine in text-based programming languages.

The VIs comprising the ASAP software is presented below. Section 4, Software Design, describes the VIs in additional detail and also presents the graphical design of the software VIs used to collect and process the ASAP FTIR spectrometer data. The VIs are:

- FTRX Applications Rev 11.vi
- Processing Interferogram
- Minimax
- ZeroPadder
- Pad to…
- Get Interferomgram
- IR Sampler- Interpolator
- Zero Phase Filter
- Decimate by 1-2-4-8
- Reference Subsampler
- Peaks and Valleys
- Subsample Indexer
- Is Even
- ZX Detector
- Threshold Detector with Hysteresis
- Configure DAQmx Read Parameters
- Configure, Load, Enable, and Wire Breakpoint
- Configure motion and move to startpoint
- Config Analog Input Channels
- Config FTIR Scan Parameters

Presentation of the ASAP system software will be primarily graphical in nature as the LabView software functionality is described very concisely with significant

supporting detail using its graphical programming language structure. For each of the VIs listed above, the following descriptions or graphical information will be presented:

- General Notes
- Connector Pane
- Front Panel
- Controls and Indicators
- Block Diagram
- List of SubVIs and Express VIs with Configuration Information

APPENDIX A

Part 3. ASAP SDD Software Headers

4.1 FTRX Applications Rev 11.vi

4.2 Processing Interferogram Rev7.vi

4.3 Minimax Rev1.vi

4.4 ZeroPadder Rev3.vi

4.5 Pad to… Rev1.vi

4.6 Get Interferogram Rev1.vi

4.7 IR Sampler- Interpolator Rev1.vi

4.8 Zero Phase Filter Rev2.vi

4.9 Decimate by 1-2-4-8 Rev2.vi

4.10 Reference Subsampler Rev2.vi

4.11 Peaks and Valleys Rev2.vi

4.12 Subsample Indexer Rev5.vi

4.13 Is Even .vi

4.14 ZX Detector rev5.vi

4.15 Threshold Detector with Hysteresis Rev2.vi

4.16 Configure DAQmx Read Parameters Rev3.vi

4.17 Configure, Load, Enable, and Wire Breakpoint Rev1

4.18 Configure motion and move to startpoint Rev3.vi

4.19 Config Analog Input Channels Rev1.vi

4.20 Config FTIR Scan Parameters Rev1.vi

APPENDIX A

Part 4. ASAP Final Report Software Diagrams

FTRX Application Rev11.vi

FTRX Applic Rev3

1. Manually scanning in one direction
2. Double-sided interferogram limited to OPD for 4cm-1 resolution, -203250 counts from approximate center.
3. 20% too many samples on each side.
4. Interferogram is centered on breakpoint, which is found and entered manually.
5. No data saving yet.

Connector Pane

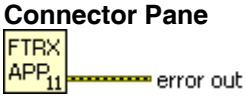

Front Panel

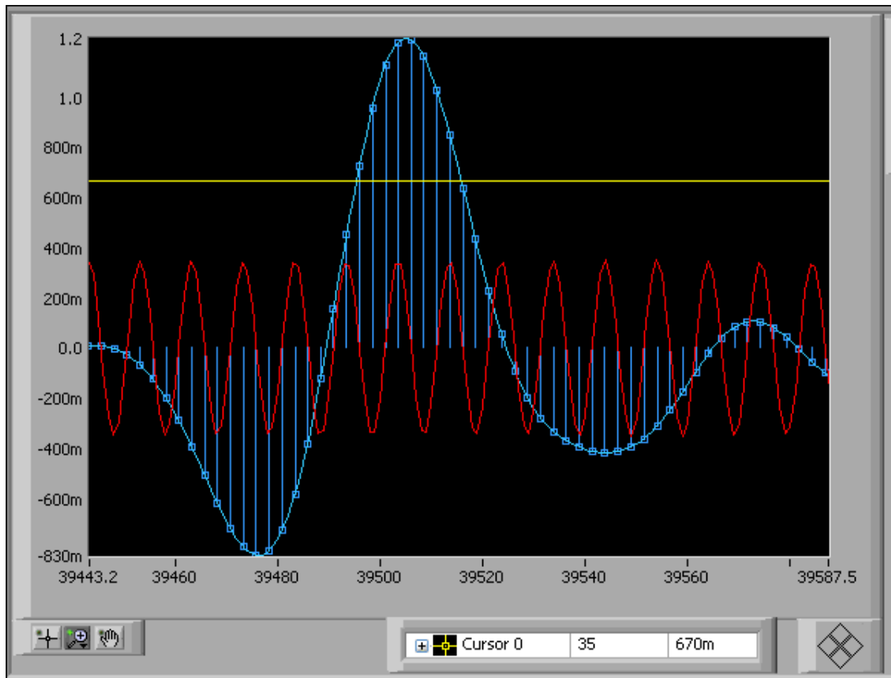

Input Ref
Input IR
Filtered Ref
Filtered IR
Resampled IR

Peak
1.22559
CB Peak
39505
Min
-0.881042
Min Index
39476

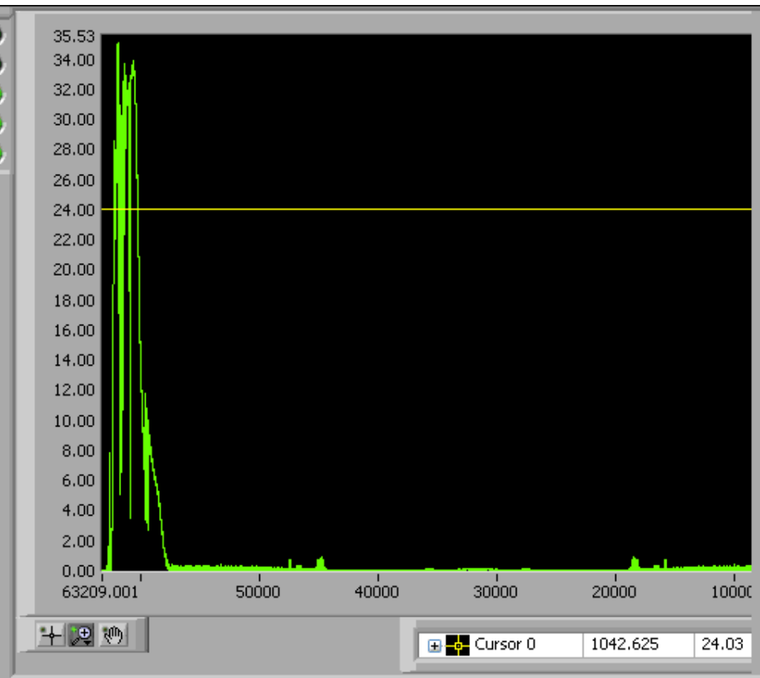

Scan Parameters
Resolution cm-1
4
Sample Rate
100000
Centerburst Pos
-203036
Active edge
Rising

Scan Positions Out
Start Position
-184073
Target Position
-221999
Breakpt Pos
-203036

Startpoint reached?
BP1

AA Filter
AAF Enabled
Lowpass Cutoff Freq
100000

New CB I32
-203036

Scan Dynamics
Velocity
40000

Dataset Sampling
Samples per Scan
79012
Sample Rate
100000

INTERFEROGRAM

Sample Freq (Hz)
100.000k
Decimate...
by 1 (No Decim.)

Input Ref
157993
0.575256

Input IR
395058
0.0189209

Ref Smoothing Filter
Filter Design
Chebyshev
Filter type
Bandpass
Order

IR Smoothing Filter
Filter Design
Chebyshev
Filter type
Bandpass
Order

IF Size
30785
Samples/Ref Wave
4

Resampled IR
39298
0

SPECTRUM

Scale Factor Used (cm-1/bin)
0.48225

Wind, Padded, FFT Size
131072

Window / Padding
window
Hamming
window parameter
NaN
Pad to...
131072

window properties
eq noise BW
1.36
coherent gain
0.54

Win Pad FFT
32003
49.7m -56.1m i

FFT Mag
131063
0.00494752

YScale.Maximum
32.5
X Scale.Range:Minimum
2280
X Scale.Range:Maximum
2400

Keep Expansion?

Enter Number of Runs
1
Enter Base Path
C:\Documents and Settings\User\My Documents\FTRX\Data Files

error out
status
source

Signal Channel Input Parameters
Reference Channel Input Parameters
DAQmx Read Input Parameters
DAQmx Read Input Parameters
Set by User

Controls and Indicators

Reference Channel Input Parameters

HeNe Reference Channel physical channels specifies the names of the physical channels to use to create virtual channels. The DAQmx physical channel constant lists all physical channels on devices and modules installed in the system.

Maximum Value

Minimum Value

Terminal Configuration

Input Coupling

Signal Channel Input Parameters

IR Signal Channel physical channels specifies the names of the physical channels to use to create virtual channels. The DAQmx physical channel constant lists all physical channels on devices and modules installed in the system.

Maximum Value

Minimum Value

Terminal Configuration

Input Coupling

DAQmx Read Input Parameters

RelativeTo

Offset

ChannelsToRead

WfmAttr

ReadAllAvailSamp

AutoStart

OverWrite

WaitMode

SleepTime

Scan Dynamics

Velocity

Acceleration

S Curve Time

Scan Parameters

Resolution cm-1

Sample Rate

Centerburst Pos

Active edge edge specifies on which edge of the digital signal the Reference Trigger occurs.

IR Smoothing Filter

Filter Design

Filter type

Order

Lower

Higher

Ref Smoothing Filter

Filter Design

Filter type filter type specifies the passband of the filter.

Order order is the order of the IIR filter and must be greater than zero. If **order** is less than or equal to zero, the VI sets **Reverse Coefficients** and **Forward Coefficients** to empty arrays and returns an error.

Reference Freq low cutoff freq: fl is the low cutoff frequency and must observe the Nyquist criterion.

Track.Percentage low cutoff freq: fl is the low cutoff frequency and must observe the Nyquist criterion.

Decimate...

Keep Expansion?

YScale.Maximum

X Scale.Range:Maximum

X Scale.Range:Minimum

Window / Padding

window window is the window to apply to **X**.

window parameter window parameter is the beta parameter for a Kaiser window, the standard deviation for a Gaussian window, and the ratio, s, of the mainlobe to the sidelobe for a Dolph-Chebyshev window. If **window** is any other window, this VI ignores this input.

The default value of **window parameter** is NaN, which sets beta to 0 for a Kaiser window, the standard deviation to 0.2 for a Gaussian window, and s to 60 for a Dolph-Chebyshev window.

Pad to...

IF Plots Selector

Enter Number of Runs

Enter Base Path

BP1

Startpoint reached?

Dataset Sampling

Samples per Scan

Sample Rate

+OPD Samples

Active edge

Reference Channel Verify

Verify Reference Channel physical channels specifies the names of the physical channels to use to create virtual channels. The DAQmx physical channel constant lists all physical channels on devices and modules installed in the system.

Range Set High

Range Set Low

Signal Channel Verify

Verify Signal Channel physical channels specifies the names of the physical channels to use to create virtual channels. The DAQmx physical channel constant lists all physical channels on devices and modules installed in the system.

Range Set High

Range Set Low

AA Filter

AAF Enabled

Lowpass Cutoff Freq

DAQmx Read Input Parameters Set by User

RelativeTo

Offset

ChannelsToRead

WfmAttr

ReadAllAvailSamp

AutoStart

OverWrite

WaitMode

SleepTime

Scan Positions Out

Start Position

Target Position

Breakpt Pos

New CB I32

IF Size

Samples/Ref Wave

Input IR

Interferogram

Input Ref

Reference

Sample Freq (Hz)

Resampled IR

Numeric

FFT Mag

Win Pad FFT FFT {X} is the FFT of **X**.

FFT {X} is the FFT of **X**.

Scale Factor Used (cm-1/bin)

window properties window properties returns the coherent gain and equivalent noise bandwidth of the window.

eq noise BW eq noise BW returns the equivalent noise bandwidth of the window. You can use **eq noise BW** to divide a sum of individual power spectra or to compute the power in a given frequency span.

coherent gain coherent gain returns the inverse of the scaling factor this VI applies to the window.

Wind, Padded, FFT Size

Interferogram Cluster

Resampled Interferogram

Interferogram Minimax

Peak

CB Peak


Min


Min Index


Spectrum Cluster


Spectrum


Interferogram Minimax


Peak


Peak cm-1


Min


Min cm-1


error out error in can accept error information wired from VIs previously called. Use this information to decide if any functionality should be bypassed in the event of errors from other VIs.

Right-click the **error in** control on the front panel and select **Explain Error** or **Explain Warning** from the shortcut menu for more information about the error.


status status is TRUE (X) if an error occurred or FALSE (checkmark) to indicate a warning or that no error occurred.

Right-click the **error in** control on the front panel and select **Explain Error** or **Explain Warning** from the shortcut menu for more information about the error.


code code is the error or warning code.

Right-click the **error in** control on the front panel and select **Explain Error** or **Explain Warning** from the shortcut menu for more information about the error.


source source describes the origin of the error or warning.

Right-click the **error in** control on the front panel and select **Explain Error** or **Explain Warning** from the shortcut menu for more information about the error.

Block Diagram

Dataset Sampling
Scan Positions Out
Reference Channel Verify
AA Filter
Signal Channel Verify

1. Configure In-Scan analog input channels
Configure DAQmx read parameters
2. Configure motion and move to startpoint
3. Configure In-Scan centerburst Breakpoint

5. Load first target position (negative OPD)
6. Configure In-Scan Reference Trigger
7. Configure DAQmx read parameters
8. Start In-Scan Read
The In-Scan Read should return Samples per Scan samples, of which +OPD Samples are pre-trigger samples as configured by the Reference Digital Edge.
9. Start In-Scan Move
10. When first breakpoint, at entered centerburst position, is encountered, load and arm second breakpoint.
11. Read the In-Scan data and display it.
12. Store In-Scan data
13. Stop Task [In-Scan]
14. Clear Task [In-Scan]

Enter Number of Runs
DAQmx Read Input Parameters
Reference Channel Input Parameters
Board ID
Axis 1
/Dev1/PFI0
Scan Dynamics
Scan Parameters
Signal Channel Input Parameters

Startpoint reached?
DAQmx Read Input Parameters Set by User

Timeout
Profile Complete
Motor Off
Position Brkpt
BP1
status
NOR
If BP1 reached, pass Enable 2d Bp, and light BP1 lamp.
EXIT ENTIRE LOOP IF PROFILE COMPLETE, MOTOR OFF OR ERROR TRUE

Analog 2D DBL NChan NSamp
Input Ref
Input IR
New CB I32

Start Position
Breakpt Pos
Target Position
Velocity
Samples per Scan
+OPD Samples
Active edge
Reference Digital Edge

Centerburst Pos
Sample Rate

IF Plots Selector
Keep Expansion?
X Scale.Range:Minimum
Window / Padding
Sample Freq (Hz)
Decimate...
Ref Smoothing Filter
IR Smoothing Filter
YScale.Maximum
X Scale.Range:Maximum

Interferogram Cluster
IF Size
Spectrum Cluster
Samples/Ref Wave
Scale Factor Used (cm-1/bin)
Wind, Padded, FFT Size
Win Pad FFT
window properties
FFT Mag
Resampled IR

Spectrum Cluster
Cluster
Cluster (strict)
Array (strict)
Cluster (strict)
XYGraph (strict)
XYGraph (strict)
IF Plots Selector
Array
Interferogram Cluster
Cluster
Spectrum
XYGraph
Resampled Interferogram
XYGraph
Spectrum Cluster
IF Plots Selector
Interferogram Cluster
Spectrum X-Y Graph
Resampled Interferogram X-Y Graph

Rev 7 replaces Conf Motion and move to startpoint Rev1 with Rev2, which contains Enable axes, which instantiates 62.5usec update rate, not possible in MAX with PCI cards.

To use Innova PCI system, without internal RTSI jumper, we are trying:
(a) Set Source input of DAQmx Reference Trigger to /Dev1/PFI0.
The source physical terminals become pins 11 and 12 of the 56120 breakout.
(b) We are leaving alone Configure, Load, Enable and Wire Breakpoint Rev1 to send Breakpoint to RTSI0 line, although we will not use that line.
(c) We physically connect the Breakpoint 1 output, pins 26 and 25 of the 7354 to the pins mentioned in (a) using a twisted pair jumper.

Rev 8 removes entirely the trajectory monitoring and displaying, and redundant display of the interferogram. Both interferogram and spectrum are now displayed at once.

Rev9 adds coadding and defers front panel updates.

Disabled
Choose filepath to write
open or create
write-only
little-endian
Write data arrays into binary files.
Root directory is input.
Number of arrays or runs is input.
An array of refnums to the files is generated.

Open/Create/Replace File
open or create
write-only
little-endian
error out

Enter Base Path

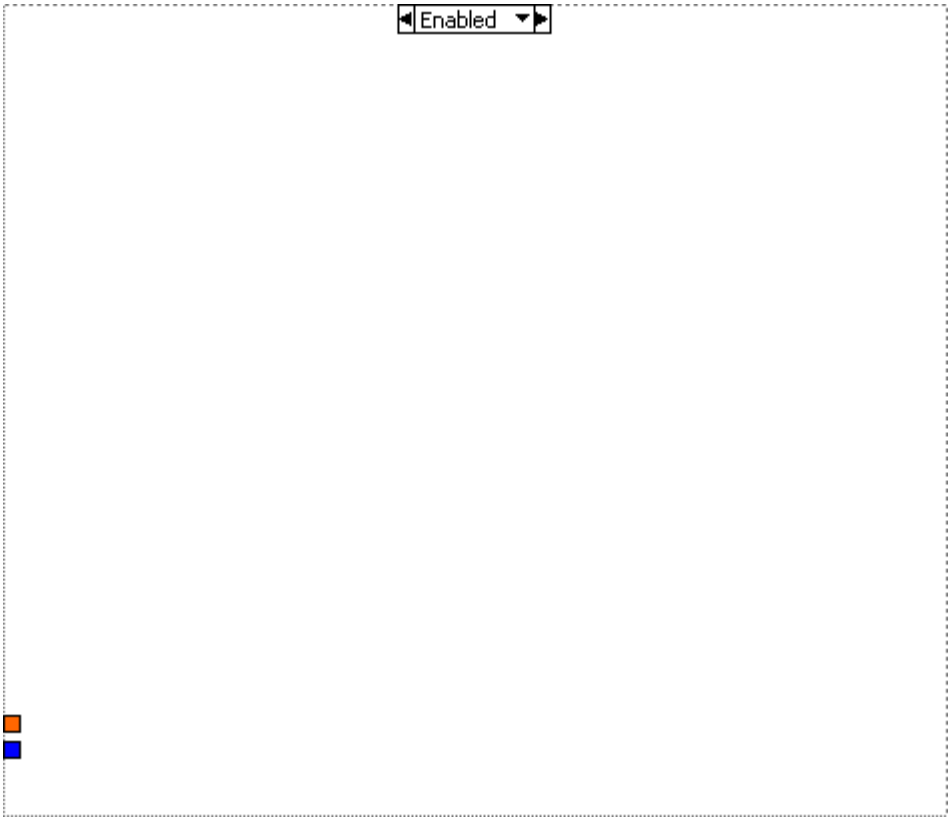

List of SubVIs and Express VIs with Configuration Information

DAQmx Clear Task.vi
C:\Program Files\National Instruments\LabVIEW 8.5\vi.lib\DAQmx\configure\task.llb\DAQmx Clear Task.vi

Processing Interferogram Rev7.vi
C:\Documents and Settings\User\My Documents\FTRX\Processing Interferogram Rev7.vi

Pad to...Rev1.ctl
C:\Documents and Settings\User\My Documents\FTRX\Pad to...Rev1.ctl

DAQmx Stop Task.vi
C:\Program Files\National Instruments\LabVIEW 8.5\vi.lib\DAQmx\configure\task.llb\DAQmx Stop Task.vi

DAQmx Read (Analog 2D DBL NChan NSamp).vi
C:\Program Files\National Instruments\LabVIEW 8.5\vi.lib\DAQmx\read.llb\DAQmx Read (Analog 2D DBL NChan NSamp).vi

DAQmx Read.vi
C:\Program Files\National Instruments\LabVIEW 8.5\vi.lib\DAQmx\read.llb\DAQmx Read.vi

Read per Axis Status.flx
C:\Program Files\National Instruments\LabVIEW 8.5\vi.lib\Motion\FlexMotion\FunctionsVIs\Trajectory.llb\Read per Axis Status.flx

Board Id
C:\Program Files\National Instruments\LabVIEW 8.5\vi.lib\Motion\FlexMotion\CustomControls\CustomControls.llb\Board Id

Start Motion (8 axes).flx
C:\Program Files\National Instruments\LabVIEW 8.5\vi.lib\Motion\FlexMotion\FunctionsVIs\StartStopMotion.llb\Start Motion (8 axes).flx

Start Motion.flx
C:\Program Files\National Instruments\LabVIEW 8.5\vi.lib\Motion\FlexMotion\FunctionsVIs\StartStopMotion.llb\Start Motion.flx

DAQmx Start Task.vi
C:\Program Files\National Instruments\LabVIEW 8.5\vi.lib\DAQmx\configure\task.llb\DAQmx Start Task.vi

Configure DAQmx Read Parameters Rev3.vi
C:\Documents and Settings\User\My Documents\FTRX\Configure DAQmx Read Parameters Rev3.vi

Load Target Position.flx
C:\Program Files\National Instruments\LabVIEW 8.5\vi.lib\Motion\FlexMotion\FunctionsVIs\Trajectory.llb\Load Target Position.flx

Axis To Control.flx
C:\Program Files\National Instruments\LabVIEW 8.5\vi.lib\Motion\FlexMotion\CustomControls\CustomControls.llb\Axis To Control.flx

Configure, Load, Enable and Wire Breakpoint Rev1.vi
C:\Documents and Settings\User\My Documents\FTRX\Configure, Load, Enable and Wire Breakpoint Rev1.vi

Configure motion and move to startpoint Rev3.vi
C:\Documents and Settings\User\My Documents\FTRX\Configure motion and move to startpoint Rev3.vi

DAQmx Reference Trigger (Digital Edge).vi
C:\Program Files\National Instruments\LabVIEW 8.5\vi.lib\DAQmx\configure\trigger.llb\DAQmx Reference Trigger (Digital Edge).vi

DAQmx Trigger.vi
C:\Program Files\National Instruments\LabVIEW 8.5\vi.lib\DAQmx\configure\trigger.llb\DAQmx Trigger.vi

Config Analog Input Channels Rev1.vi
C:\Documents and Settings\User\My Documents\FTRX\Config Analog Input Channels Rev1.vi

Config FTIR Scan Parameters Rev1.vi
C:\Documents and Settings\User\My Documents\FTRX\Config FTIR Scan Parameters Rev1.vi

Processing Interferogram Rev7.vi
See the BD for explanation.

Connector Pane

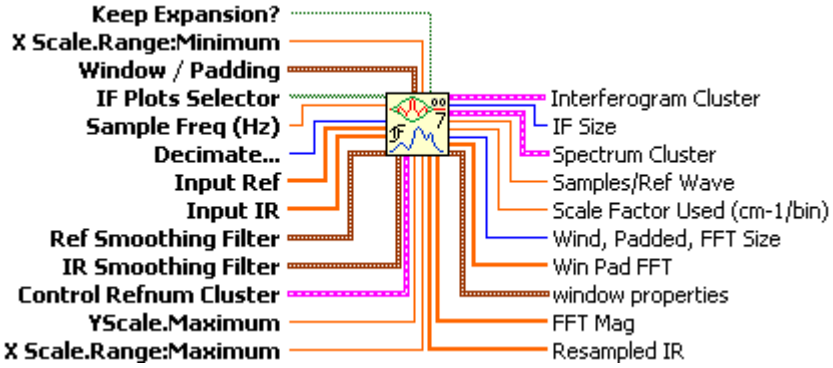

Front Panel

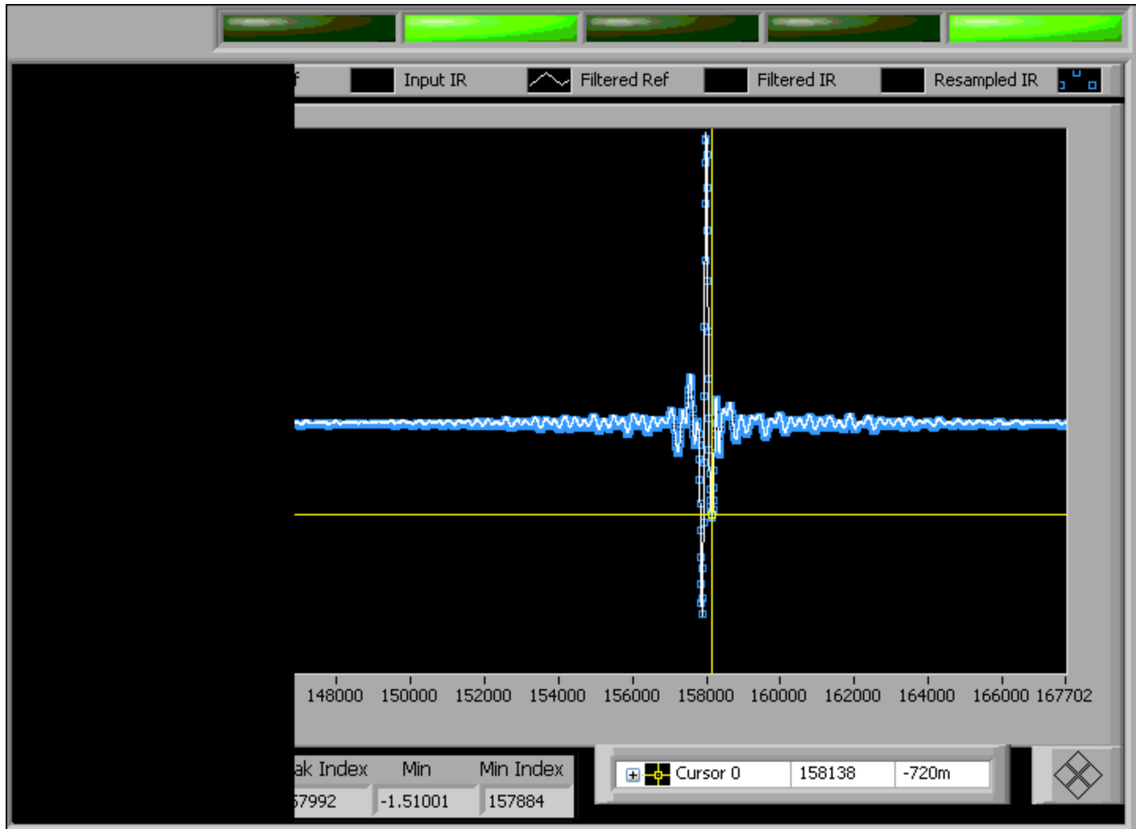

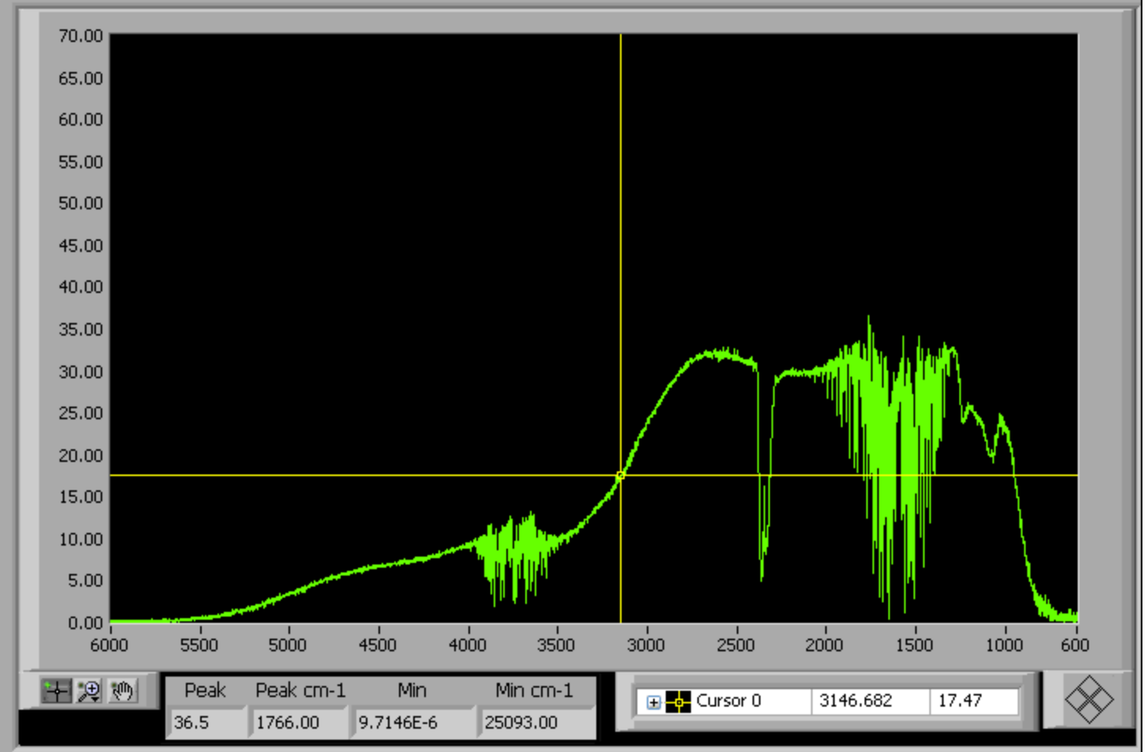

INTERFEROGRAM

Sample Freq (Hz) 400.000k

Decimate... by 1 (No Decim.)

Input Ref 316360 0.575256

Input IR 158179 -0.64209

Ref Smoothing Filter

Filter Design Chebychev

IR Smoothing Filter

Filter Design Chebychev

SPECTRUM

Scale Factor Used (cm-1/bin) 0.48225

Wind, Padded, FFT Size 131072

Window / Padding

window Rectangle

window parameter NaN

Pad to... 131072

window properties

eq noise BW 1.00

coherent gain 1.00

Win Pad FFT 131071 11.4m +17.7m i

FFT Mag 0 0.0273671

YScale.Maximum 32.5

Controls and Indicators

Window / Padding

window window is the window to apply to **X**.

window parameter window parameter is the beta parameter for a Kaiser window, the standard deviation for a Gaussian window, and the ratio, s, of the mainlobe to the sidelobe for a Dolph-Chebyshev window. If **window** is any other window, this VI ignores this input.

The default value of **window parameter** is NaN, which sets beta to 0 for a Kaiser window, the standard deviation to 0.2 for a Gaussian window, and s to 60 for a Dolph-Chebyshev window.

Pad to...

X Scale.Range:Minimum

X Scale.Range:Maximum

Keep Expansion?

YScale.Maximum

Decimate...

Sample Freq (Hz)

Input Ref

Reference

Input IR

Interferogram

Ref Smoothing Filter

Filter Design

Filter type filter type specifies the passband of the filter.

Order order is the order of the IIR filter and must be greater than zero. If **order** is less than or equal to zero, the VI sets **Reverse Coefficients** and **Forward Coefficients** to empty arrays and returns an error.

Reference Freq low cutoff freq: fl is the low cutoff frequency and must observe the Nyquist criterion.

Track.Percentage low cutoff freq: fl is the low cutoff frequency and must observe the Nyquist criterion.

IR Smoothing Filter

Filter Design

Filter type

Order

Lower

Higher

IF Plots Selector

Control Refnum Cluster

Spectrum Cluster

IF Plots Selector

Interferogram Cluster

Spectrum X-Y Graph

Resampled Interferogram X-Y Graph

IF Size

Wind, Padded, FFT Size

window properties window properties returns the coherent gain and equivalent noise bandwidth of the window.

eq noise BW eq noise BW returns the equivalent noise bandwidth of the window. You can use **eq noise BW** to divide a sum of individual power spectra or to compute the power in a given frequency span.

coherent gain coherent gain returns the inverse of the scaling factor this VI applies to the window.

Windowed, Padded IF

Scale Factor Used (cm-1/bin)

Win Pad FFT FFT {X} is the FFT of **X**.

FFT {X} is the FFT of **X**.

Samples/Ref Wave

Resampled IR

Numeric

Interferogram Cluster

Resampled Interferogram

Interferogram Minimax

Peak

Peak Index

Min

Min Index

Spectrum Cluster

Spectrum

Interferogram Minimax

Peak

Peak cm-1

Min

Min cm-1

FFT Mag

Block Diagram

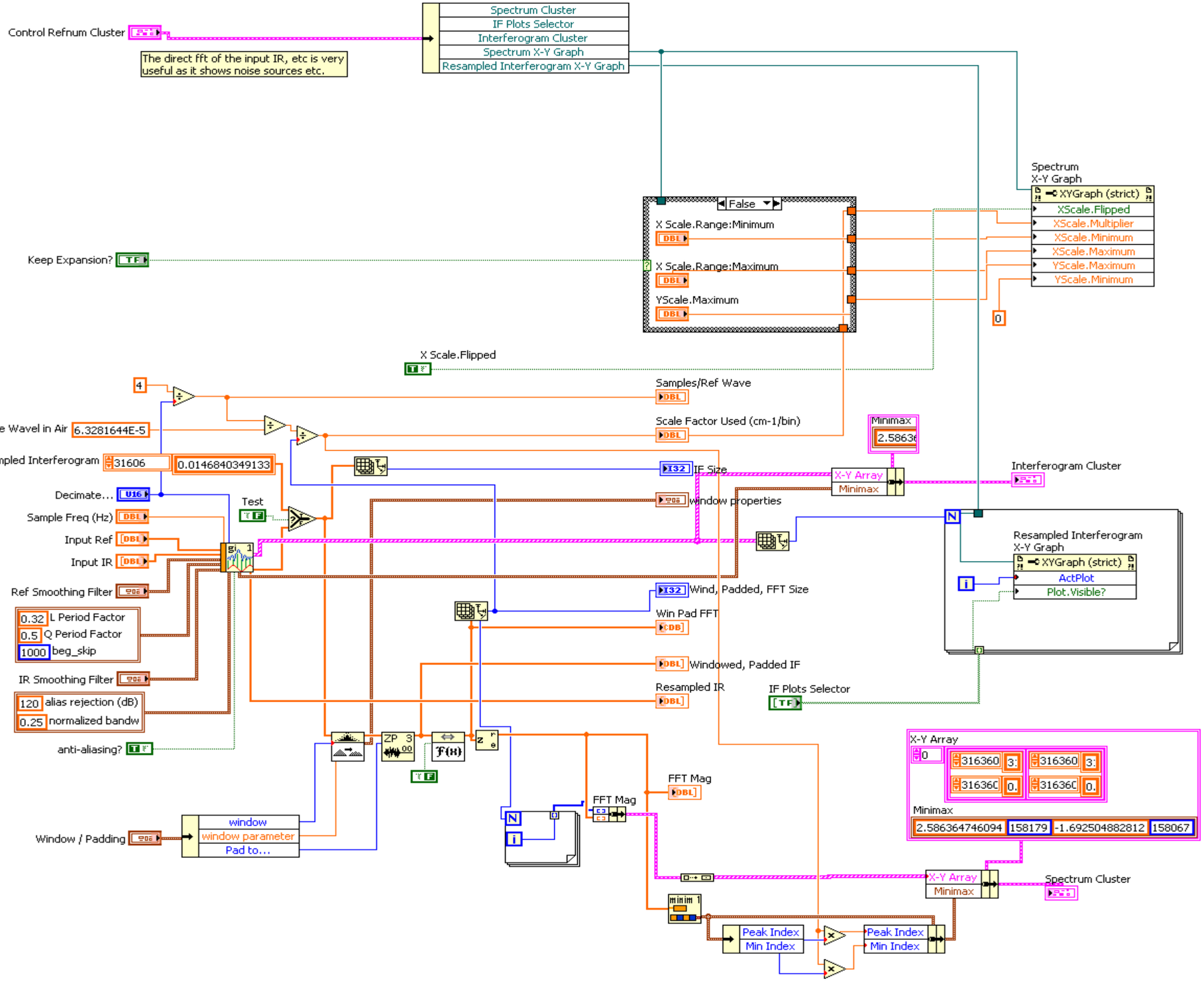
Control Refnum Cluster
The direct fft of the input IR, etc is very useful as it shows noise sources etc.
Spectrum Cluster
IF Plots Selector
Interferogram Cluster
Spectrum X-Y Graph
Resampled Interferogram X-Y Graph
Keep Expansion?
False
X Scale.Range:Minimum
X Scale.Range:Maximum
YScale.Maximum
Spectrum
X-Y Graph
XYGraph (strict)
XScale.Flipped
XScale.Multiplier
XScale.Minimum
XScale.Maximum
YScale.Minimum
0
X Scale.Flipped
4
Samples/Ref Wave
HeNe Wavel in Air
6.3281644E-5
Scale Factor Used (cm-1/bin)
Minimax
2.5863
Test Resampled Interferogram
31606
0.0146840349133
IF Size
X-Y Array
Minimax
Interferogram Cluster
Decimate...
Test
window properties
Sample Freq (Hz)
Input Ref
Input IR
Resampled Interferogram
X-Y Graph
XYGraph (strict)
ActPlot
Plot.Visible?
Ref Smoothing Filter
Wind, Padded, FFT Size
0.32 L Period Factor
0.5 Q Period Factor
1000 beg_skip
Win Pad FFT
IR Smoothing Filter
Windowed, Padded IF
120 alias rejection (dB)
0.25 normalized bandw
Resampled IR
IF Plots Selector
anti-aliasing?
ZP 3
FFT Mag
FFT Mag
X-Y Array
0
316360
3
316360
0.
Minimax
2.586364746094
158179
-1.692504882812
158067
window
window parameter
Pad to...
Window / Padding
X-Y Array
Minimax
Spectrum Cluster
minim 1
Peak Index
Min Index
Peak Index
Min Index

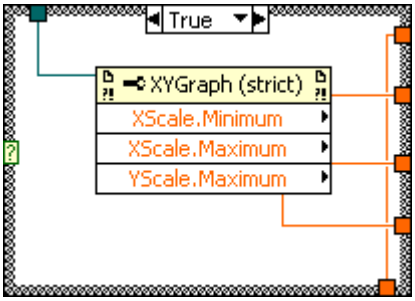

List of SubVIs and Express VIs with Configuration Information

Minimax Rev1.vi
C:\Documents and Settings\User\My Documents\FTRX\Minimax Rev1.vi

NI_AALPro.lvlib:Real FFT.vi
C:\Program Files\National Instruments\LabVIEW 8.5\vi.lib\Analysis\2dsp.llb\Real FFT.vi

NI_AALPro.lvlib:FFT.vi
C:\Program Files\National Instruments\LabVIEW 8.5\vi.lib\Analysis\2dsp.llb\FFT.vi

ZeroPadder Rev3.vi
C:\Documents and Settings\User\My Documents\FTRX\ZeroPadder Rev3.vi

Pad to...Rev1.ctl
C:\Documents and Settings\User\My Documents\FTRX\Pad to...Rev1.ctl

NI_AALPro.lvlib:Scaled Time Domain Window (DBL).vi
C:\Program Files\National Instruments\LabVIEW 8.5\vi.lib\Analysis\0measdsp.llb\Scaled Time Domain Window (DBL).vi

NI_AALPro.lvlib:Scaled Time Domain Window.vi
C:\Program Files\National Instruments\LabVIEW 8.5\vi.lib\Analysis\0measdsp.llb\Scaled Time Domain Window.vi

Get Interferogram Rev1.vi
C:\Documents and Settings\User\My Documents\FTRX\Get Interferogram Rev1.vi

Minimax Rev1.vi

Connector Pane

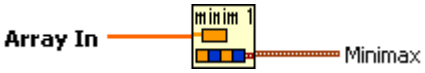

Front Panel

Controls and Indicators

Array In

Interferogram

Minimax

Peak

Peak Index

Min

Min Index

Block Diagram

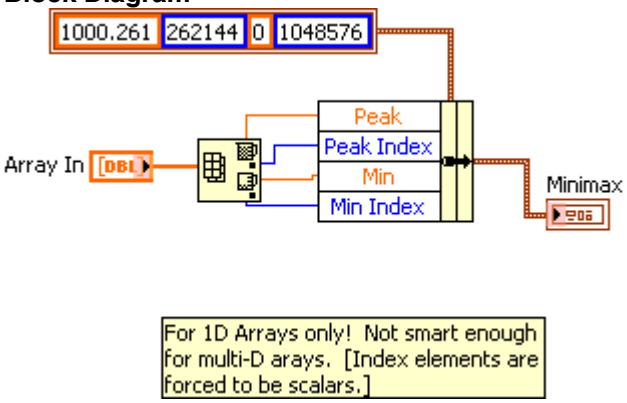

List of SubVIs and Express VIs with Configuration Information

ZeroPadder Rev3.vi
Zero-Padder Rev1

If Pad to... .LE. Size[X] Padded X = X
Else Padded X = (X with zeros concatenated on the end, for an array size shown by Pad to...)

Zero-Padder Rev1 does not truncate X if Size [X] < Pad to... value

Zero-Padder Rev1 works for 1D arrays and is not smart about higher dimensional arrays.

Connector Pane

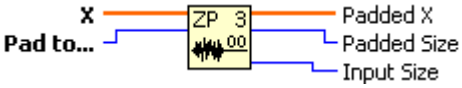

Front Panel

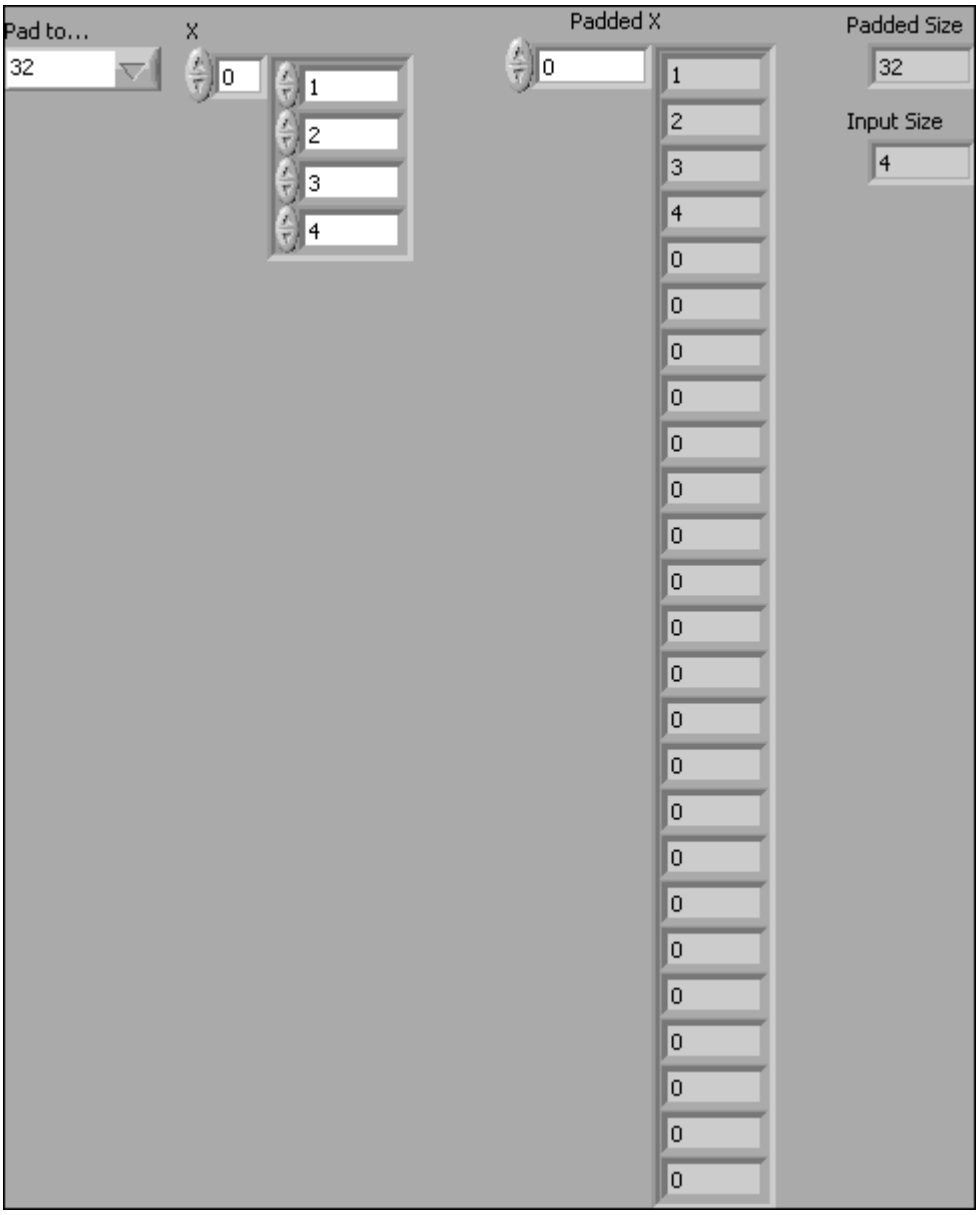

Controls and Indicators

X

Numeric

Pad to...

Padded X

element

Padded Size

Input Size

Block Diagram

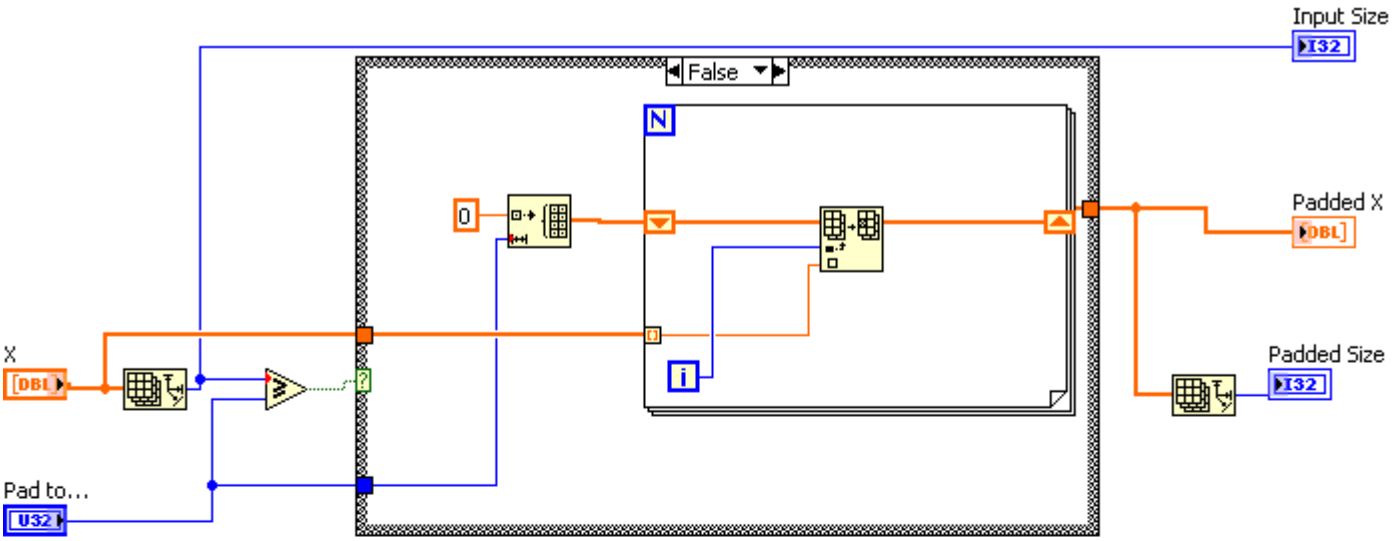

Zero-Padder Rev2

If Pad to... < Size[X] Padded X = X
Else Padded X = (X with zeros concatenated on the end, for an array size shown by Pad to...)

Zero-Padder does not truncate X if Size [X] < Pad to... value

Zero-Padder works for 1D arrays and is not smart about higher dimensional arrays.

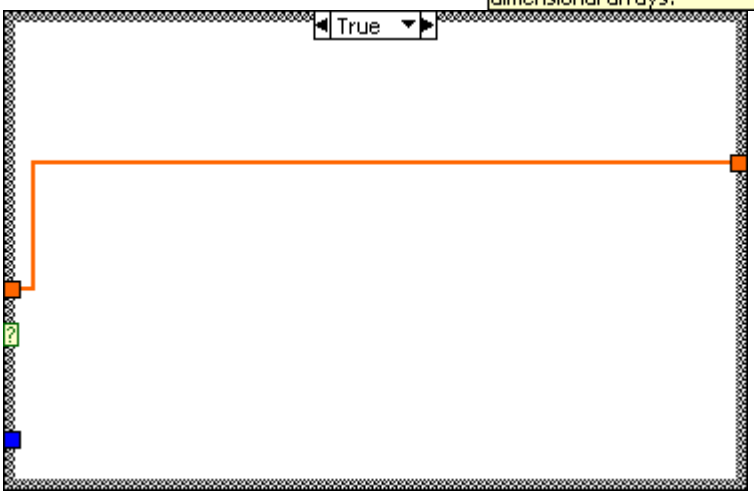

List of SubVIs and Express VIs with Configuration Information

Pad to...Rev1.ctl

C:\Documents and Settings\User\My Documents\FTRX\Pad to...Rev1.ctl

Pad to...Rev1.ctl

Connector Pane

Front Panel

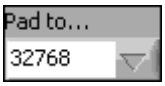

Controls and Indicators

U32 **Pad to...**

List of SubVIs and Express VIs with Configuration Information

Get Interferogram Rev1.vi

Connector Pane

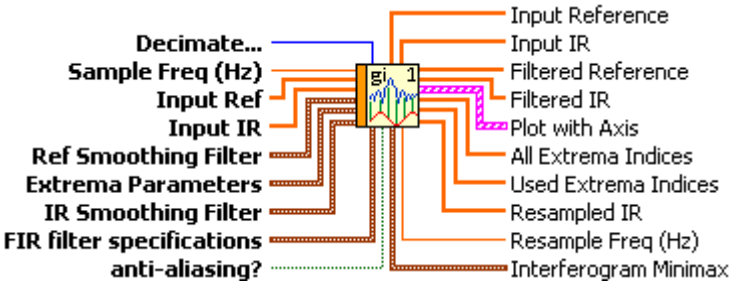

Front Panel

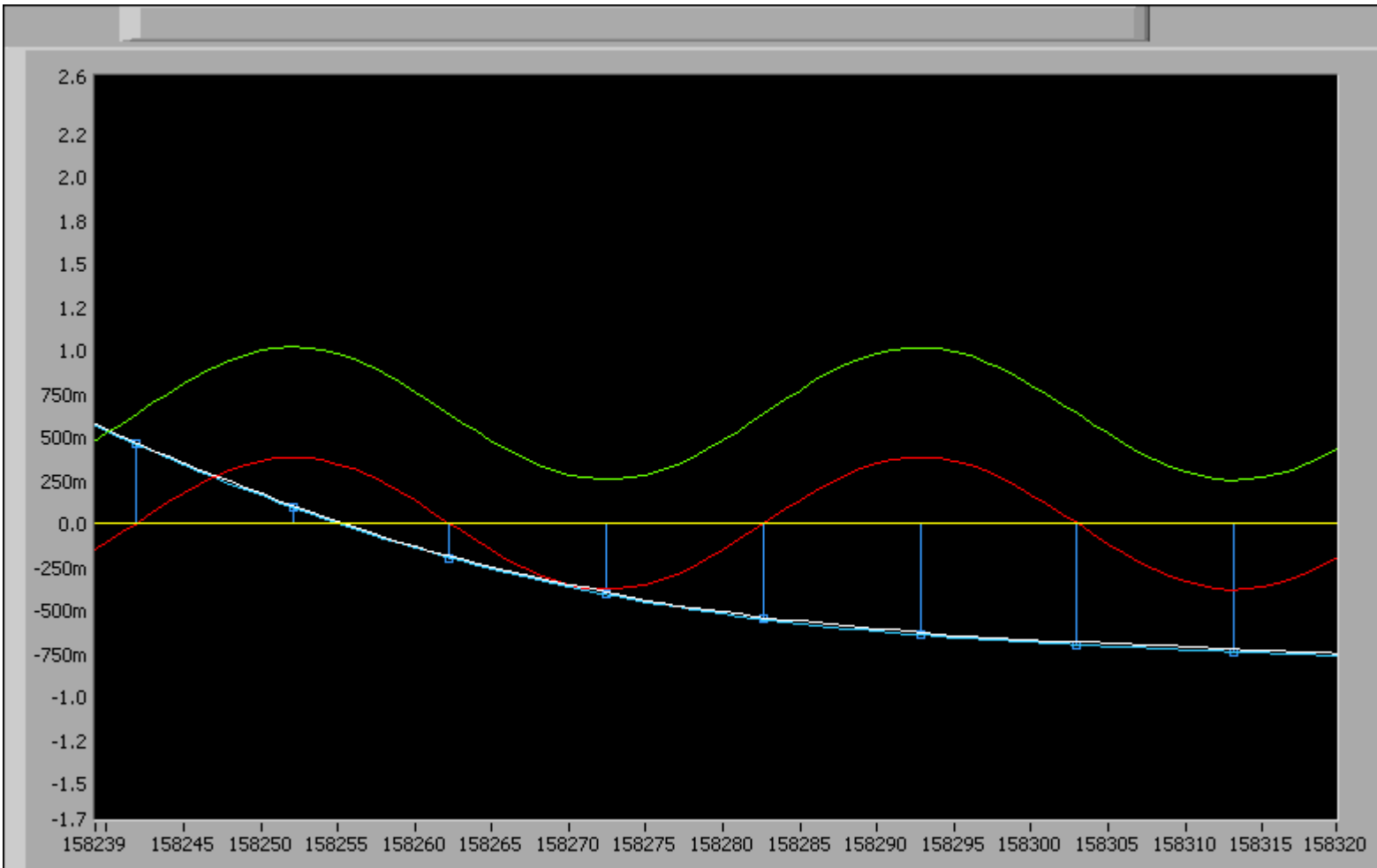

Peak	Peak Index	Min	Min Index
2.58636	158179	-1.6925	158067

Cursor 0	47387	1.8m

Sample Freq (Hz): 400.000k

Decimate... by 1 (No Decim.) 1

Input Ref: 316360 | 0.293579

Input IR: 158179 | 2.58636

Input Reference: 316360 | 0.293579

Input IR: 158179 | 2.58636

Filtered Reference: 316360 | 9.24413E-5

Filtered IR: 158179 | 2.56769

Used Extrema Indices: 31410 | 315358.2

Resampled IR: 16030 | 0.00505906

All Extrema Indices: 31410 | 315358.2

Resample Freq (Hz): 40.0000k

Ref Smoothing Filter

- Filter Design: Chebyshev
- Filter type: Bandpass
- Order: 5
- Reference Freq: 10.00k
- Track.Percentage: 1.250

IR Smoothing Filter

- Filter Design: Chebyshev
- Filter type: Bandpass
- Order: 3
- Lower: 360
- Higher: 3800

Extrema Parameters

- L Period Factor

anti-aliasing?

Controls and Indicators

Sample Freq (Hz)

anti-aliasing? anti-aliasing? specifies whether the input signal undergoes lowpass filtering when LabVIEW downsamples the signal.

Ref Smoothing Filter

- **Filter Design**
- **Filter type filter type** specifies the passband of the filter.
- **Order order** is the order of the IIR filter and must be greater than zero. If **order** is less than or equal to zero, the VI sets **Reverse Coefficients** and **Forward Coefficients** to empty arrays and returns an error.
- **Reference Freq low cutoff freq: fl** is the low cutoff frequency and must observe the Nyquist criterion.
- **Track.Percentage low cutoff freq: fl** is the low cutoff frequency and must observe the Nyquist criterion.

Extrema Parameters

- **L Period Factor**
- **Q Period Factor**
- **beg_skip**

IR Smoothing Filter

- **Filter Design**
- **Filter type**
- **Order**
- **Lower**
- **Higher**

FIR filter specifications FIR filter specifications specifies the minimum values this VI needs to specify the FIR filter.

- **alias rejection (dB) alias rejection (dB)** specifies the minimum attenuation level of signal components aliased after any resampling operation. The default is 120.
- **normalized bandw normalized bandwidth** specifies the fraction of the new sampling rate that is not attenuated. The default is 0.4536.

Decimate...

Input IR

- **Interferogram**

Input Ref

Reference

Interferogram Minimax

Peak

Peak Index

Min

Min Index

Plot with Axis

All Extrema Indices

Used Extrema Indices

Numeric

Filtered IR

Numeric

Resampled IR

Numeric

Filtered Reference

Numeric

Input IR

Interferogram

Input Reference

Reference

Resample Freq (Hz)

Block Diagram

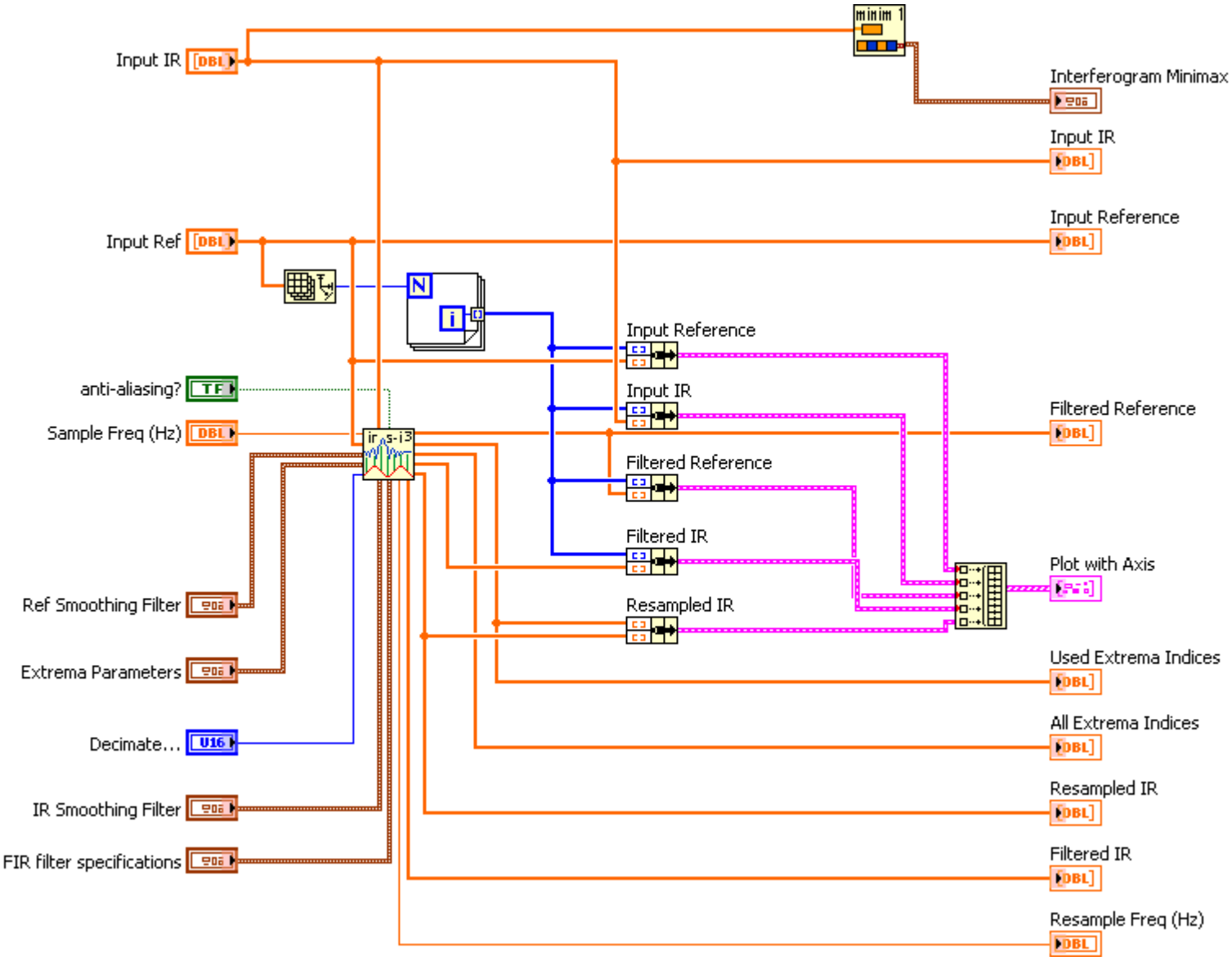

List of SubVIs and Express VIs with Configuration Information

Minimax Rev1.vi
C:\Documents and Settings\User\My Documents\FTRX\Minimax Rev1.vi

IR Sampler - Interpolator Rev3.vi
C:\Documents and Settings\User\My Documents\FTRX\IR Sampler - Interpolator Rev3.vi

IR Sampler - Interpolator Rev3.vi

IR Sampler - Interpolator uses **Reference Signal**, a quasi-sinusoid at approximately **HeNe Freq Est**, to resample a filtered version of **IR Signal**.

Reference Signal and **IR Signal** are simultaneously sampled at **Sample Frequency**, and have the same number of elements. **Sample Frequency** may be derived by decimation; it may not be the same frequency as the original sample frequency. **HeNe Freq Est** is used to determine the averaging parameters to acquire the zero crossings and peaks and valleys of the HeNe waveform. The **Ref S-G Period Factor** is that fraction of a nominal HeNe period to perform a moving Savitsky-Golay zero phase smoothing of the HeNe waveform. **Ref Q Period Factor** is that fraction of a nominal HeNe period over which to perform a quadratic fit to extract the peak and valley indices. **Ref L Period Factor** is that fraction of a nominal HeNe period over which to perform a straight line fit to acquire zero crossing data. It needs to be adjusted so that an odd number of points are used. This is not automatically done in Rev1. The input IR signal array itself has a highest frequency which limits the smoothing proces. The **IR S-G Period Factor** governs that.

Ouput are the Filtered Reference, Extrema Indices, an array consisting of the consecutive zero crossings and peaks and valley expressed as fractional indices, the Input and Filtered IR, and the Resampled IR at the Extrema fractional indices.

The Hermite Interpolation routine is extremely time-consuming. The interpolation is essentially a convolution operation, in which the kernel is controlled by the Extrema array. Therefore it is suggested strongly that in Rev 2, decimation of the IR and Reference arrays occur immediately after filtering, to minimize the size of the interpolating array, and hence the execution time.

Connector Pane

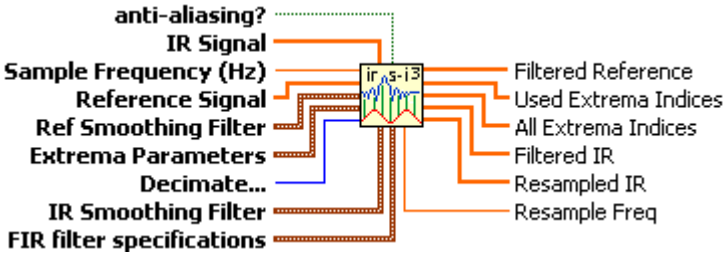

Front Panel

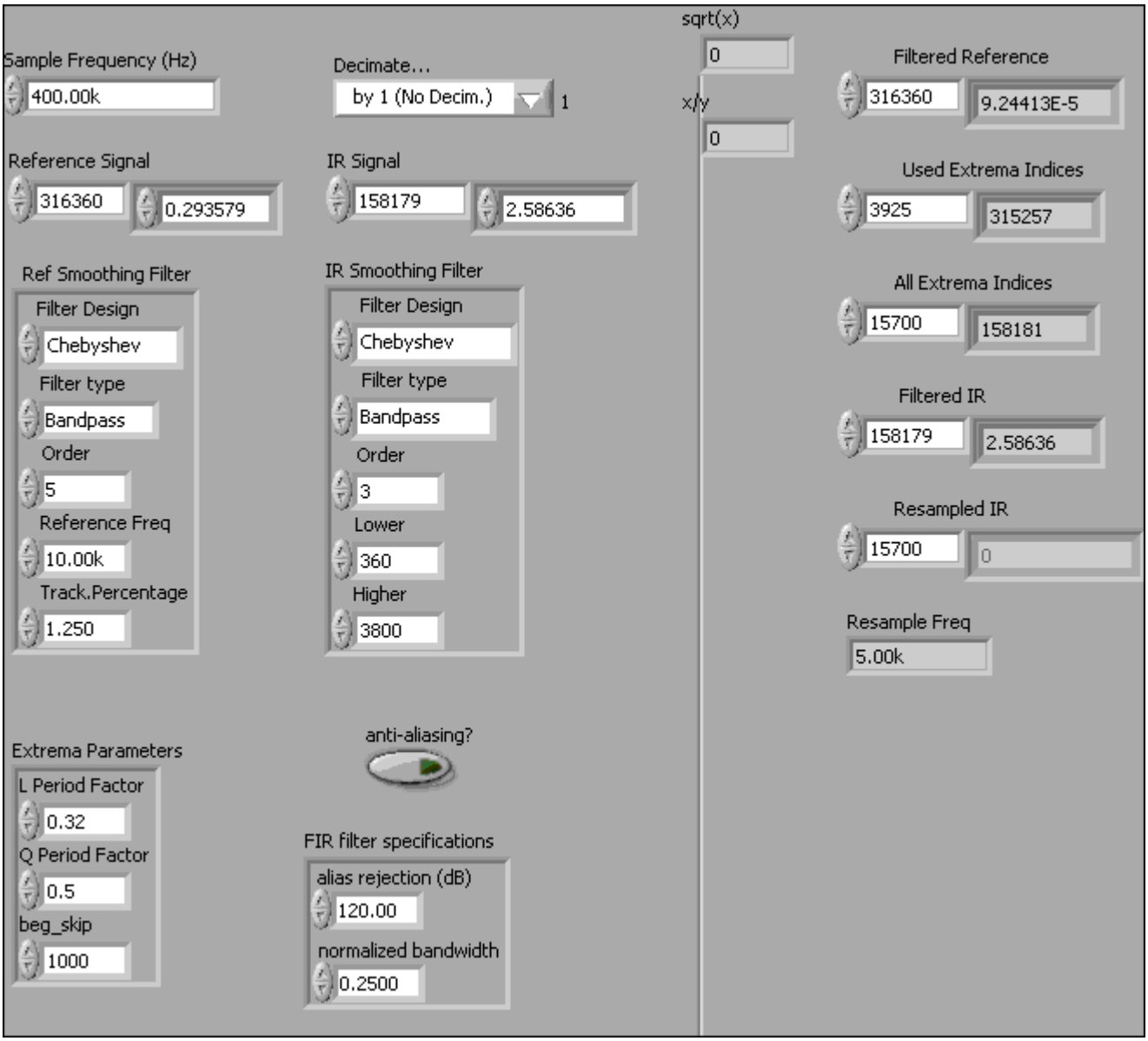

Controls and Indicators

IR Signal

Reference Signal

Sample Frequency (Hz)

Ref Smoothing Filter

Filter Design

Filter type filter type specifies the passband of the filter.

Order order is the order of the IIR filter and must be greater than zero. If **order** is less than or equal to zero, the VI sets **Reverse Coefficients** and **Forward Coefficients** to empty arrays and returns an error.

Reference Freq low cutoff freq: fl is the low cutoff frequency and must observe the Nyquist criterion.

Track.Percentage low cutoff freq: fl is the low cutoff frequency and must observe the Nyquist criterion.

Extrema Parameters

L Period Factor

Q Period Factor

beg_skip

IR Smoothing Filter

Filter Design

Filter type

Order

Lower

Higher

anti-aliasing? anti-aliasing? specifies whether the input signal undergoes lowpass filtering when LabVIEW downsamples the signal.

FIR filter specifications FIR filter specifications specifies the minimum values this VI needs to specify the FIR filter.

alias rejection (dB) alias rejection (dB) specifies the minimum attenuation level of signal components aliased after any resampling operation. The default is 120.

normalized bandwidth normalized bandwidth specifies the fraction of the new sampling rate that is not attenuated. The default is 0.4536.

Decimate...

Filtered IR

Numeric

Resampled IR

Numeric

All Extrema Indices

Filtered Reference

Numeric

Used Extrema Indices

Numeric

Resample Freq

sqrt(x)

x/y

Block Diagram

Rev3 - Decimation with Resample (constant to variable) using an FIR Filter Implementation

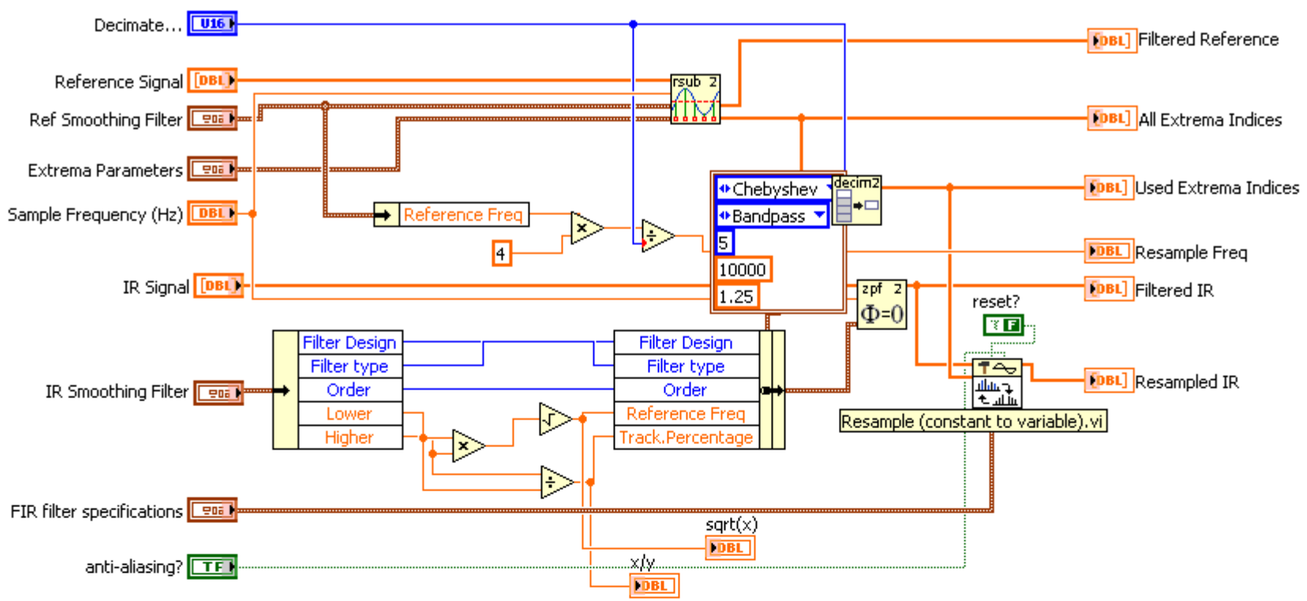

IR Sampler - Interpolator uses **Reference Signal,** a quasi-sinusoid at approximately **Reference Freq**, to resample a filtered version of **IR Signal**.

Reference Signal and **IR Signa**l are simultaneously sampled at **Sample Frequency**, and have the same number of elements.

[**Sample Frequency** may be reduced by decimation; it may not be the same frequency as the original sample frequency. Then, the 100kHz AA filter can be taken advantage of without a large output dataset. Filtering could also occur before decimation].

Reference Freq and **Track Percentage** along with other parameters in **Ref Smoothing Filter** control the bandpass filtering of the Ref Channel by a Zero Phase Digital Filter. **Track Percentage** controls the band limits above and below Reference Freq. The **Extrema Parameters** control the fitting and extraction of All Extrema Indices. **Ref Q Period Factor** is that fraction of a nominal HeNe period over which to perform a quadratic fit to extract the peak and valley indices. **Ref L Period Factor** is that fraction of a nominal HeNe period over which to perform a straight line fit to acquire zero crossing data. It needs to be adjusted so that an odd number of points are used. This is not automatically done in Rev3.

The input **IR Signal** is filtered by the Zero Phase **IR Smoothing Filter** with its parameters. Currently, it has been found that since the IR frequency band is a much smaller percentage of the sampling frequency, the IR Smoothing Filter has to be of lower order than the filter on the reference channel.

The **Filtered IR** is resampled by the decimated **Used Extrema Indices**, using the Resample (constant to variable).vi, which uses an FIR implementation

Ouput are the **Filtered Reference**, **Used Extrema Indices**, a decimated array consisting of the consecutive zero crossings and peaks and valley expressed as fractional indices, **All Extrema Indices**, the undecimated set of zx and pv fract. indices, the **Filtered IR**, and the **Resampled IR** at the Used Extrema fractional indices.

List of SubVIs and Express VIs with Configuration Information

NI_AALPro.lvlib:Resample (constant to variable,single-channel).vi
C:\Program Files\National Instruments\LabVIEW 8.5\vi.lib\Analysis\2dsp.llb\Resample (constant to variable,single-channel).vi

NI_AALPro.lvlib:Resample (constant to variable).vi
C:\Program Files\National Instruments\LabVIEW 8.5\vi.lib\Analysis\2dsp.llb\Resample (constant to variable).vi

Zero Phase Filter Rev2.vi
C:\Documents and Settings\User\My Documents\FTRX\Zero Phase Filter Rev2.vi

Decimate by 1-2-4-8 Rev2.vi
C:\Documents and Settings\User\My Documents\FTRX\Decimate by 1-2-4-8 Rev2.vi

Reference Subsampler Rev2.vi
C:\Documents and Settings\User\My Documents\FTRX\Reference Subsampler Rev2.vi

Zero Phase Filter Rev2.vi

Connector Pane

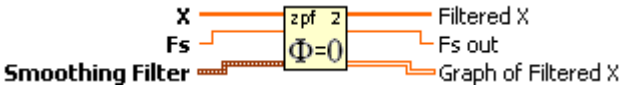

Front Panel

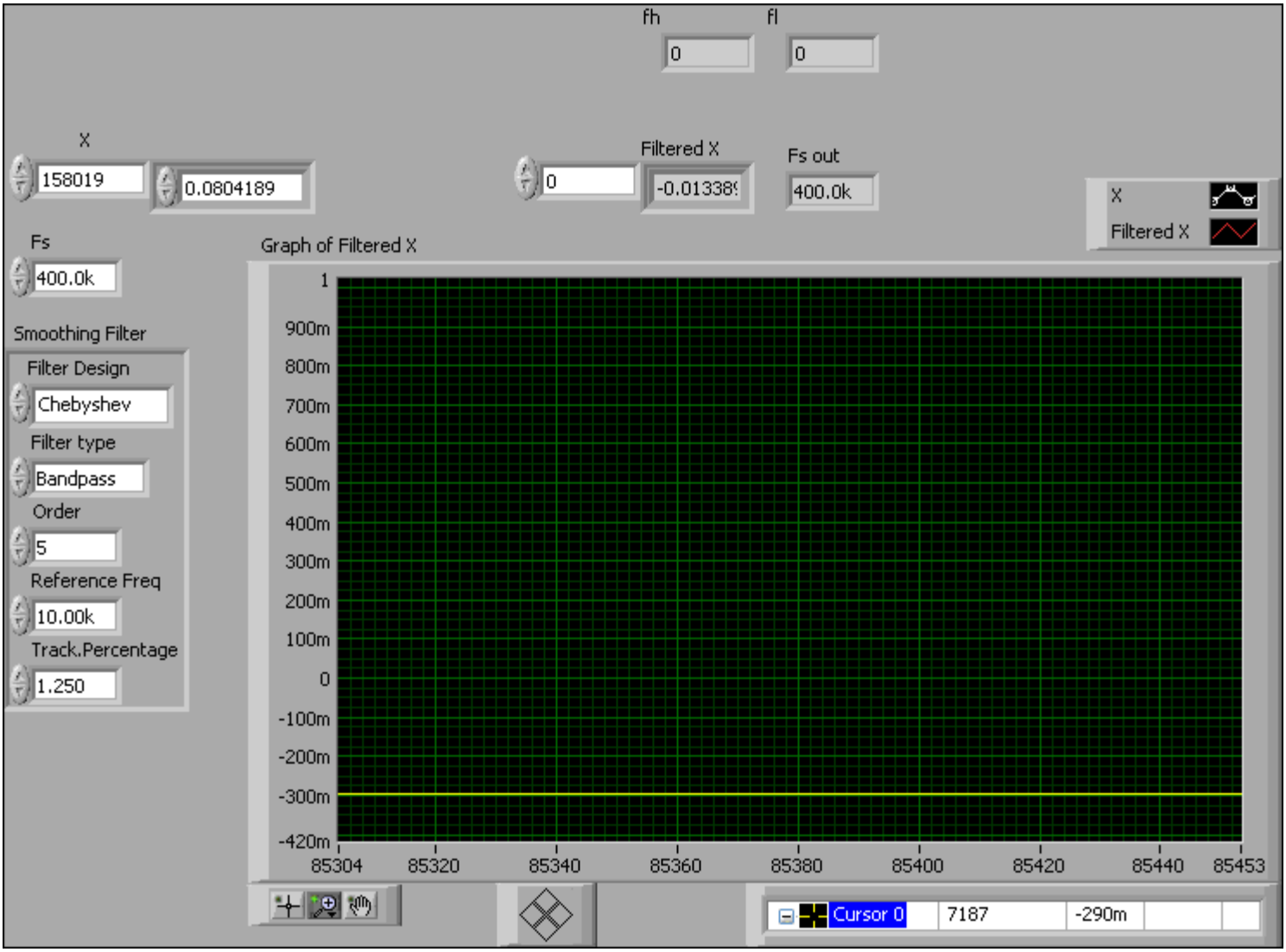

Controls and Indicators

Fs sampling freq: fs is the sampling frequency and must be greater than zero. The default is 1.0.

X

Smoothing Filter

Filter Design

Filter type filter type specifies the passband of the filter.

Order order is the order of the IIR filter and must be greater than zero. If **order** is less than or equal to zero, the VI sets **Reverse Coefficients** and **Forward Coefficients** to empty arrays and returns an error.

Reference Freq low cutoff freq: fl is the low cutoff frequency and must observe the Nyquist criterion.

Track.Percentage low cutoff freq: fl is the low cutoff frequency and must observe the Nyquist criterion.

Graph of Filtered X

Filtered X Filtered X returns the filtered signal.

Filtered X returns the filtered signal.

Fs out sampling freq: fs is the sampling frequency and must be greater than zero. The default is 1.0.

fh

fl

Block Diagram

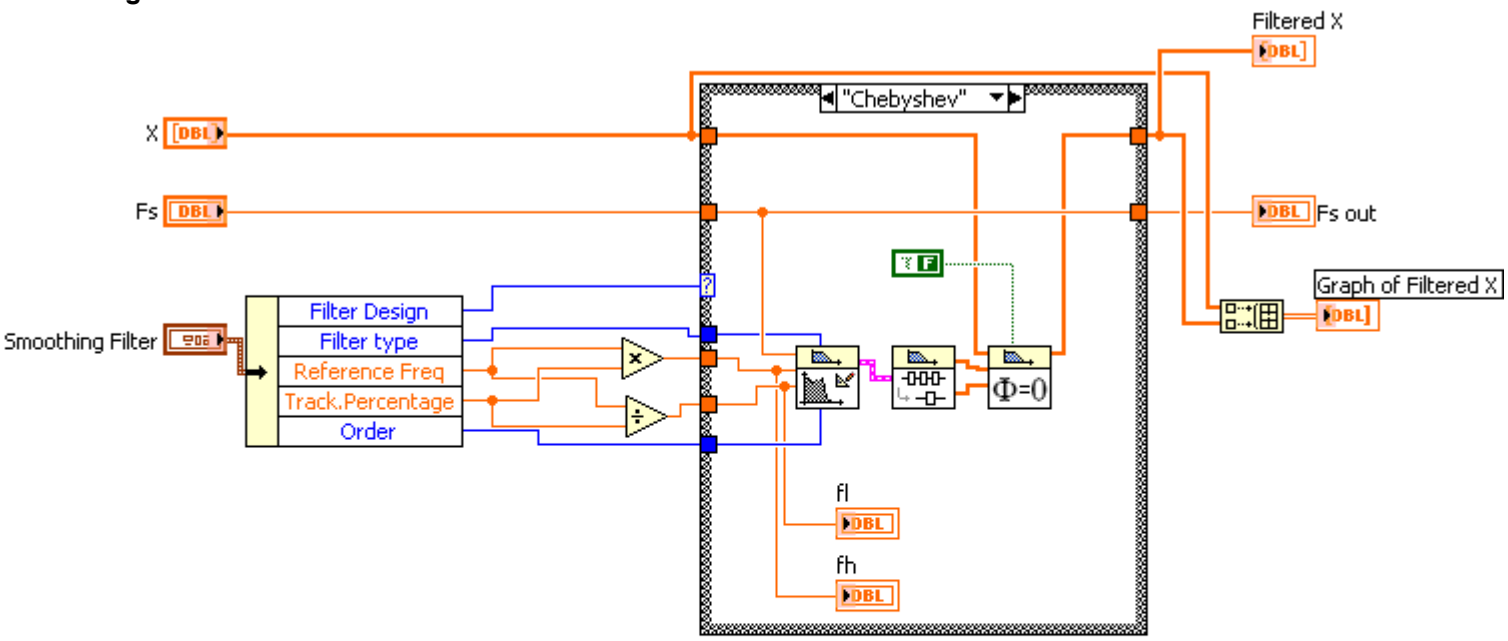

Rev 2 changes inputs to Ref Frequency and
Tracking Percentage, from Higher and Lower.
The tracking percentage is that factor that Higher
is greater than Reference Frequency and Lower is less
than Reference Frequency.

Zero Phase Filter outputs one data point for every input
point. Its nature is such that transient effects mean that
the beginning and end have bad data, the narrower the
bandwidth, the longer the transient, the more output data
that is in the transient regime and should be eliminated.

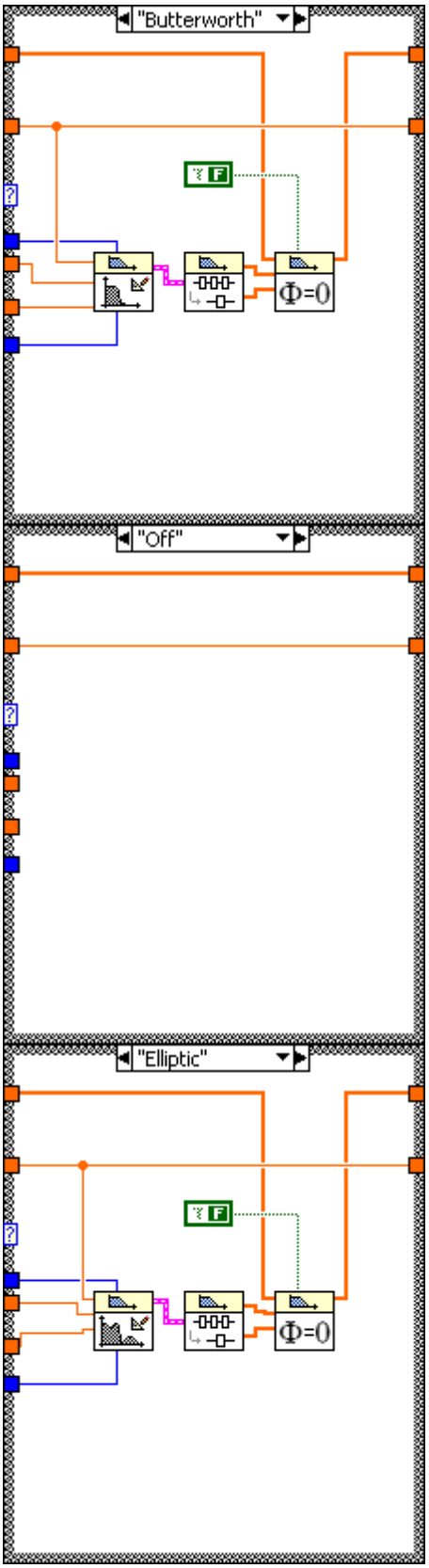

List of SubVIs and Express VIs with Configuration Information

NI_AALBase.lvlib:Elliptic Coefficients.vi
C:\Program Files\National Instruments\LabVIEW 8.5\vi.lib\Analysis\3filter.llb\Elliptic Coefficients.vi

NI_AALBase.lvlib:Chebyshev Coefficients.vi
C:\Program Files\National Instruments\LabVIEW 8.5\vi.lib\Analysis\3filter.llb\Chebyshev Coefficients.vi

NI_AALBase.lvlib:Zero Phase Filter (DBL).vi
C:\Program Files\National Instruments\LabVIEW 8.5\vi.lib\Analysis\3filter.llb\Zero Phase Filter (DBL).vi

NI_AALBase.lvlib:Zero Phase Filter.vi
C:\Program Files\National Instruments\LabVIEW 8.5\vi.lib\Analysis\3filter.llb\Zero Phase Filter.vi

NI_AALBase.lvlib:Cascade To Direct Coefficients.vi
C:\Program Files\National Instruments\LabVIEW 8.5\vi.lib\Analysis\3filter.llb\Cascade To Direct Coefficients.vi

NI_AALBase.lvlib:Butterworth Coefficients.vi
C:\Program Files\National Instruments\LabVIEW 8.5\vi.lib\Analysis\3filter.llb\Butterworth Coefficients.vi

Decimate by 1-2-4-8 Rev2.vi

Connector Pane

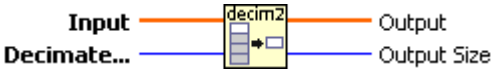

Front Panel

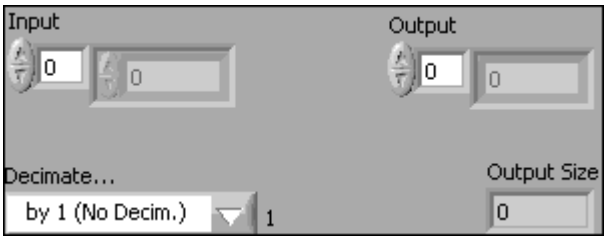

Controls and Indicators

Input

Numeric

Decimate...

Output

Numeric

Output Size

Block Diagram

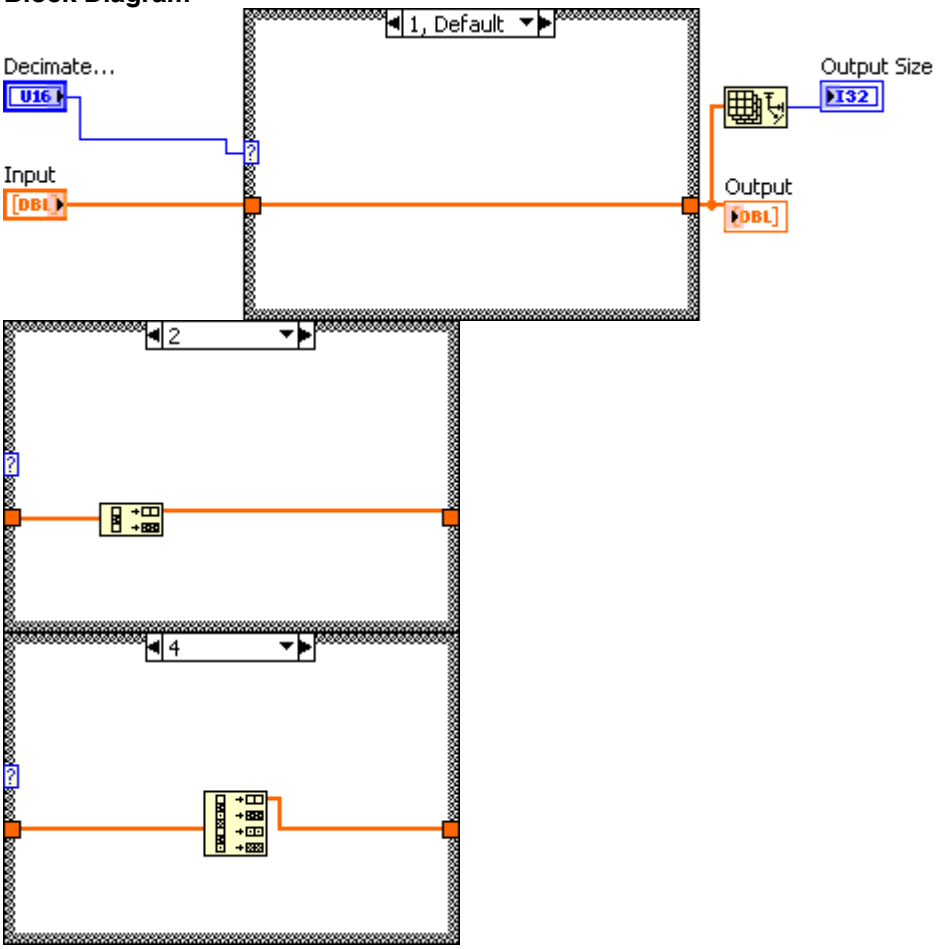

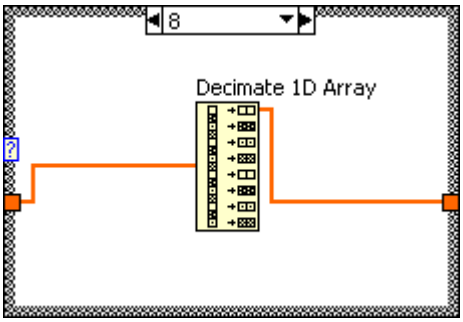

List of SubVIs and Express VIs with Configuration Information

Reference Subsampler Rev2.vi
Reference Subsampler generates a set of fractional extrema indices representing the peaks, valleys and zero crossings of a sinusoidal reference signal input. This permits a reference sinewave to sample an unknown signal at a frequency 4X its own frequency. For a visible HeNe reference, a significant decimation can be done on an infrared interferogram.

Input Signal is the [noisy] reference sinewave.
Sample Freq is the frequency it is sampled at.
Ref Freq should be chosen slightly higher than the highest frequency anticipated for the Input Signal.

Connector Pane

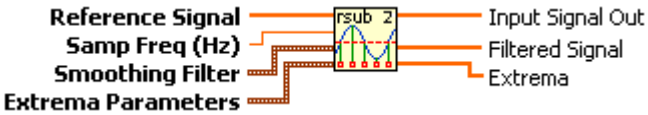

Front Panel

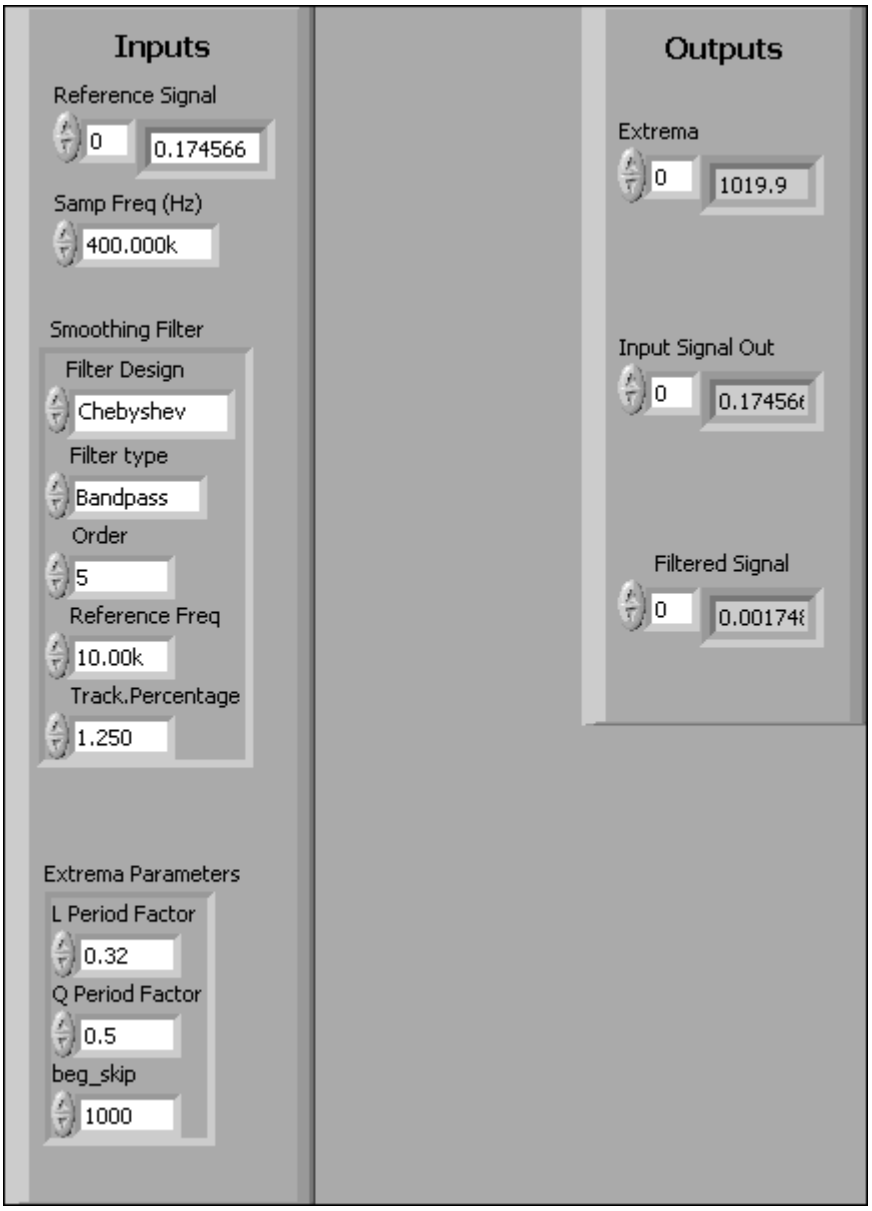

Controls and Indicators

Samp Freq (Hz)

Reference Signal X is the input array of samples to filter.

Numeric X is the input array of samples to filter.

Smoothing Filter

Filter Design

Filter type filter type specifies the passband of the filter.

Order order is the order of the IIR filter and must be greater than zero. If **order** is less than or equal to zero, the VI sets **Reverse Coefficients** and **Forward Coefficients** to empty arrays and returns an error.

Reference Freq low cutoff freq: fl is the low cutoff frequency and must observe the Nyquist criterion.

Track.Percentage low cutoff freq: fl is the low cutoff frequency and must observe the Nyquist criterion.

Extrema Parameters


L Period Factor


Q Period Factor


beg_skip


Extrema


Filtered Signal Filtered X is the output array of filtered samples.


Numeric Filtered X is the output array of filtered samples.


Input Signal Out X is the input array of samples to filter.


Numeric X is the input array of samples to filter.

Block Diagram

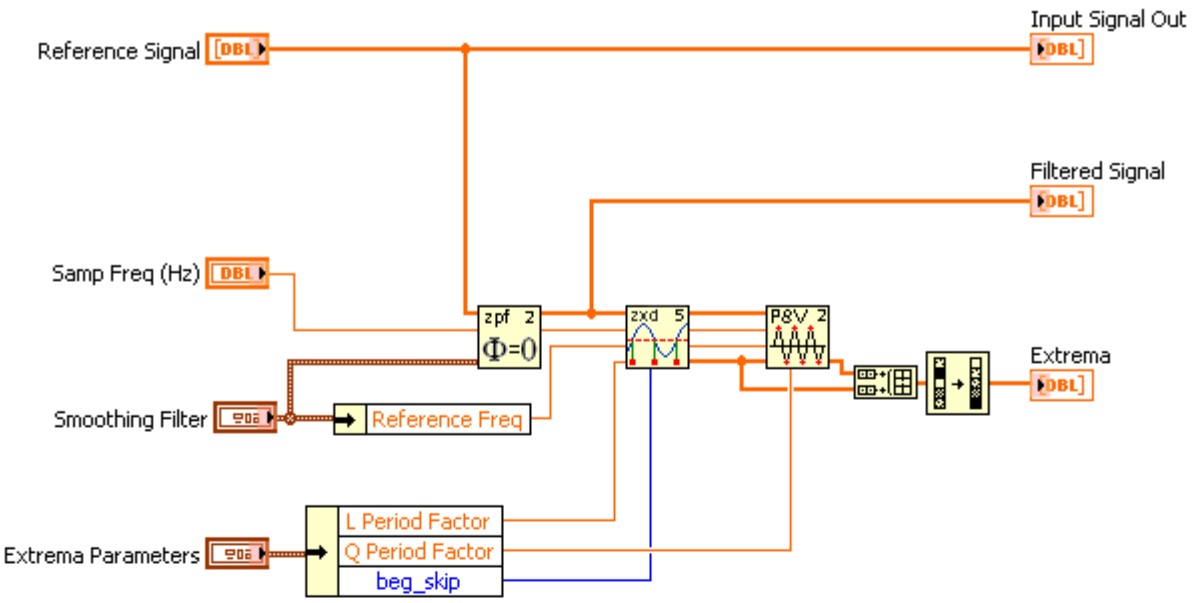

Reference Subsampler Rev2 includes

Zero Phase Filter Rev2
ZX Detector Rev5
Peaks and Valleys Rev2

Zero Phase Filter Rev2 is a true, designable, zero phase IIR bandpass filter implementation. It can have very sharp skirts, eliminating noise.

ZX Detector Rev5 is greatly improved speedwise over Rev4 due to improved array handling. It also permits the user to separately eliminate data points at the beginning and end of a dataset.

Reference Subsampler Rev2 generates a set of fractional extrema indices representing the peaks, valleys and zero crossings of a sinusoidal reference signal input.

This permits a reference sinewave to sample an unknown signal at a frequency 4X its own frequency. For a visible HeNe reference, a significant decimation can be done on an infrared interferogram.

Reference Subsampler first smooths the input Reference Signal using an optional zero phase IIR filter.

It then finds the zero crossings based on its calculation of the Reference Signal mean level, then finds the peak and valley points by quadratic fitting at their anticipated positions.

Reference Signal is an array of the signal used to create the sampling indices

Sample Frequency is the sampling frequency used to digitize the Reference Signal

Ref Frequency is the HeNe ref Frequency = velocity/4 in cps.

List of SubVIs and Express VIs with Configuration Information

Zero Phase Filter Rev2.vi
C:\Documents and Settings\User\My Documents\FTRX\Zero Phase Filter Rev2.vi

Peaks and Valleys Rev2.vi
C:\Documents and Settings\User\My Documents\FTRX\Peaks and Valleys Rev2.vi

ZX Detector Rev5.vi
C:\Documents and Settings\User\My Documents\FTRX\ZX Detector Rev5.vi

Peaks and Valleys Rev2.vi

Connector Pane

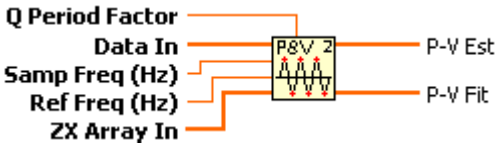

Front Panel

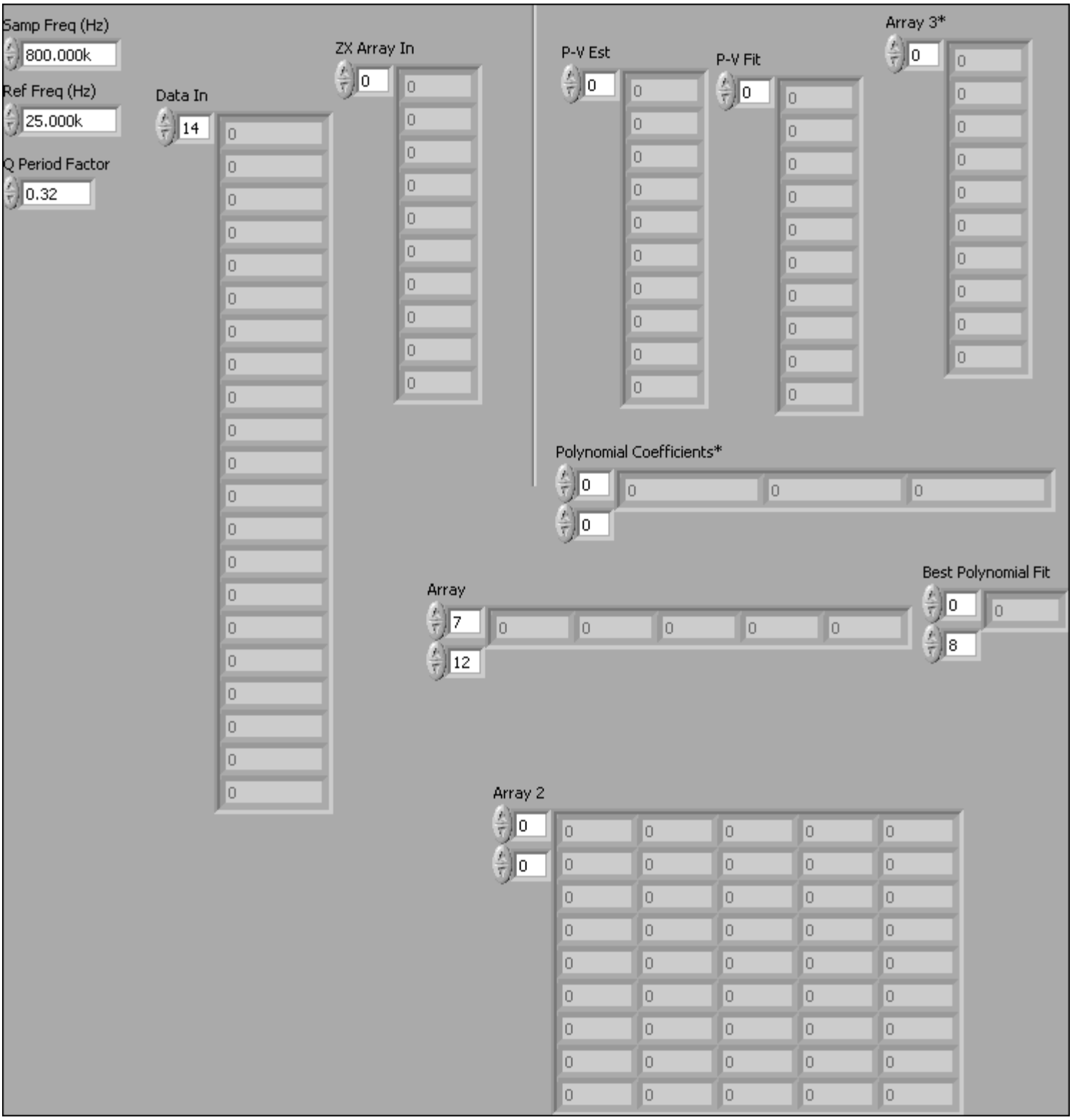

Controls and Indicators


ZX Array In


Numeric


Data In


Numeric


Ref Freq (Hz)


Samp Freq (Hz)


Q Period Factor


P-V Est


P-V Fit


Array


Numeric


Array 2


Polynomial Coefficients*


Array 3*


lower


Best Polynomial Fit

Block Diagram

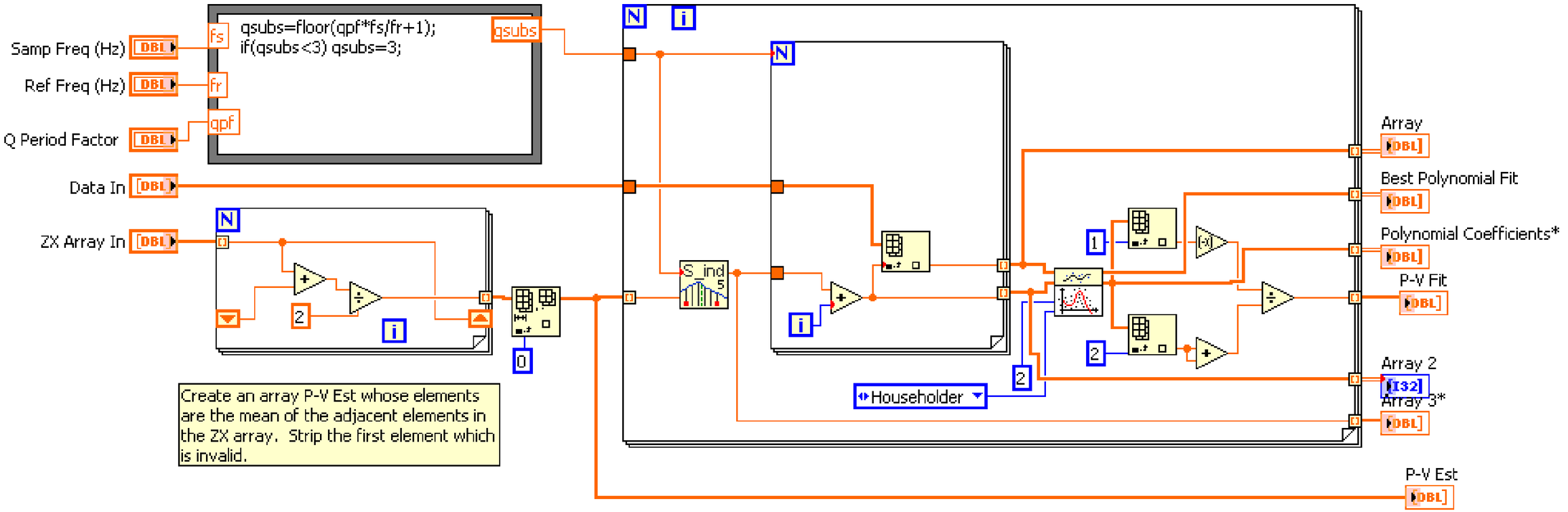

Subsample index each P-V Est, generating a lower value. Now subsample the data array creating Nsubsamples per P-V Est element centered on this element. Output the original indices and the values to the quadratic fitter. Find the extreme value over the subsamble by xext = -b/2a from the fit $y = c + bx + ax^2$. Index out that value to the P-V fit array.

List of SubVIs and Express VIs with Configuration Information

NI_AALPro.lvlib:General Polynomial Fit.vi
C:\Program Files\National Instruments\LabVIEW 8.5\vi.lib\Analysis\6fits.llb\General Polynomial Fit.vi

Subsample Indexer Rev5.vi
C:\Documents and Settings\User\My Documents\FTRX\Subsample Indexer Rev5.vi

Subsample Indexer Rev5.vi
Subsampler Indexer.vi acts only on sample indices, not sample data values.
It calculates the optimally centered upper and lower indices for a single fractional index.
These upper and lower indices are then employed in an algorithm to even better estimate a fiducial point.

For instance, if the fractional index is 4.30, and the number of subsamples is 5, the VI determines an upper index of 6 and a lower index of 2. So indices 2,3,4,5, and 6 are indicated for further fitting operations by returning lower = 2 and upper = 6. The fractional index supplied to this VI has to be obtained by a previous linear interpolation threshold operation or some other operation.

There are two cases, even and odd number of subsamples.

Define ns = Nsubsamples
f = fractional index

Even:

upper=trunc(f)+ns/2
lower=trunc(f) -ns/2+1

Odd:

upper=round(f) +(ns-1)/2
lower=round(f) -(ns-1)/2

There are no validity tests or coercions, as in previous versions.
Rev 5 simply reversed the connections on the icon so lower is on top.

Connector Pane

Front Panel

Controls and Indicators

Nsubsamples

Fractional_Index

upper

lower

Block Diagram

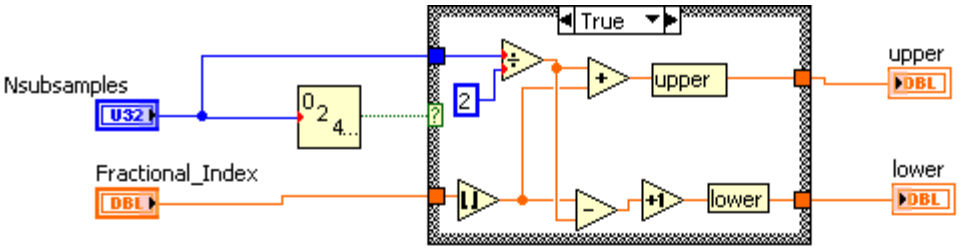

Subsampler Indexer.vi acts only on sample indices, not sample data values.
It calculates the optimally centered upper and lower indices for a single fractional index.
These upper and lower indices are then employed in an algorithm to even better estimate a fiducial point.

For instance, if the fractional index is 4.30, and the number of subsamples is 5, the VI determines an upper index of 6 and a lower index of 2. So indices 2,3,4,5, and 6 are indicated for further fitting operations by returning lower = 2 and upper = 6. The fractional index supplied to this VI has to be obtained by a previous linear interpolation threshold operation or some other operation.

There are two cases, even and odd number of subsamples.

Define ns = Nsubsamples
f = fractional index

Even:

upper=trunc(f)+ns/2
lower=trunc(f) -ns/2+1

Odd:

upper=round(f) +(ns-1)/2
lower=round(f) -(ns-1)/2

There are no validity tests or coercions, as in previous versions.
Rev 5 simply reversed the connections on the icon so lower is on top.

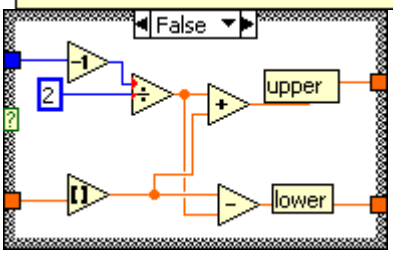

List of SubVIs and Express VIs with Configuration Information

Is Even.vi
C:\Documents and Settings\User\My Documents\FTRX\Is Even.vi

Is Even.vi

Connector Pane

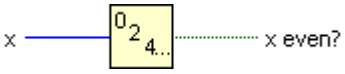

Front Panel

Controls and Indicators

x

x even?

Block Diagram

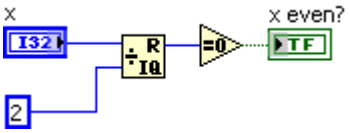

List of SubVIs and Express VIs with Configuration Information

ZX Detector Rev5.vi

Connector Pane

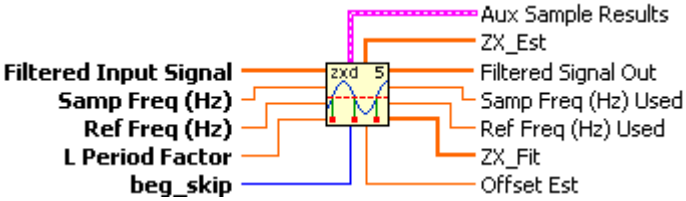

Front Panel

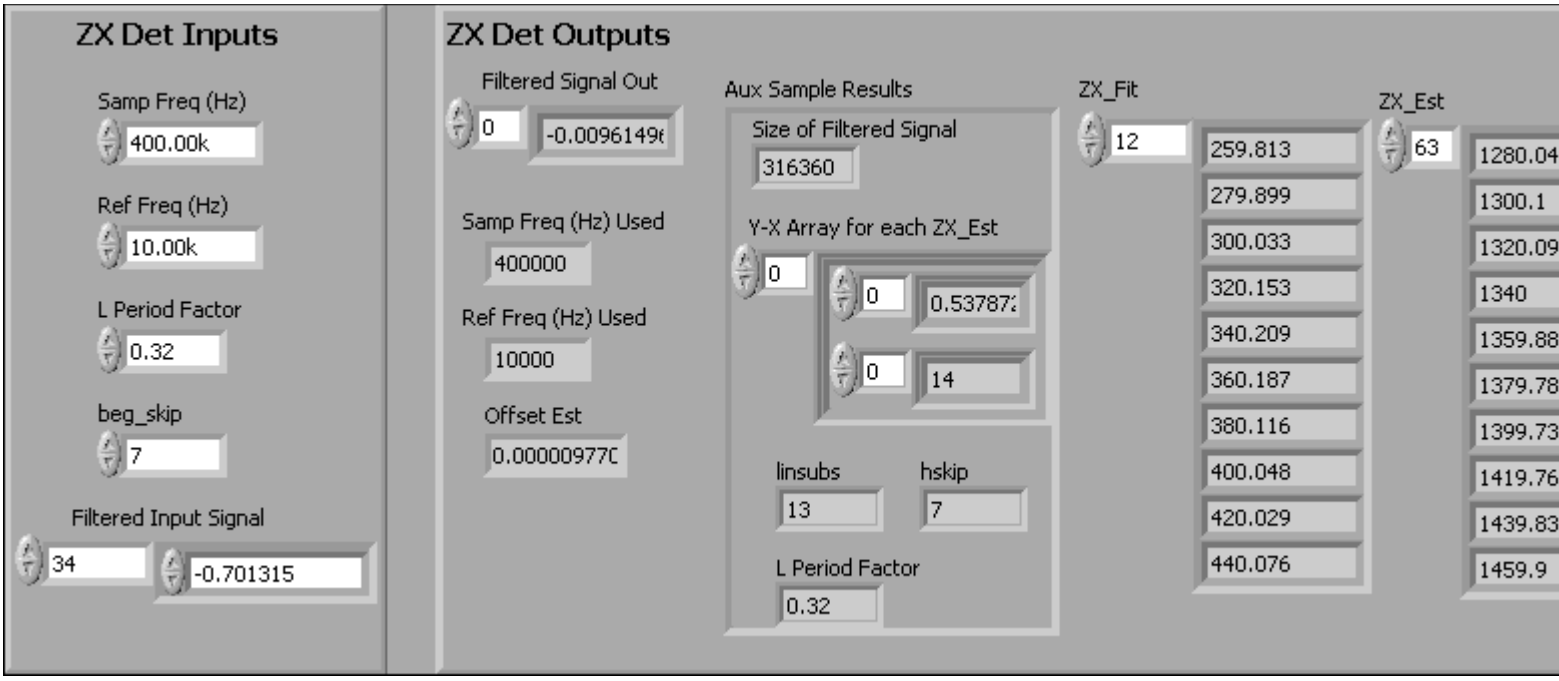

Controls and Indicators

Samp Freq (Hz)

Ref Freq (Hz)

L Period Factor

Filtered Input Signal X is the input array of samples to filter.

Numeric X is the input array of samples to filter.

beg_skip

ZX_Fit

Filtered Signal Out Filtered X is the output array of filtered samples.

Numeric Filtered X is the output array of filtered samples.

ZX_Est

Numeric

Samp Freq (Hz) Used


Ref Freq (Hz) Used


Aux Sample Results


Size of Filtered Signal


Y-X Array for each ZX_Est


Numeric


linsubs


L Period Factor


hskip


Offset Est mean is the mean, or average, of the values in the input sequence **X**.

Block Diagram

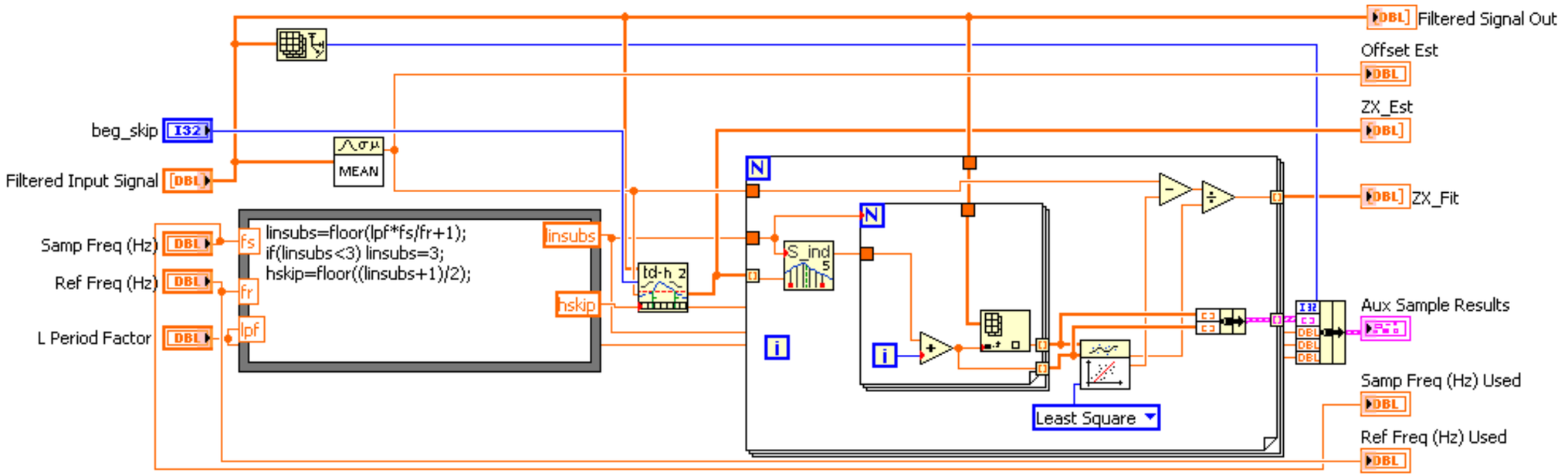

0. Revision 4 includes offset estimation within code. This is by simple mean. Finding the offset from the prefilter operation did not affect results. Offset is now an output.
1. linsubs is the number of samples that will fit into lpf*Tref. It is 1 more than the number of intervals of Ts contained in lfp*Tref. linsubs>3.
2. hskip is crucial to the algorithm. This parameter, roughly equal to half the linsubs subsampling interval, governs:
   (a) hskip signal samples are skipped at the beginning of the signal data before looking for the first zero crossing.
   (b) hskip signal samples are skipped at the end of the signal data, wherein looking for zero crossings is abandoned.

(a) and (b) assure a full subsample contributes to a zero crossing fit at beginning and end.

   (c) hskip signal samples are skipped after a zero crossing is detected, providing a temporal dead zone. This makes the algorithm very noise resistant.

3. td-h provides an array of zero crossings of the signal at level offset.
4. The zero crossings are individually clocked into the for loop. S_ind provides [upper and] lower indices of a subsample sequence of length linsubs centered on ZX_Est. Each lower is fed into an inner for loop as a parameter. This loop
   (a) indexes the data about the ZX_Est element.
   (b) creates an array of the corresponding indices of the data.

These arrays are of length linsub, from 0 to linsub-1, and are indexed out to the linear fit vi.

5. The linear fit vi finds the slope and intercept parameters of the subsample as it passes through threshold. The equation mx + b = threshold is then solved for a more accurate fractional zx index. The principal output of the vi is ZX_ Fit, a more accurate estimation of the fractional zx index that ZX_Est, as provided by td-h vi.

List of SubVIs and Express VIs with Configuration Information

Subsample Indexer Rev5.vi
C:\Documents and Settings\User\My Documents\FTRX\Subsample Indexer Rev5.vi

NI_AALPro.lvlib:Linear Fit.vi
C:\Program Files\National Instruments\LabVIEW 8.5\vi.lib\Analysis\6fits.llb\Linear Fit.vi

Threshold Detector with Hysteresis Rev2.vi
C:\Documents and Settings\User\My Documents\FTRX\Threshold Detector with Hysteresis Rev2.vi

NI_AALBase.lvlib:Mean.vi
C:\Program Files\National Instruments\LabVIEW 8.5\vi.lib\Analysis\baseanly.llb\Mean.vi

Threshold Detector with Hysteresis Rev2.vi
Creates an array of bidirectional Fractional Indices at Threshold.

Tests passing of an Input Signal array through Threshold value by computing local line segments between adjacent points of array. The intersection of the local line segment between i and i+1 with with y=Thresh is at the fractional index Test[i]:

Test[i] =(Thresh-y[i])/(y[i+1]-y[i]) +i. Form the array of possible threshold crossings:

Raw[i]=if(Test[i]>=i.and.Test[i]<i+1,test[i],0)

In Raw[i], 0 is appended as a marker if no crossing found. Create loop increments

Loop_Incr[i]=if(Raw[i]=0,1,hskip)

Use delay hysteresis. If no crossing found, make Loop_Incr=0, test very next index pair. If crossing found, make Loop_Incr=hskip_int, skip ahead hskip_int indices. This creates noise immunity.

Additionally, the first and last beg_skip array points of Input Signal are skipped to avoid end effects. The provider of Input Signal should take enough additional points so that this is not an issue.

Connector Pane

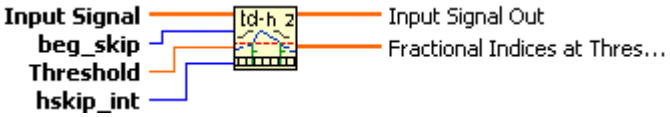

Front Panel

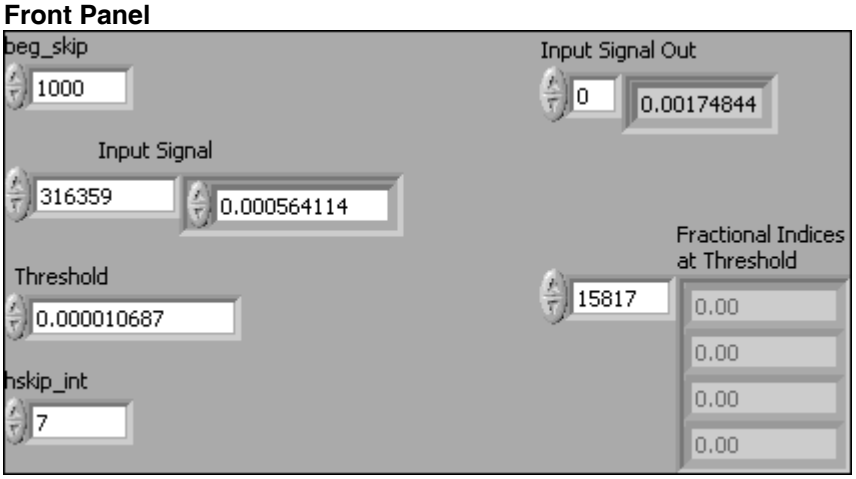

Controls and Indicators

hskip_int

Threshold

Input Signal

beg_skip

Fractional Indices at Threshold

Numeric

Input Signal Out

Block Diagram

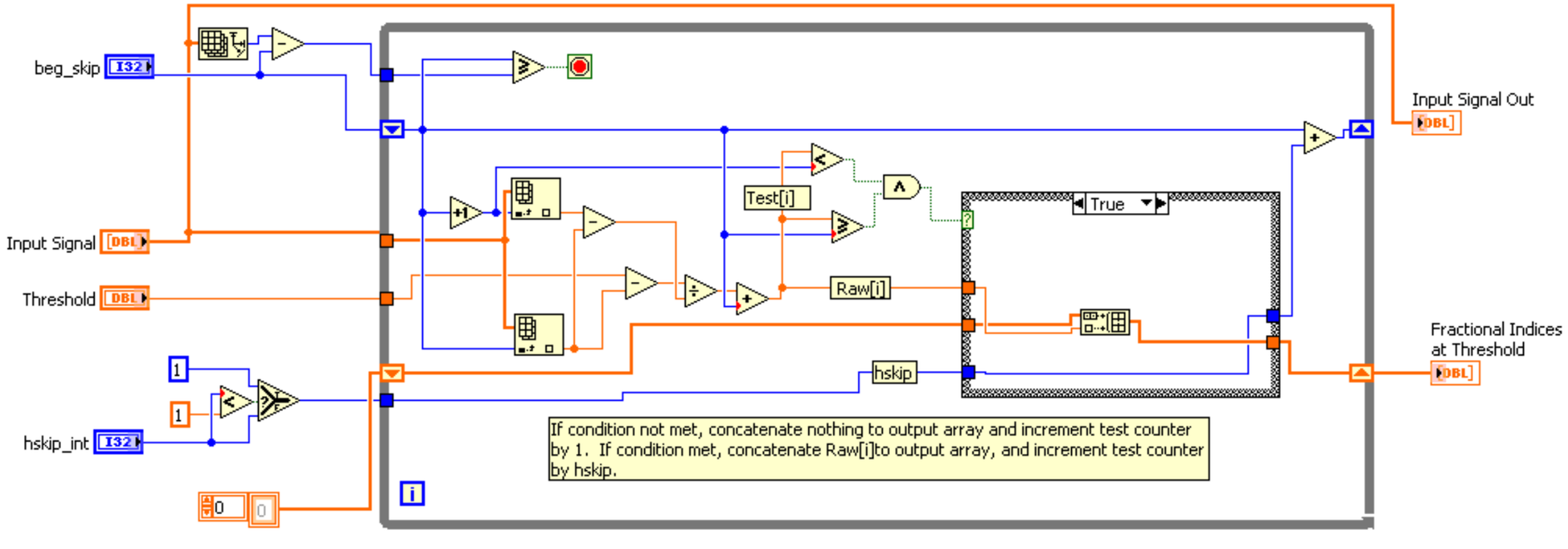

REV2

Here, the Raw[i] array is built only upon detection of a zero crossing. Previously, a dummy 0 was appended to the array as a marker. A separate routine stripped 0's from the final array. This was extremely time-consuming.

New input: beg_skip Number of "invalid" samples at beginning and end to skip over before finding zero crossings. Necessary because the new zero phase filters have a long kernel and hence a long transient response, and they shift zero crossings at beginning and end.

An array of ignored indices was removed.

0. Assure hskip is at least 1.
1. Load Size_of_Input_Signal-hskip-1 into loop exit test value.
   Load hskip-1 into index register. Recall indexing is from zero. These choices guarantee there will be at least hskip samples before and after zero crossing is found. Noise can still vary the output array size. It should be stable if filtering is effective.
2. Compute
   Test[i] =(Thresh-y[i])/(y[i+1]-y[i]) +i
as i ranges from hskip (to eliminate an invalid beginning range)
to Size_of_Input_Signal-hskip-1 (to elim an invalid end range).
Test[i] is the trial index where the interval y[i] will intersect thresh based on y[i+1] and y[i].
If Test[i] falls between i and i+1, a crossing has been found and the best [here linear] estimate is Test[i]
3. Compute
   Raw[i]=if(Test[i]>=i.and.Test[i]<i+1,test[i],0)
If Raw[i] is a valid crossing, output it. If not, append 0 as a marker.
If no crossing found, increment loop counter by 1. If crossing found increment loop counter by hskip. I.e.
   Loop_Incr=if(Raw[i]=0,1,hskip)
This use of delay by hskip samples to provide dead zone. Not actually hysteresis.

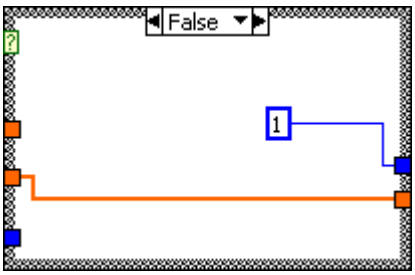

List of SubVIs and Express VIs with Configuration Information

Configure DAQmx Read Parameters Rev3.vi

Connector Pane

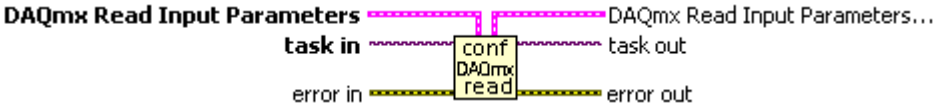

Front Panel

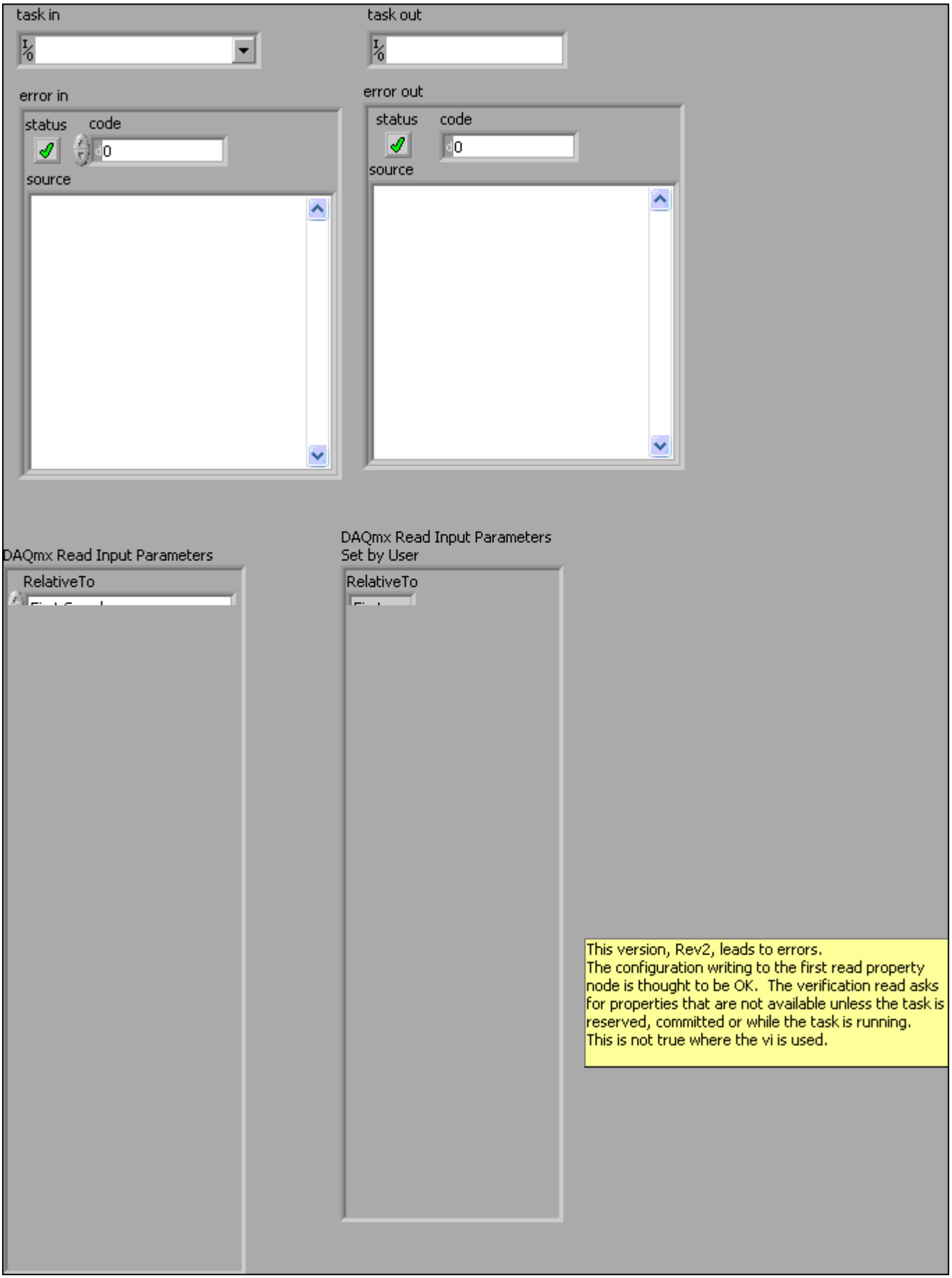

Controls and Indicators

error in error in can accept error information wired from VIs previously called. Use this information to decide if any functionality should be bypassed in the event of errors from other VIs.

Right-click the **error in** control on the front panel and select **Explain Error** or **Explain Warning** from the shortcut menu for more information about the error.

status status is TRUE (X) if an error occurred or FALSE (checkmark) to indicate a warning or that no error occurred.

Right-click the **error in** control on the front panel and select **Explain Error** or **Explain Warning** from the shortcut menu for more information about the error.

code code is the error or warning code.

Right-click the **error in** control on the front panel and select **Explain Error** or **Explain Warning** from the shortcut menu for more information about the error.

source source describes the origin of the error or warning.

Right-click the **error in** control on the front panel and select **Explain Error** or **Explain Warning** from the shortcut menu for more information about the error.

task in

DAQmx Read Input Parameters

RelativeTo

Offset

ChannelsToRead

WfmAttr

ReadAllAvailSamp

AutoStart

OverWrite

WaitMode

SleepTime

task out

error out error in can accept error information wired from VIs previously called. Use this information to decide if any functionality should be bypassed in the event of errors from other VIs.

Right-click the **error in** control on the front panel and select **Explain Error** or **Explain Warning** from the shortcut menu for more information about the error.

status status is TRUE (X) if an error occurred or FALSE (checkmark) to indicate a warning or that no error occurred.

Right-click the **error in** control on the front panel and select **Explain Error** or **Explain Warning** from the shortcut menu for more information about the error.

code code is the error or warning code.

Right-click the **error in** control on the front panel and select **Explain Error** or **Explain Warning** from the shortcut menu for more information about the error.

source source describes the origin of the error or warning.

Right-click the **error in** control on the front panel and select **Explain Error** or **Explain Warning** from the shortcut menu for more information about the error.

DAQmx Read Input Parameters Set by User

RelativeTo

Offset

ChannelsToRead

WfmAttr

ReadAllAvailSamp

AutoStart

OverWrite

WaitMode

SleepTime

Block Diagram

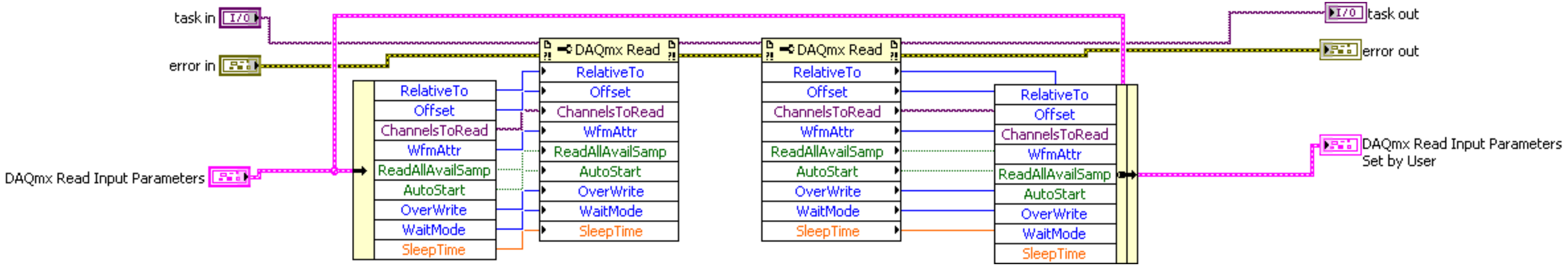
task in
error in
DAQmx Read Input Parameters
DAQmx Read
RelativeTo
Offset
ChannelsToRead
WfmAttr
ReadAllAvailSamp
AutoStart
OverWrite
WaitMode
SleepTime
DAQmx Read
RelativeTo
Offset
ChannelsToRead
WfmAttr
ReadAllAvailSamp
AutoStart
OverWrite
WaitMode
SleepTime
RelativeTo
Offset
ChannelsToRead
WfmAttr
ReadAllAvailSamp
AutoStart
OverWrite
WaitMode
SleepTime
task out
error out
DAQmx Read Input Parameters
Set by User

List of SubVIs and Express VIs with Configuration Information

Configure, Load, Enable and Wire Breakpoint Rev1.vi

Connector Pane

Front Panel

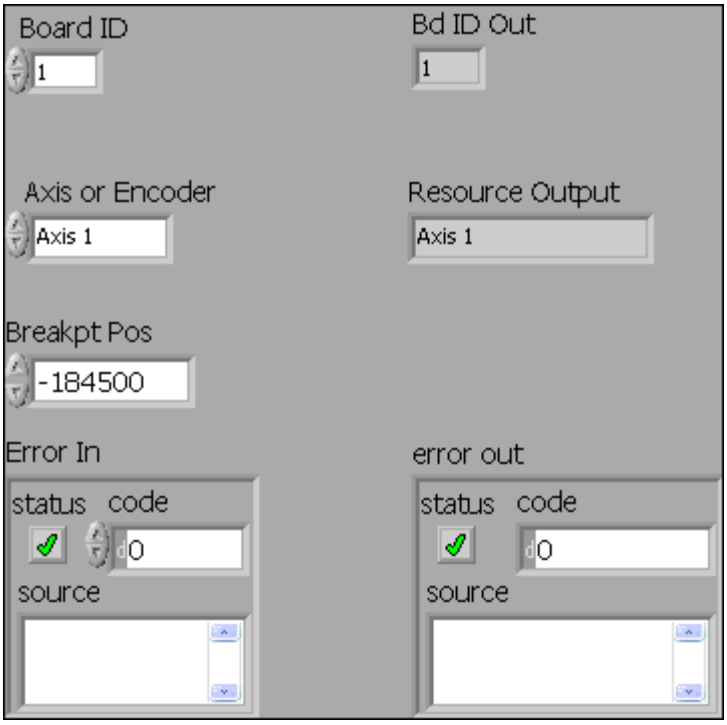

Controls and Indicators

Breakpt Pos

Board ID

Axis or Encoder

Error In The error in cluster can accept error information wired from VIs previously called. Use this information to decide if any functionality should be bypassed in the event of errors from other VIs.

The pop-up option Explain Error (or Explain Warning) gives more information about the error displayed.

status The **status** boolean is either TRUE (X) for an error, or FALSE (checkmark) for no error or a warning.

The pop-up option **Explain Error** (or Explain Warning) gives more information about the error displayed.

code The **code** input identifies the error or warning.

The pop-up option **Explain Error** (or Explain Warning) gives more information about the error displayed.

source The **source** string describes the origin of the error or warning.

The pop-up option **Explain Error** (or Explain Warning) gives more information about the error displayed.

Bd ID Out

error out error in can accept error information wired from VIs previously called. Use this information to decide if any functionality should be bypassed in the event of errors from other VIs.

Right-click the **error in** control on the front panel and select **Explain Error** or **Explain Warning** from the shortcut menu for more information about the error.

status status is TRUE (X) if an error occurred or FALSE (checkmark) to indicate a warning or that no error occurred.

Right-click the **error in** control on the front panel and select **Explain Error** or **Explain Warning** from the shortcut menu for more information about the error.

code code is the error or warning code.

Right-click the **error in** control on the front panel and select **Explain Error** or **Explain Warning** from the shortcut menu for more information about the error.

source source describes the origin of the error or warning.

Right-click the **error in** control on the front panel and select **Explain Error** or **Explain Warning** from the shortcut menu for more information about the error.

Resource Output

Block Diagram

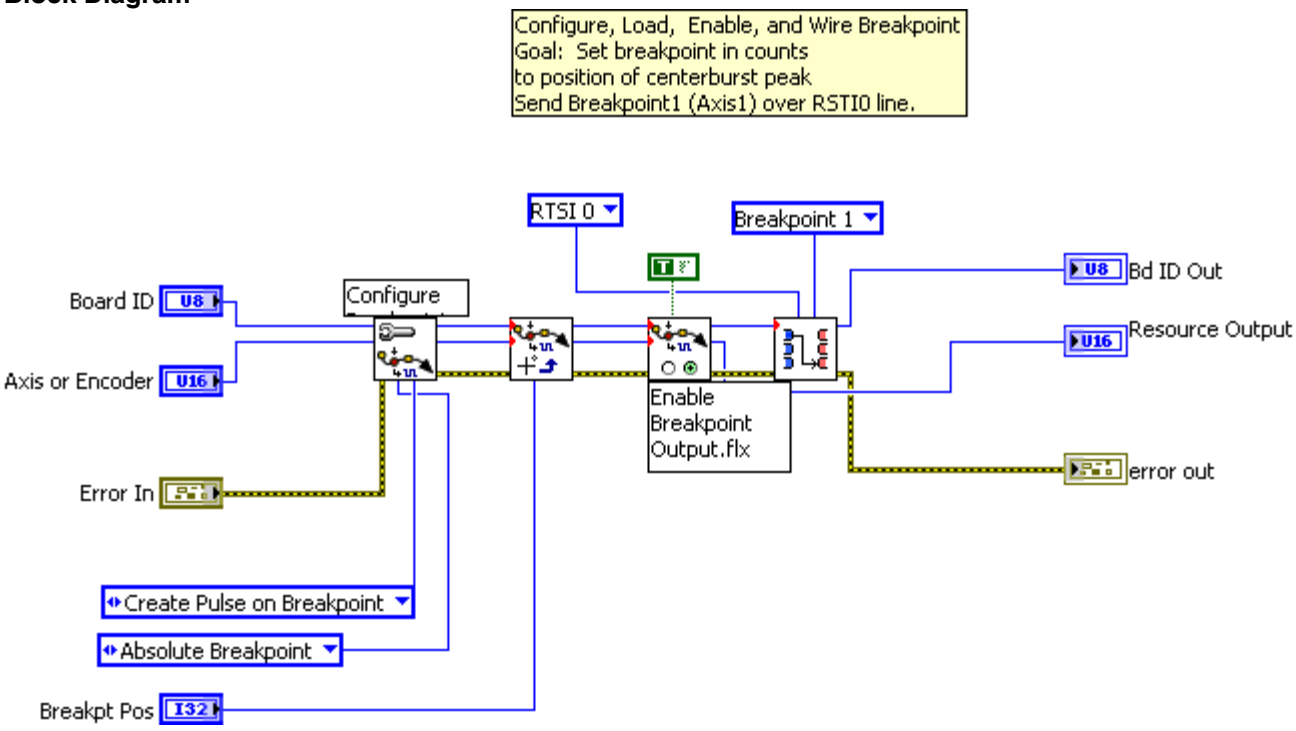

List of SubVIs and Express VIs with Configuration Information

Bd Id Out

C:\Program Files\National Instruments\LabVIEW 8.5\vi.lib\Motion\FlexMotion\CustomControls\CustomControls.llb\Bd Id Out

Resource Out (Enum).flx
C:\Program Files\National Instruments\LabVIEW 8.5\vi.lib\Motion\FlexMotion\CustomControls\CustomControls.llb\Resource Out (Enum).flx

Board Id
C:\Program Files\National Instruments\LabVIEW 8.5\vi.lib\Motion\FlexMotion\CustomControls\CustomControls.llb\Board Id

Select Signal.flx
C:\Program Files\National Instruments\LabVIEW 8.5\vi.lib\Motion\FlexMotion\FunctionsVIs\AnalogDigitalIO.llb\Select Signal.flx

Enable Breakpoint Output.flx
C:\Program Files\National Instruments\LabVIEW 8.5\vi.lib\Motion\FlexMotion\FunctionsVIs\MotionIO.llb\Enable Breakpoint Output.flx

AxisOrEncoder To Control.flx
C:\Program Files\National Instruments\LabVIEW 8.5\vi.lib\Motion\FlexMotion\CustomControls\CustomControls.llb\AxisOrEncoder To Control.flx

Load Breakpoint Position.flx
C:\Program Files\National Instruments\LabVIEW 8.5\vi.lib\Motion\FlexMotion\FunctionsVIs\MotionIO.llb\Load Breakpoint Position.flx

Configure Breakpoint.flx
C:\Program Files\National Instruments\LabVIEW 8.5\vi.lib\Motion\FlexMotion\FunctionsVIs\MotionIO.llb\Configure Breakpoint.flx

Configure motion and move to startpoint Rev3.vi

Connector Pane

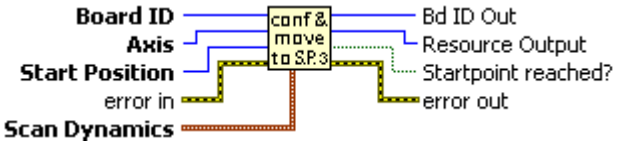

Front Panel

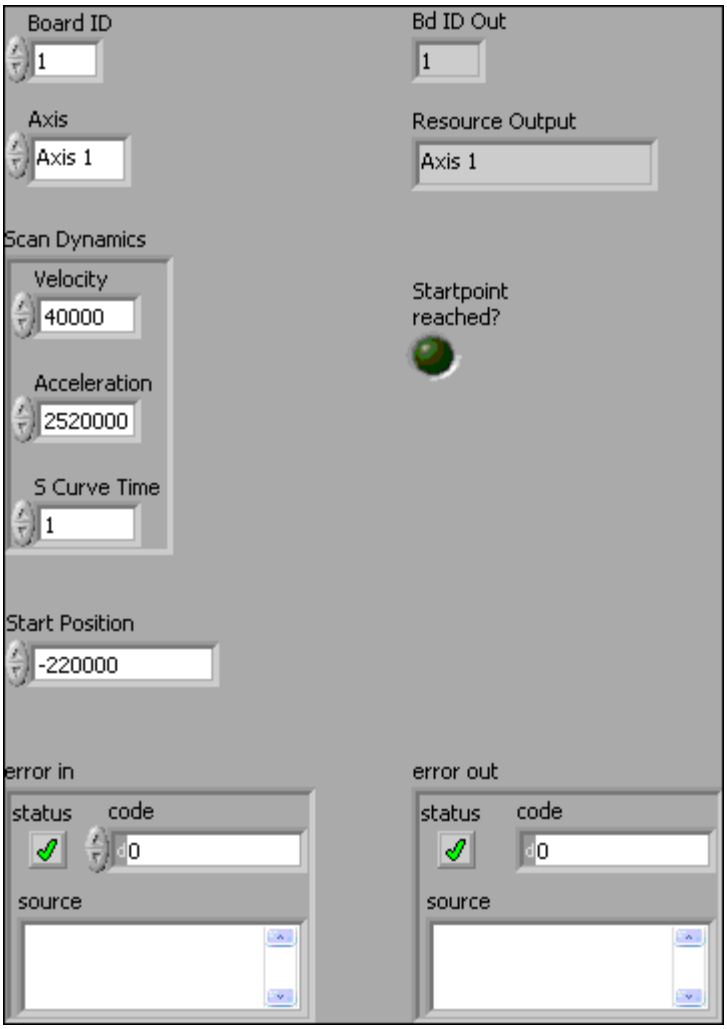

Controls and Indicators

Scan Dynamics

Velocity

Acceleration

S Curve Time

Start Position

error in error in can accept error information wired from VIs previously called. Use this information to decide if any functionality should be bypassed in the event of errors from other VIs.

Right-click the **error in** control on the front panel and select **Explain Error** or **Explain**

Warning from the shortcut menu for more information about the error.

status status is TRUE (X) if an error occurred or FALSE (checkmark) to indicate a warning or that no error occurred.

Right-click the **error in** control on the front panel and select **Explain Error** or **Explain Warning** from the shortcut menu for more information about the error.

code code is the error or warning code.

Right-click the **error in** control on the front panel and select **Explain Error** or **Explain Warning** from the shortcut menu for more information about the error.

source source describes the origin of the error or warning.

Right-click the **error in** control on the front panel and select **Explain Error** or **Explain Warning** from the shortcut menu for more information about the error.

Board ID

Axis

Startpoint reached?

Resource Output

error out error in can accept error information wired from VIs previously called. Use this information to decide if any functionality should be bypassed in the event of errors from other VIs.

Right-click the **error in** control on the front panel and select **Explain Error** or **Explain Warning** from the shortcut menu for more information about the error.

status status is TRUE (X) if an error occurred or FALSE (checkmark) to indicate a warning or that no error occurred.

Right-click the **error in** control on the front panel and select **Explain Error** or **Explain Warning** from the shortcut menu for more information about the error.

code code is the error or warning code.

Right-click the **error in** control on the front panel and select **Explain Error** or **Explain Warning** from the shortcut menu for more information about the error.

source source describes the origin of the error or warning.

Right-click the **error in** control on the front panel and select **Explain Error** or **Explain Warning** from the shortcut menu for more information about the error.

Bd ID Out

Block Diagram

Axis # (8 axes).flxPosition Mode always absolute
a, v, and S time same whether
In-Scan or Outscan.

62 usec

Absolute Position

Board ID U8

Axis U16

error in

Scan Dynamics

Velocity
Acceleration
S Curve Time

Start Position I32

Breakpoint Window

U32

10

Move to Start Position
Retro in general should be at
start position from last scan

Check that startpoint reached

status

U8 Bd ID Out

U16 Resource Output

error out

TF Startpoint reached?

Rev2 adds Enable Axes vi, and enables Axis 1 only via a constant.
Rev3 adds Enable Encoder vi, and enables onlyencoders 1 and 5 via
a constant.
This is needed to instantiate PID update rate
and enable axis 1 independent of MAX.

List of SubVIs and Express VIs with Configuration Information

Resource Out (Enum).flx
C:\Program Files\National Instruments\LabVIEW 8.5\vi.lib\Motion\FlexMotion\CustomControls\CustomControls.llb\Resource Out (Enum).flx

Bd Id Out
C:\Program Files\National Instruments\LabVIEW 8.5\vi.lib\Motion\FlexMotion\CustomControls\CustomControls.llb\Bd Id Out

Board Id
C:\Program Files\National Instruments\LabVIEW 8.5\vi.lib\Motion\FlexMotion\CustomControls\CustomControls.llb\Board Id

Axis To Control.flx
C:\Program Files\National Instruments\LabVIEW 8.5\vi.lib\Motion\FlexMotion\CustomControls\CustomControls.llb\Axis To Control.flx

Axis # (8 axes).flx
C:\Program Files\National Instruments\LabVIEW 8.5\vi.lib\Motion\FlexMotion\CustomControls\CustomControls.llb\Axis # (8 axes).flx

Load Target Position.flx
C:\Program Files\National Instruments\LabVIEW 8.5\vi.lib\Motion\FlexMotion\FunctionsVIs\Trajectory.llb\Load Target Position.flx

Start Motion.flx
C:\Program Files\National Instruments\LabVIEW 8.5\vi.lib\Motion\FlexMotion\FunctionsVIs\StartStopMotion.llb\Start Motion.flx

Start Motion (8 axes).flx
C:\Program Files\National Instruments\LabVIEW 8.5\vi.lib\Motion\FlexMotion\FunctionsVIs\StartStopMotion.llb\Start Motion (8 axes).flx

Check Move Complete Status (8 axes).flx
C:\Program Files\National Instruments\LabVIEW 8.5\vi.lib\Motion\FlexMotion\FunctionsVIs\Trajectory.llb\Check Move Complete Status (8 axes).flx

Check Move Complete Status.flx
C:\Program Files\National Instruments\LabVIEW 8.5\vi.lib\Motion\FlexMotion\FunctionsVIs\Trajectory.llb\Check Move Complete Status.flx

Configure Move Complete Criteria.flx
C:\Program Files\National Instruments\LabVIEW 8.5\vi.lib\Motion\FlexMotion\FunctionsVIs\AxisResourceConfig.llb\Configure Move Complete Criteria.flx

Set u32.flx
C:\Program Files\National Instruments\LabVIEW 8.5\vi.lib\Motion\FlexMotion\FunctionsVIs\ErrorUtility.llb\Set u32.flx

Load Velocity.flx
C:\Program Files\National Instruments\LabVIEW 8.5\vi.lib\Motion\FlexMotion\FunctionsVIs\Trajectory.llb\Load Velocity.flx

Load Acceleration/Deceleration.flx
C:\Program Files\National Instruments\LabVIEW 8.5\vi.lib\Motion\FlexMotion\FunctionsVIs\Trajectory.llb\Load Acceleration/Deceleration.flx

Load S-Curve Time.flx
C:\Program Files\National Instruments\LabVIEW 8.5\vi.lib\Motion\FlexMotion\FunctionsVIs\Trajectory.llb\Load S-Curve Time.flx

Enable Axes (8 axes).flx
C:\Program Files\National Instruments\LabVIEW 8.5\vi.lib\Motion\FlexMotion\FunctionsVIs\AxisResourceConfig.llb\Enable Axes (8 axes).flx

Enable Axes.flx
C:\Program Files\National Instruments\LabVIEW 8.5\vi.lib\Motion\FlexMotion\FunctionsVIs\AxisResourceConfig.llb\Enable Axes.flx

Enable Encoders (8 axes).flx
C:\Program Files\National Instruments\LabVIEW 8.5\vi.lib\Motion\FlexMotion\FunctionsVIs\AnalogDigitalIO.llb\Enable Encoders (8 axes).flx

Enable Encoders.flx
C:\Program Files\National Instruments\LabVIEW 8.5\vi.lib\Motion\FlexMotion\FunctionsVIs\AnalogDigitalIO.llb\Enable Encoders.flx

Set Operation Mode.flx
C:\Program Files\National Instruments\LabVIEW 8.5\vi.lib\Motion\FlexMotion\FunctionsVIs\Trajectory.llb\Set Operation Mode.flx

Config Analog Input Channels Rev1.vi

Connector Pane

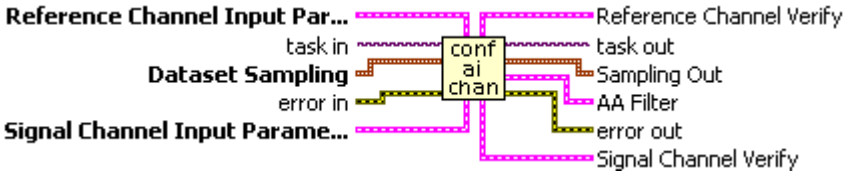

Front Panel

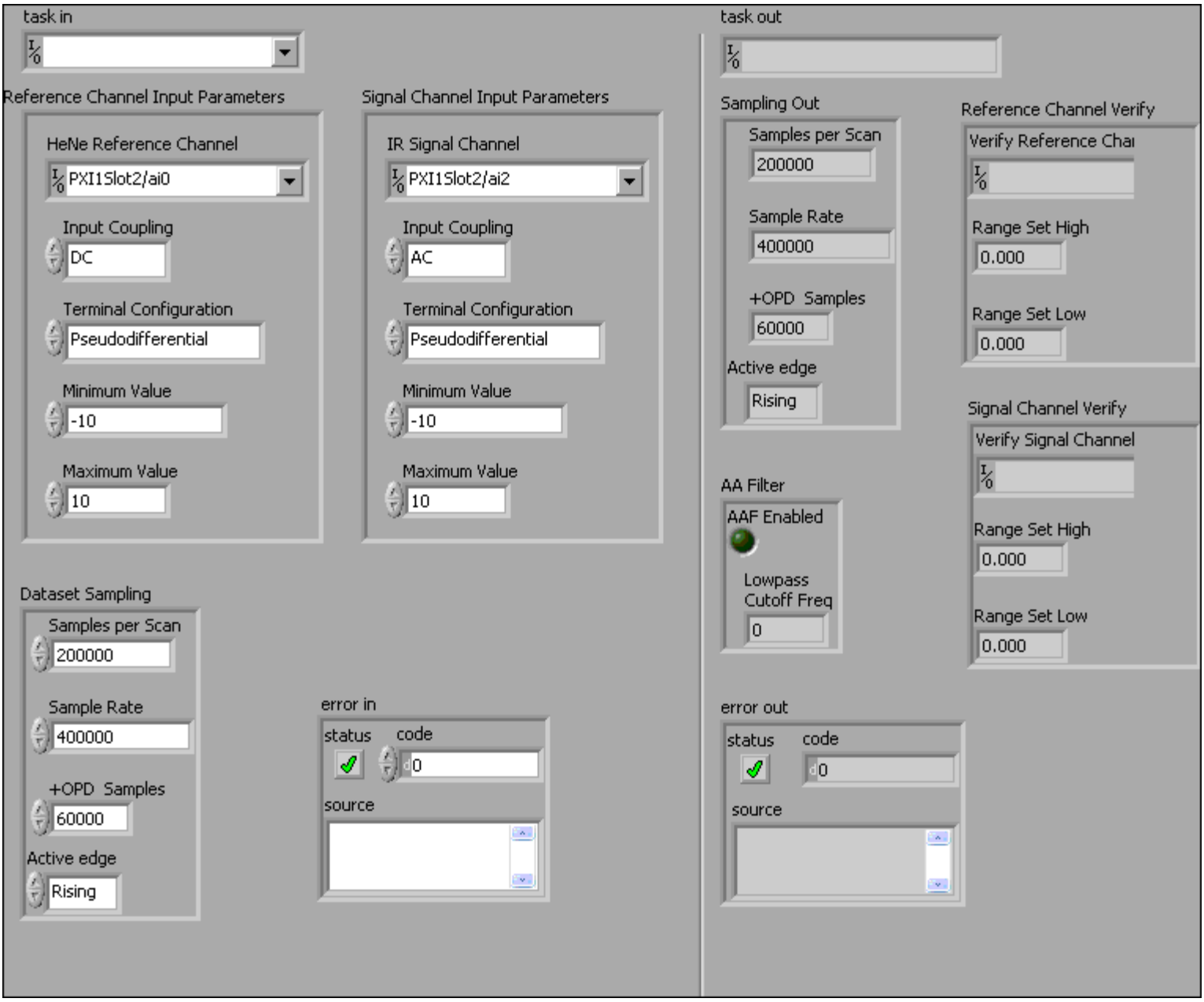

Controls and Indicators

Dataset Sampling

- **Samples per Scan**
- **Sample Rate**
- **+OPD Samples**
- **Active edge**

Reference Channel Input Parameters

HeNe Reference Channel physical channels specifies the names of the physical channels to use to create virtual channels. The DAQmx physical channel constant lists all physical channels on devices and modules installed in the system.

Maximum Value

Minimum Value

Terminal Configuration

Input Coupling

Signal Channel Input Parameters

IR Signal Channel physical channels specifies the names of the physical channels to use to create virtual channels. The DAQmx physical channel constant lists all physical channels on devices and modules installed in the system.

Maximum Value

Minimum Value

Terminal Configuration

Input Coupling

task in task in specifies the task to which to add the virtual channels this VI creates. If you do not specify a task, NI-DAQmx creates a task for you and adds the virtual channels this VI creates to that task.

error in error in describes error conditions that occur before this VI or function runs.

status status is TRUE (X) if an error occurred before this VI or function ran or FALSE (checkmark) to indicate a warning or that no error occurred before this VI or function ran. The default is FALSE.

code code is the error or warning code. The default is 0. If **status** is TRUE, **code** is a negative error code. If **status** is FALSE, **code** is 0 or a warning code.

source source identifies where an error occurred. The source string includes the name of the VI that produced the error, what inputs are in error, and how to eliminate the error.

error out error in can accept error information wired from VIs previously called. Use this information to decide if any functionality should be bypassed in the event of errors from other VIs.

Right-click the **error in** control on the front panel and select **Explain Error** or **Explain Warning** from the shortcut menu for more information about the error.

status status is TRUE (X) if an error occurred or FALSE (checkmark) to indicate a warning or that no error occurred.

Right-click the **error in** control on the front panel and select **Explain Error** or **Explain Warning** from the shortcut menu for more information about the error.

code code is the error or warning code.

Right-click the **error in** control on the front panel and select **Explain Error** or

Explain Warning from the shortcut menu for more information about the error.

source source describes the origin of the error or warning.

Right-click the **error in** control on the front panel and select **Explain Error** or **Explain Warning** from the shortcut menu for more information about the error.

task out

Reference Channel Verify

Verify Reference Channel physical channels specifies the names of the physical channels to use to create virtual channels. The DAQmx physical channel constant lists all physical channels on devices and modules installed in the system.

Range Set High

Range Set Low

Signal Channel Verify

Verify Signal Channel physical channels specifies the names of the physical channels to use to create virtual channels. The DAQmx physical channel constant lists all physical channels on devices and modules installed in the system.

Range Set High

Range Set Low

Sampling Out

Samples per Scan

Sample Rate

+OPD Samples

Active edge

AA Filter

AAF Enabled

Lowpass Cutoff Freq

Block Diagram

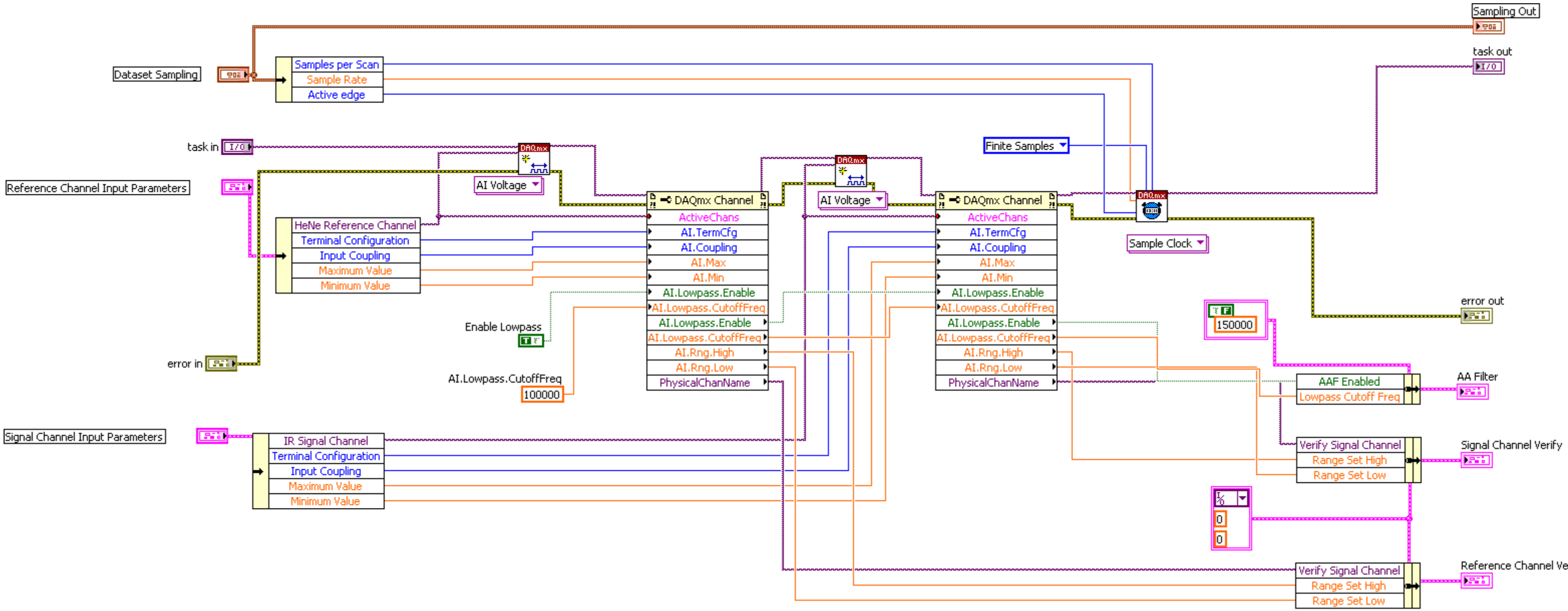

Rev1
1. The antialias filters is turned on for both channels by a single shared BD constant.
2. The Range Set High and Low are Separately settable per channel.

List of SubVIs and Express VIs with Configuration Information

DAQmx Timing (Sample Clock).vi
C:\Program Files\National Instruments\LabVIEW 8.5\vi.lib\DAQmx\configure\timing.llb\DAQmx Timing (Sample Clock).vi

DAQmx Timing.vi
C:\Program Files\National Instruments\LabVIEW 8.5\vi.lib\DAQmx\configure\timing.llb\DAQmx Timing.vi

DAQmx Create Channel (AI-Voltage-Basic).vi
C:\Program Files\National Instruments\LabVIEW 8.5\vi.lib\DAQmx\create\channels.llb\DAQmx Create Channel (AI-Voltage-Basic).vi

DAQmx Create Virtual Channel.vi
C:\Program Files\National Instruments\LabVIEW 8.5\vi.lib\DAQmx\create\channels.llb\DAQmx Create Virtual Channel.vi

Config FTIR Scan Parameters Rev1.vi

Connector Pane

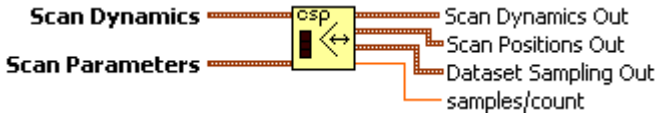

Front Panel

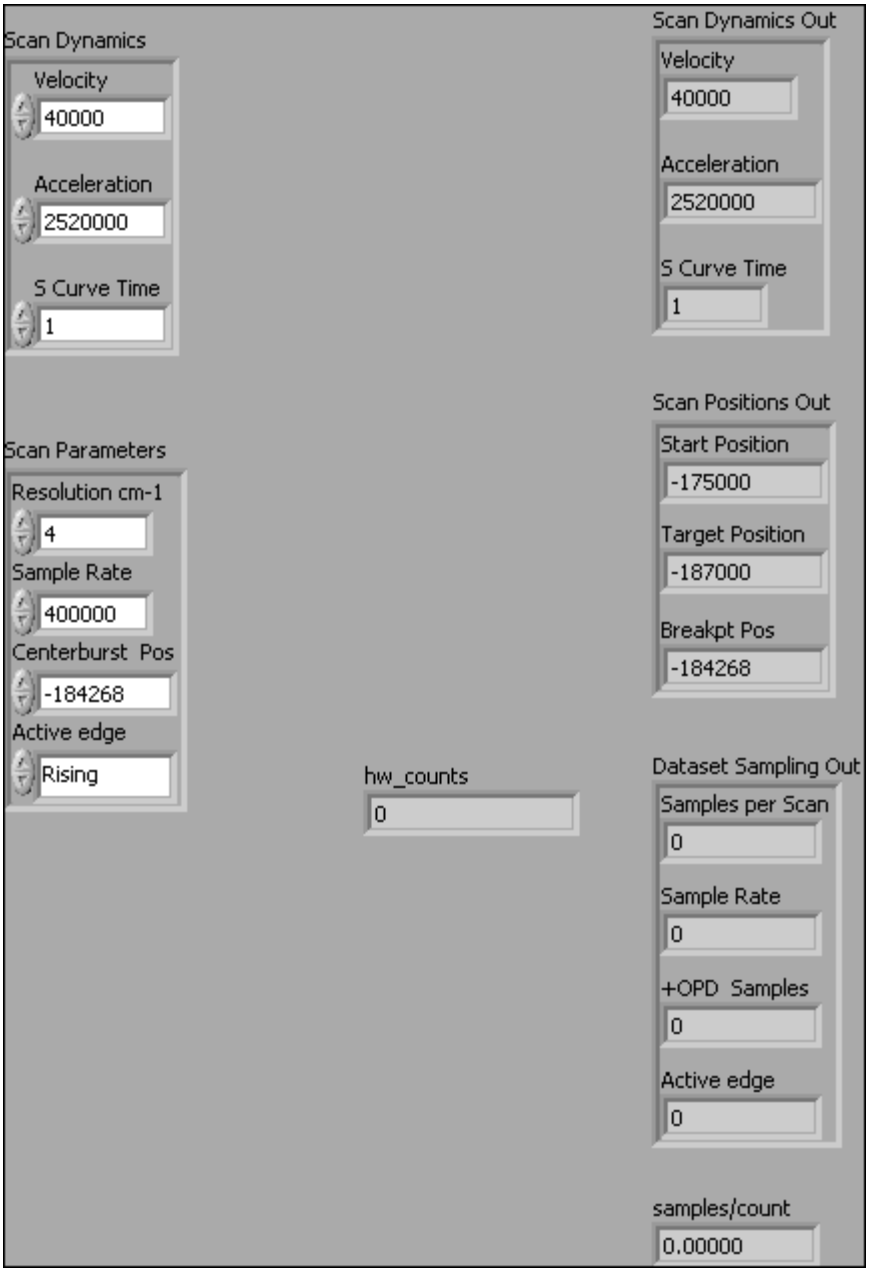

Controls and Indicators

- **Scan Dynamics**
  - **Velocity**
  - **Acceleration**
  - **S Curve Time**
- **Scan Parameters**


Resolution cm-1


Sample Rate


Centerburst Pos


Active edge edge specifies on which edge of the digital signal the Reference Trigger occurs.


hw_counts


samples/count


Scan Positions Out


Start Position


Target Position


Breakpt Pos


Dataset Sampling Out


Samples per Scan


Sample Rate


+OPD Samples


Active edge


Scan Dynamics Out


Velocity


Acceleration


S Curve Time

Block Diagram

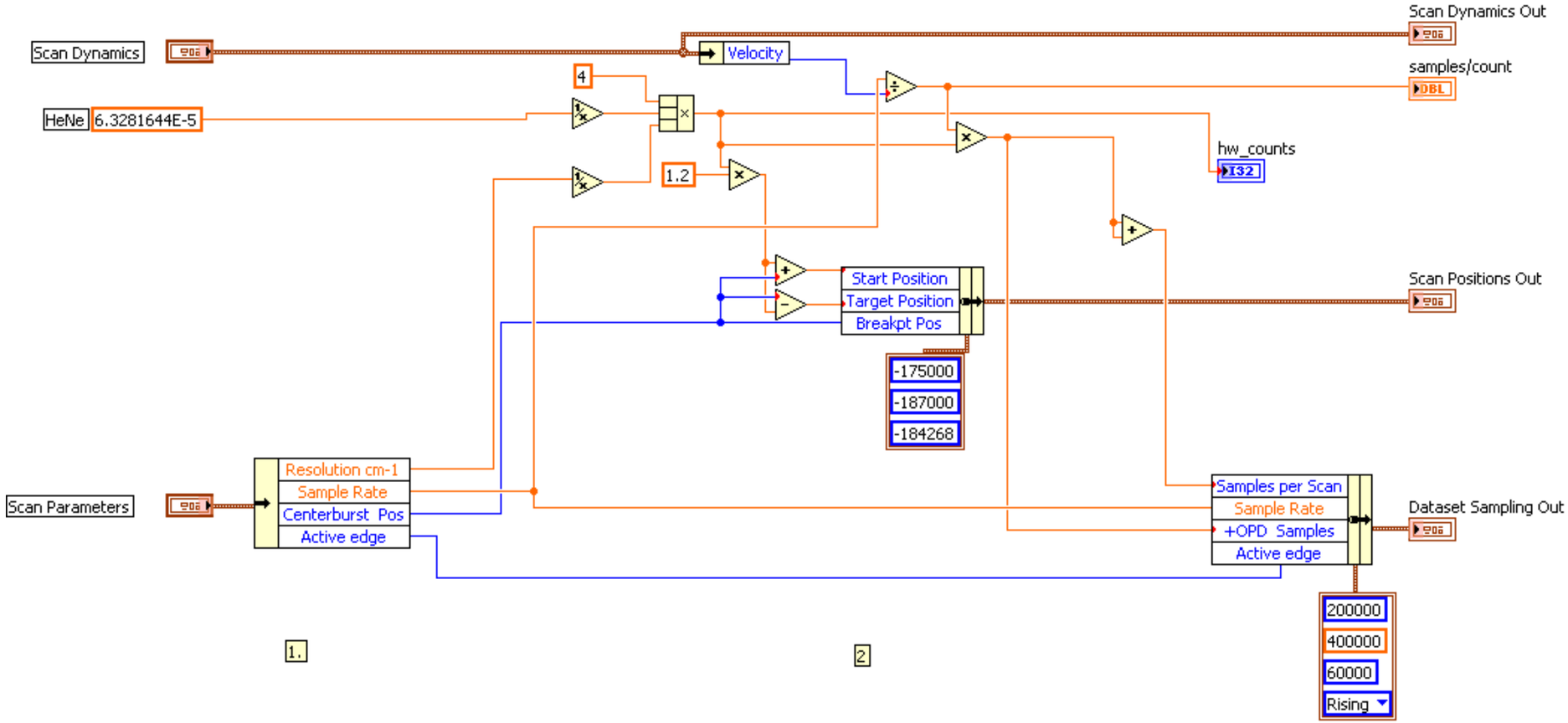

1.

2

1. Inputs

Scan Dyanmics
Velocity
Acceleration
S-Curve time

Scan Parameters
Resolution
Sample rate
Centerburst Pos
Trigger Edge

2. Compute

Breakpt Pos = Centerburst Pos
hw_counts = travel in counts needed to achieve resolution
=4*OPD/lambda = 4*(1/res)*(1/lambda)
Start Pos = bp + 1.2* hw_counts
Target Pos = bp -1.2*hw_counts

Note this is a double sided interferogram!

Samples/scan (double-sided) =
sample rate [samples/sec]/velocity [cts/sec]
*hw_counts*2
+OPD samples = .5*samples/scan

3. Outputs

Scan Dynamics
pass-thru

Scan Positions
Start position
Target position
Breakpoint position

Dataset Sampling Out
Samples per scan
Sample rate (pass-thru)
+OPD samples
Active Edge (pass-thru)

List of SubVIs and Express VIs with Configuration Information